Designing of Capecitabine Loaded Gum Odina-Alginate Based Microsphere for Targeted Delivery for Colon Cancer Management

Thesis submitted by Ahana Hazra

Doctor of Philosophy (Pharmacy)

Department of Pharmaceutical Technology
Faculty Council of Engineering & Technology
Jadavpur University
Kolkata, India

2023

INDEX NO. 300/20/Ph.

1. **Title of the thesis:**

   Designing of Capecitabine Loaded Gum Odina-Alginate Based Microsphere for Targeted Delivery for Colon Cancer Management

2. **Name, Designation & Institute of the Supervisor**

   Dr. Amalesh Samanta, Professor, Division of Microbiology & Biotechnology, Department of Pharmaceutical Technology, Jadavpur University, Kolkata-700032,India.

3. **List of Publications:**

A. Journal publication:

a) Related to this work

1. Hazra A, Sanyal D, De A, Chatterjee S, Chattopadhyay K, Samanta A. Development and in vitro characterization of capecitabine loaded biopolymeric vehicle for the treatment of colon cancer. Journal of Applied Polymer Science. 2022 Jul 10;139(26):e52374.
2. Hazra A, Tudu M, Mohanta A, Samanta A. Gum odina prebiotic induced gut modulation for the treatment of colon cancer on Swiss albino mice: By using capecitabine loaded biopolymeric microsphere. International Journal of Biological Macromolecules. 2024 Apr 4:131410.

b) Other publications during the period of doctoral research

1. Hazra A, Chatterjee S, Mohanta A, Paul Pankaj, Samanta A. A review on fungal pullulan as a natural polymer focusing on targeted therapy for colon cancer and other pharmaceutical applications. Polymers for Advanced Technologies. 2023.

4. List of Patents

Nil

5. List of Presentation in National/ International

- **Oral presentation** at National Conference on "Bioengineering-2019" during the period of December 06-07, 2019, organized by Department of Biotechnology and Medical Engineering National Institute of Technology, Rourkela Odisha, India.

- **Participation** in virtual scientific conclave- 2021 during the period of 27-29, 2021 organized by Faculty of Pharmaceutical Science Assam Down Town University in association with DRDO, Tezpur, Assam.

- **Oral presentation** at International Conference on "Recent Trends in Material Science and Device"-2023 during the period of July 22-23,2023, organized by Research Plateau Publishers & G.A.V. Degree College, Patauda, Jhajjar, Haryana, India

- **Poster Presentation** at International Conference on "Advanced Materials for Better Tomorrow-II" during the period of October 10-13,2023, organized by Banaras Hindu University, India.

"STATEMENT OF ORIGINALITY"

I, Ahana Hazra registered on 21/07/2020 hereby declare that the thesis entitled **"Designing of Capecitabine Loaded Gum Odina-Alginate Based Microsphere for Targeted Delivery for Colon Cancer Management"** contains a literature survey and original research work has been done by myself under the general supervision of my supervisor.

I have followed the academic rules, norms and the guidelines given in the Ethical Code of Conduct provided by Institute in the writing the thesis.

Whenever I have quoted written materials from other sources, I have put them under quotation marks and given credit to the sources by citing them and giving required details in the references.

I also declare that I have checked this thesis as per the "Policy on Anti Plagiarism, Jadavpur University, 2019", and the level of similarity as checked by iThenticate software is 7%.

14.5.24.

Certified by Supervisor: Prof. (Dr.) Amalesh Samanta
Department of Pharmaceutical Technology
Jadavpur University
Kolkata-700032

Ahana Hazra

Signature of the Candidate

Date: 9.11.23

Prof. (Dr.) Amalesh Samanta
Div. of Microbiology & Biotechnology
Dept. of Pharmaceutical Technology
Jadavpur University
Kolkata-700032, India

CERTIFICATE FROM THE SUPERVISOR

This is to certify that the thesis entitled **"Designing of Capecitabine Loaded Gum Odina-Alginate Based Microsphere for Targeted Delivery for Colon Cancer Management"** submitted by Miss. Ahana Hazra who got her name registered on 21.07.2020 for the award of Ph. D. (Pharmacy) degree of Jadavpur University is based solely upon her work under the supervision of Prof. (Dr.) Amalesh Samanta and that neither her thesis nor any part of the thesis has been submitted as a basis for the award of any previous degree to anyone else.

14.5.24.

Signature of the Supervisor
Prof. (Dr.) Amalesh Samanta
Department of Pharmaceutical Technology
Jadavpur University
Kolkata-700032

Prof. (Dr.) Amalesh Samanta
Div. of Microbiology & Biotechnology
Dept. of Pharmaceutical Technology
Jadavpur University
Kolkata-700032, India

DECLARATION

This research work is entitled "**Designing of Capecitabine Loaded Gum Odina-Alginate Based Microsphere for Targeted Delivery for Colon Cancer Management**" has been carried out by me under the supervision of Prof. (Dr.) Amalesh Samanta in the Department of Pharmaceutical Technology, Faculty Council of Engineering & Technology, Jadavpur University, Kolkata-700032, India. I hereby declare that the work is original and has not been submitted so far, in part or full, or any degree/diploma course of any university.

Date: 9.11.23

Place: Asansol

Ahana Hazra

Signature of the Candidate

Date: 9.11.23

ACKNOWLEDGEMENT

The path to success needs hard work and dedication but this path to success is paved in the right direction by proper guidance, help, and cooperation of several well-wishers. I hereby thank all of them who with their help and cooperation paved the way to completion of my dissertation work.

I express my deep sense of gratitude towards my respected guide, Prof. (Dr.) Amalesh Samanta, Professor, Division of Pharmaceutical Microbiology & Biotechnology, Department of Pharmaceutical Technology, Jadavpur University, Kolkata – 700032, for his guidance, innovative ideas, constant inspiration, uttering efforts, and spontaneous valuable suggestions, immense support and encouragement during my study. I am thankful to him to trust me which made me realize my potential. Without his help, this dissertation would not be as it is.

I express my sincere thanks to the Head of the Department of Pharmaceutical Technology, Jadavpur University, Kolkata, for cooperation in the completion of this research work.

I am also thankful to Dr. Krishnananda Chattopadhyay, Chief Scientist & Head, Structural Biology & Bioinformatics, Division of Structural Biology & Bioinformatics, CSIR-Indian Institute of Chemical Biology, for providing all facilities and skillful operation of cell culture study.

I am also obliged to Dwipanjan Sanyal Senior Research Fellow, CSIR-Indian Institute of Chemical Biology, Kolkata for his enormous support to complete my Ph. D. work.

I would like to express my special thanks to myall lab mates: Dr. Arnab De, Dr. Piu Das, Miss Mousumi Tudu, Miss Sohini Chatterjee, Mr. Abhishek Mohanta, Mr. Pankaj Paul, Mr. Totan Roy, and all other who have extended their cooperation to carry out this work successfully.

I am also thankful to UGC RUSA2.0 and SVMCM for providing the financial support to conduct research work smoothly.

I hereby express my heartfelt thanks to my dear parents for their support, sincere advice, and constant inspiration all the way.

Last but most importantly I am very much thankful to THE ALMIGHTY GOD, for providing me the desired strength and enthusiasm to enable me to complete this project successfully.

Ahana Hazra

Date: 9.11.23

Ahana Hazra

PREFACE

Colon cancer is one of the fourth most disastrous cancer and causes mortality and morbidity worldwide. Colon cancer-associated death is mostly found in western countries due to changes in their habitual lifestyle and food habit. In recent years more than 66,000 cases of colon cancer are also reported in India. Several types of natural and synthetic drugs have been used as a chemotherapeutic agent for the treatment of colon cancer but they have been associated with lots of biochemical side effects which predominantly destroy the healthy cells of patients.

Capecitabine is one of the potent chemotherapeutic agent widely used for several decades for the treatment of colon cancer. The major challenges related to oral administration of capecitabine is attributed due to the short plasma half-life, rapid rate of elimination, high dose of capecitabine is needed twice per day, unwanted dose-related toxicity like bone marrow depression, cardiotoxicity, diarrhea, nausea, and dermatitis, etc. Keeping this view, the present study focused on the development of a natural polymer gum odina-sodium alginate based capecitabine loaded microsphere for the treatment of colon cancer.

The subject matter of the thesis has been divided into several chapters containing the development of gum odina- sodium alginate based capecitabine loaded microsphere, optimization of formulations, physicochemical characterizations, and biological evaluation of formulation and *in vitro* and *in vivo* studies of optimized formulation to investigate the role of the formulated microsphere as an ideal formulation for the treatment of colon cancer.

CONTENTS

LIST OF ABBREVIATIONS

HDI	Human development index
FAP	Familial adenomatous polyposis
HNPCC	Hereditary nonpolyposis colon can
AFAP	Attenuated familial adenomatous polyposis
HNPCC	Hereditary nonpolyposis colorectal cancer
IBD	Inflammatory bowel diseases
CEA	Carcinoembryonic antigen
EGFR	Epidermal growth factor receptor
HCL	Hydrochloric acid
PBS	Phosphate buffer solution
5-FU	5-fluorouracil
$CaCl_2$	Calcium chloride
GIT	Gastrointestinal tract
GO	Gum odina
SA	Sodium alginate
DPPH	2, 2-diphenyl-1-picrylhydrazyl
FBS	Fetal Bovine Serum

DMEM	Dublbecco's Modified Eagle's medium
DMH	1,2 -dimethylhydrazine
DSS	Dextran sodium sulphate
mg	Milligram
N	Nitrogen
mL	Milliliter
nm	Nanometer
SEM	Surface morphology analysis
cm	Centimeter
AFM	Atomic force microscopy
mm	Millimeter
kHz	Kilohertz
FTIR	Fourier Transform Infrared
XRD	X-ray diffraction (XRD)
kV	Kilovolt
mA	Milliampere
DSC	Differential scanning calorimetry
TGA	Thermogravimetric analysis

W/V	Weight in volume
kJ	Kilojoule
min	Minutes
M	Molar
SGF	Simulated gastric fluid
SCF	Simulated colonic fluid
CA 19-9	Cancer antigen 19-9
CA 125	Cancer antigen 125
kU	Kilo unit
ANOVA	Analysis of variance
SD	Standard deviation
%	Percentage
AUC	Area under the curve
ALT	Alanine transaminase
AST	Aspartate aminotransferase
IC50	Half maximal inhibitory concentration

LIST OF TABLES

LIST OF FIGURES

CHAPTER 1

INTRODUCTION

1 Introduction

This section covers the background and significance of colon cancer prevention, the cause of colon cancer, and the importance of colon-targeted drug delivery systems. It also explores the use of naturally obtained biopolymers for formulation development and addresses the drawbacks of conventional dosage forms. The thesis offers a concise overview of gum odina and sodium alginate-based biopolymeric microspheres as promising biomaterials for colon cancer prevention.

1.1 Background and importance of the study

Colon cancer increased most in economically developed countries due to changes of life style, dietary changes, obesity, smoking, alcohol consumption, and physical inactivity. However, more than 66,000 cases of colon cancer have been documented in India in recent years [1]. The likelihood of developing colon cancer can range from medium to high. Individuals without advanced colorectal adenoma, intestinal bowel disease, polyposis syndrome, hereditary colorectal cancer syndrome, or a family history of colon cancer have an average risk of acquiring colon cancer after the age of 50 years. Most people with a high risk of colon cancer start showing symptoms at a young age, which makes them candidates for a specific screening and surveillance program [1]. Colon cancer is the result of numerous multi-step mutational processes that occur in succession. Seventy percent of colon cancer was mostly caused by spontaneous adenoma and familial adenoma polyps, whereas thirty percent of colon cancer was caused by

abnormalities in DNA mismatch repair, B-Raf proto-oncogene mutation, and base-excision repair genes linked to mutY DNA glycosylase polyposis syndrome [2]. Numerous chemotherapeutic drugs have been used to treat colon cancer, but they have a negative impact on public health because to their high toxicity, noxiousness, low permeability, excess solubility, and lack of target specificity. Regular administration of medications that have been developed to preserve their stability, activity, and bioavailability is often required for conventional therapy [3]. The basic goal of a drug delivery system is to sustain medication levels in the body for an extended length of time while still being within the therapeutic window. Sustained or controlled release formulations that could maintain a steady state plasma level for a long time are designed to address this issue with conventional therapy [4]. Such formulations result in the least amount of drug plasma level variation with fewer side effects. The most recent development in drug delivery technology is the use of microspheres to circumvent some of the drawbacks of traditional methods, including poor oral bioavailability, lack of precise targeting, poorer aqueous solubility, and lower therapeutic indices. Numerous studies have recently concentrated on using synthetic polymers instead of natural biopolymers as drug delivery methods. Due to their biodegradability, biocompatibility, affordability, sustainability, passive tumor-targeting, high encapsulation efficiency, and capacity to transport a wide variety of therapeutic drugs to the targeted spot, natural polymers are preferable to synthetic polymers [5]. In order to create the microspheres for this study, we employed gum odina, a

natural polysaccharide that was naturally liberated from the bark of *Odina wodier* family Anacardiaceae. Gum odina-based microencapsulation enhances the solubility of the drug, prevents early degradation in the upper gastrointestinal tract, and supports targeted drug delivery and controlled drug release [6].

In this thesis work, the biopolymer gum odina-sodium alginate-based microsphere will have all possible characteristics for being the ideal material for colon cancer prevention at a realistic cost with improvement of patient compliance.

1.2 Cancer

Cancer develops when a few body cells proliferate uncontrollably and spread to other physical organs. Cancer can grow virtually anywhere among the billions of cells that make up the human body. Human cells frequently divide to produce new cells as needed by the body (a procedure known as cell proliferation and multiplication). When aging or damage causes a cell to die, new ones replace the old ones [7].

1.3 Types of tumor

Tumors can be classified as either benign or malignant, depending entirely on how they spread. Unproblematic benign tumors typically remain in their original locations rather than spreading to other parts of the body. Benign tumors grow slowly and steadily, and their borders are clearly defined. Malignant tumors, on the other hand, spread rapidly and uncontrollably from one area of the body to another [8].

1.4 Incidence of colon cancer

The frequency of colon cancer is rising in industrialized nations including Western Europe, North America, Australia, New Zealand, and Japan. Colon cancer is the third most prevalent type of cancer worldwide [9]. Each year, 250000 new cases of colon cancer are recorded in Europe, making up 10.3% of all new cases in women and 7.4% of all new cases in men. There isn't a recent, extensive population study available in Europe that details the incidence of colon cancer in young people. Industrialization and urbanization both raise the rates of this colon cancer-related death [10]. Overall, there are up to eight-fold differences between countries in the incidence of colon cancer, which varies greatly by location. There are substantial differences in the occurrence of colon cancer worldwide. These differences are closely linked to the level of development in each region, as measured by the Human Development Index (HDI) [9].

It also highlights that within individual countries, like the United States, there can be significant disparities in colon cancer rates. For example, there's a nearly threefold difference in colon cancer incidence between Alaska and the Southwest region of the United States, and these differences are influenced by variations in factors like access to screening and people's behaviors [3].

1.5 Earlier lesions

In terms of molecular genetics, colon cancer is the most complex (multistep) malignancy that is now understood. The emergence of particular varieties of neoplastic polyps in the intestinal mucosa is the initial stage of carcinogenesis.

For assessing the possibility for malignancy, polyp histology is essential. The two most prevalent histologic categories are adenomatous and hyperplastic. Histologically, hyperplastic polyps have fewer cytoplasmic mucus and more glandular cells, although they typically don't have nuclear hyperchromatism [11].

1.6 Histology

Based on the degree of preservation of typical glandular architecture and cytologic features, colon tumors are categorized as highly differentiated, moderately well differentiated, or poorly differentiated. Although the mutations responsible for poor differentiation are yet unclear, poor differentiation is likely a histologic indication of serious underlying genetic abnormalities. Undifferentiated colon tumors make up about 20% of cases [12].

1.7 Signs and symptoms

Patients may experience a range of symptoms of colon cancer, depending on the stages of the disease. Changes in bowel habits, general abdominal discomfort, weight loss, aggressive attempts, and constipation are some of the early signs of colorectal cancer in adults between the ages of 65 and 79. When a patient is 80 years old, the signs and symptoms of colon cancer are slightly different [13].

1.8 Risk factors for colon cancer

Multiple risk factors have been involved in the development of colon cancer have been established. It has been shown that conditions such as familial polyposis syndromes, inflammatory bowel illnesses, Type 2 diabetes might be increased a person's risk of developing colon cancer. There is evidence that dietary factors

are a significant contributor to development in colon cancer. Individuals with overweight, physical inactivity, cigarette smoking, alcohol consumption, and inappropriate dietary patterns are associated with an elevated risk of colon cancer. Moreover, gut microbiome, age, gender race, and socioeconomic status are known to influence colorectal cancer risk [14].

Hereditary colon cancer syndromes :

A number of particular genetic diseases, the majority of which are inherited in an autosomal-dominant manner, are linked to an extremely high risk of developing colon cancer.

The most prevalent familial colon cancer syndromes are lynch syndrome and familial adenomatous polyposis (FAP), which together account for just 5% of all colon cancer occurrences, with lynch syndrome accounting for the bulk of instances of hereditary nonpolyposis colon cancer (HNPCC)[15].

FAP:

Less than 1% of colon cancers are caused by familial adenomatous polyposis (FAP) and its variations. Colonic adenomas proliferate in large numbers during childhood in the typical FAP. Average onset of symptoms is around 16 years, and 90% of untreated cases of colon cancer are discovered by the age of 45. Although AFAP (attenuated familial adenomatous polyposis) has a higher than usual risk of developing colon cancer, it is distinguished by fewer adenomas and a 54-year-old median age at cancer diagnosis. In the same family, there may be age-matched

people with oligo-polyposis as well as people with thousands of adenomas, thus clinical experience supports less differentiation between FAP and AFAP [16].

MAP:

The autosomal-recessive syndrome MAP, or MUTYH-associated polyposis, is brought on by biallelic germline mutations in the base excision repair gene mutY homolog (MUTYH). Although the phenotypic of MAP varies, it can manifest as polyposis, usually with less than 500 adenomas. The APC (adenomatous polyposis coli) gene appears to be particularly vulnerable to oxidative DNA damage, which is repaired by the base excision repair mechanism. Somatic mutations in APC and KRAS, particularly G:C to T:A transversions, are frequently caused by base excision repair system failure and can result in a polyposis phenotype [17].

Lynch syndrome:

About 3% of all colonic adenocarcinomas are caused by the autosomal-dominant disease known as lynch syndrome, also known as HNPCC (hereditary nonpolyposis colorectal cancer). It is more frequent than FAP. If there is a significant family history of colon cancer, endometrial, or other malignancies, lynch syndrome may be suspected [18].

Smoking:

Long-term smokers have a higher risk of developing colorectal cancer and dying from it than non-smokers do [19].

Unhealthy diets and nutrition:

Some malignancies have a strong relationship with poor diets, nutrition, and the food we eat. Consuming processed meats like ham, bacon, salami, and sausages has been linked to bowel cancer in numerous studies [20].

Obesity:

A higher risk of 12 cancers is associated with being overweight or obese, where the body is carrying extra weight. Endometrial, breast, ovarian, prostate, liver, gallbladder, kidney, and colon cancers are among them [21].

Age and colorectal cancer with early start:

A significant risk factor for sporadic colon cancer is age. Before the age of 40, large bowel cancer is uncommon. Between the ages of 40 and 50, the incidence starts to considerably increase, and age-specific incidence rates rise in each decade following that [21].

Risk of colon cancer and IBD (inflammatory bowl diseases):

In contrast to the general population, patients with IBD appear to have a significantly higher risk of colorectal cancer, with one recent study showing a 7% risk of the illness after 30 years. Patients with at least 8 years of illness duration and colonic involvement are at an elevated risk of colorectal cancer. Dysplasia surveillance plans should be made available to patients at risk for colorectal cancer because they appear to lower that risk. Depending on the risk of each patient, surveillance normally comprises a colonoscopy every 1-3 years [22].

1.9 The following tests and methods are used to diagnose colon cancer

Colonoscopy:

The whole colon and rectum may be seen during a colonoscopy thanks to the use of a long, flexible, and thin tube connected to a camera and monitor. Surgery tools may be inserted via the tube by a doctor to take tissue samples and remove polyps [23].

Biopsy:

An operation called a biopsy is used to take a sample of tissue for laboratory analysis. The tissue sample for colon cancer is frequently obtained during a colonoscopy. Surgery may occasionally be required to obtain the tissue sample. Tests performed in the lab can reveal the cells' growth rate and malignant status. Additional examinations may reveal more details about the cancer cells [24].

Blood test:

Colon cancer cannot be diagnosed by blood tests. Blood tests, however, can provide information about general health, including how well the liver and kidneys are functioning. To check for low red blood cell levels, a blood test may be utilized. This outcome might suggest that bleeding is being caused by colon cancer [24]. Carcinoembryonic antigen, usually known as CEA, is a protein that is occasionally produced by colon tumors. The level of CEA can be monitored over time through blood tests.

1.10 Gut microbiota and colon cancer:

Colon cancer developed when the intestinal epithelium, mucosal barrier, and 40 trillion microorganisms in the human gut microbiota interacted with the host cell to sustain physiological activities such as energy production, metabolism, and immune response. The kind of diet, age, region, race, external environmental microorganisms, usage of antibiotics, infectious diarrhoea, or foreign immigration all affect the composition and presence of microbes in the gut. Numerous elements, such as inactivity, antibiotics, a western diet, advanced age, smoking, and obesity may increase gut microbiota imbalance. Other cancers, including hepatocellular carcinomas, pancreatic cancer, and breast cancer, are also caused by changes in the gut flora [6]. *Fusobacterium nucleatum*, *Bacteroides fragilis*, *Streptococcus bovis/gallolyticus*, *Clostridium septicum*, and *Enterococcus faecalis* are the species most frequently associated with colon carcinogenesis. According to recent findings, some bacteria like *Bacteroides fragilis*, and *Peptostreptococcus anaerobius* may contribute to the development of colon cancer by generating DNA damage and promoting the Th17 cell response. The phagocytosis of pathogenic Salmonella and E. coli could have been caused by a variety of gut commensal Gram-negative bacteria inducing an IgG response. Recent studies have suggested that the makeup of the gut bacteria may play a part in affecting how cancer develops [25].

1.11 Treatment of colon cancer:

Colon cancer is the third most common cause of cancer related deaths world wide. The primary treatment of colon cancer depending on stages and an extent of the recurrent tumor, treatment modalities including surgery alone or with radiation therapy has been recommended. The people who are diagnosed with metastatic colon cancer might be treated with cytotoxic chemotherapy, antibodies to cellular growth factors, immunotherapy, and their combinations. Several studies through clinical trials have demonstrated that variation in somatic cell and tumor progression might be halt by tailoring treatment and genomic profiling respectively. Most of the patients with metastatic colon cancer treated with monoclonal antibodies (cetuximab and panitumumab), targeted combination therapy with B-Raf Proto Oncogene and EGFR (epidermal growth factor receptor) inhibitors might be effective treatment probably extend survival upto 6 to 9 months compared with standard chemotherapeutic agent [26]. Howevere, for the 5% patients with abruptly variation in genetic sequence, numerous insertions or deletions at repetitive DNA units, mismatch repair deficiency, immunotherapy might be used as first line defence mechanism that might be improved treatment outcomes and extended overall survival to 31.4 months [27].

Chemotherapy:

Chemotherapy kills cancer cells by using potent medications. If the colon cancer is big or has progressed to the lymph nodes, chemotherapy is typically administered following surgery. Cancer cells that could remain after surgery can be eliminated by chemotherapy. This lessens the possibility of the cancer returning [28].

Palliative medicine:

Providing pain relief and addressing other symptoms of a serious illness are the main goals of palliative care. A further level of support throughout cancer treatment is provided by palliative care. People with cancer may feel better and live longer when palliative care is combined with all other approved treatments [29].

Immunotherapy:

Immunotherapy is a medical procedure that aids in the body's immune system's ability to eradicate cancer cells. By targeting germs and other cells that shouldn't be in the body, the immune system fends against infections. Cancer cells evade the immune system in order to survive. Immunotherapy aids in the discovery and destruction of cancer cells by immune system cells[30].

Targeted treatment:

In targeted therapy, drugs are used to target specific compounds found in cancer cells. Targeted therapy can kill cancer cells by inhibiting these substances. Chemotherapy is frequently used with targeted therapy. Advanced colon cancer patients often receive targeted therapy [31].

Radiation treatment:

Strong energy beams are used in radiation therapy to eliminate cancer cells. Protons, X-rays, and other types of energy are the possible sources [32]. Before surgery, radiation therapy can help a large cancer shrink so that it is easier to remove.

1.12 Drug profile

The pro-drug of 5-fluorouracil (5-FU), capecitabine, is transformed to 5-FU in the cancer cell through enzymatic breakdown. Due to its great tolerability and high intra-tumor drug concentration following absorption from the gastrointestinal system, capecitabine has been utilized extensively during the past ten years in the treatment of metastatic colorectal cancer and breast cancer [33]. However, because capecitabine must be administered at a high dose of 1250 mg/m^2, it is quickly eliminated from the body with a short plasma half-life of less than 0.85 hours. The most common overdose toxicities caused by capecitabine's adverse effects are dermatitis, diarrhoea, nausea, and vomiting, as well as

cardiotoxicity and bone marrow depression [34]. It is critical to develop a targeted delivery method that is efficient and long-acting in order to reduce the drug's high clearance rates, which is an ongoing issue. Several different pharmacological controlled release dosage forms have been developed to lessen gastrointestinal adverse effects. A medication delivery system should have all the following qualities: it should be inert, biocompatible, biodegradable, patient compliance, mechanical strength, safety, and effectiveness. There are several various methods that have been used to create controlled drug delivery systems. Microparticle systems are one such formulation that can be employed for regulated medication delivery [35].

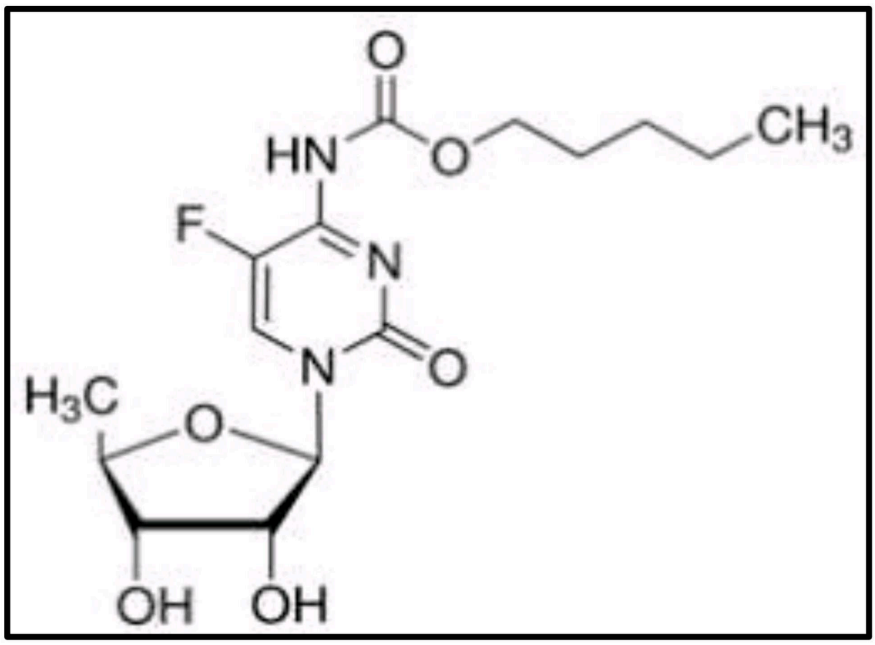

Figure 1.1 Structure of capecitabine

1.13 Description of polymer

Utilizing natural polymers in the creation of various drug delivery systems has drawn a lot of research interest over the past few decades. There are many benefits to using natural polymers, including their availability, affordability, biodegradability, and biocompatibility. One of the polyanionic polysaccharides that the FDA considers to be generally regarded as safe (GRAS) is alginate. Brown seaweeds are the source of the natural polysaccharide known as alginate. Alginate has been employed in numerous fields since it was first discovered by Stanford1 in 1881, including food, textile printing, paper, pharmaceuticals, and many more cutting-edge end uses. Alginate is a great gel-forming substance that can contain a lot of water because, it is a water-soluble polymer. Chemically, alginates are unbranched, linear polysaccharides made of β-D mannuronic acid (M) and its C-5 epimer α-l guluronic acid (G) residues that are linked by (1-4) glycoside linkages [36]. The remains are often organized along the chain in a block-like arrangement and vary greatly in composition and order. These homopolymeric β-D mannuronic acid and α-l guluronic acid block sections are interspersed with β-D mannuronic acid and - α-l guluronic acid block regions of alternating structure. The molecular weight, sequence composition, and length affect the physical characteristics of alginates. Cold water slowly dissolves sodium alginates, forming a thick, colloidal solution. Alcohol and hydroalcoholic

solutions with an alcohol level of more than 30% by weight do not allow it to dissolve. Additionally, it is insoluble in acids if the resulting solution's pH is below 3.0 as well as in other organic solvents like ether and chloroform. The pH of a 1% solution in distilled water is roughly 7.2 [37]. It does have certain drawbacks, though, like an unregulated hydration rate, which might be diminished by altering the solubility through cross-linking or complexation. According to Nayak et al., an open lattice structure (egg-box) made of alginate frequently results in porous beads and has a poorer retention capacity for medications with a high water solubility [36]. Numerous authors have developed a system to deal with the problem by ionotropically gelating alginate with Ca^{2+} ions; however, the system's swelling capacity at pH 7.4 was subpar due to the relatively strong coordination interaction between the carboxylic groups of alginate and $Ca^{2+,}$ which makes it difficult for drugs to be released into the liquid of the gastro intestinal tract [38].

The bark of the *Odina wodier* plant, in the Anacardiaceae family, is where gum odina(GO), an anionic polysaccharide, is found. It is a natural, biodegradable, nontoxic substance that costs less to produce [39]. According to reports, it is a negatively charged polyelectrolyte that is related to gum Arabic chemically and is a member of the glycuronogalactan family of polysaccharides. Prior reports on the structural compositions of the original GO and after degradation [40]. In essence, it is a polymer with d-galactose (63.7%), l-arabinose (19.5%), two types of uronic acids (11.5-17%), and one aldobiouronic acid, specifically 3-

O-(d-galactopyranosyl uronic acid)-d-galactopyranose, which is responsible for the gum's polyanionic nature. The 1,6-linked d-galactopyranosyl residue is found in the core of GO, according to the examination of its chemical makeup. A single unit side chain of the uronic acid (galactouronic and aldobiouronic acid) is linked to the C3 of this galactose residue, and the side chains are made up of singly branched galactopyranose units that are linked through C1, C3, and C6 while those that are doubly branched are linked through C1, C3, C4, and C6 in the main chain. However, C1, C3, and C5 are used to join the branching arabinose units that result from the main chain. The negative rotation of the degraded gum and its methylated product causes the bulk of the glycosidic connections to be of the -type. According to a static calculation, the molecular weight was stated to be 1.68×10^5 [41]. The safe pharmaceutical excipient GO is suggested. Mukherjee et al. recently assessed the gum's binding power by contrasting it with the conventional starch paste used as a tablet binder [42]. This investigation proved that the gum, when used in proportions noticeably less than those of starch paste, gives the formulation the necessary hardness, binding, and disintegration time. According to the rheology, the gum's aqueous dispersion displayed pseudoplastic flow [43]. A promising choice for the creation of continuous release delivery systems, according to the most recent studies, is GO.Gum odina -based systems have gained widespread acceptance as potential site-specific, controlled drug delivery tools for the colon targeting of medications among other naturally

occurring biopolymer-derived drug delivery systems [44]. In order to change the diffusion rate of the pharmaceuticals that are encapsulated, polyelectrolyte complexes between the carboxyl and amino groups have been formed in alginate and gum odina composite drug delivery studies. By electrostatic attraction, these systems enable close contact with the negatively charged mucus membrane [36]. Gum odina (GO) might be increase the bioadhesive strength to some parts of the digestive tract, such as the colon, ileum, and small intestine [45]. Additionally, an advantageous water solubility, high biocompatibility, and probiotic-boosting property in a polysaccharide prebiotic point to its potential for use in biomedical applications. It's interesting to note that gum odina is excellent for intestine-targeting drug delivery because it is unaltered in the upper gastrointestinal tract (GIT) and only destroyed by microorganisms in the lower GIT [25]. In order to extend capecitabine's half-life, achieve its intestine-targeted distribution, and control the gut microbiota for colon cancer treatment, we created a capecitabine-delivering microsphere in this study. In the colon cancer mouse model, oral treatment of capecitabine loaded formulation raises intra-tumoral capecitabine concentration while delaying drug elimination in the circulation.

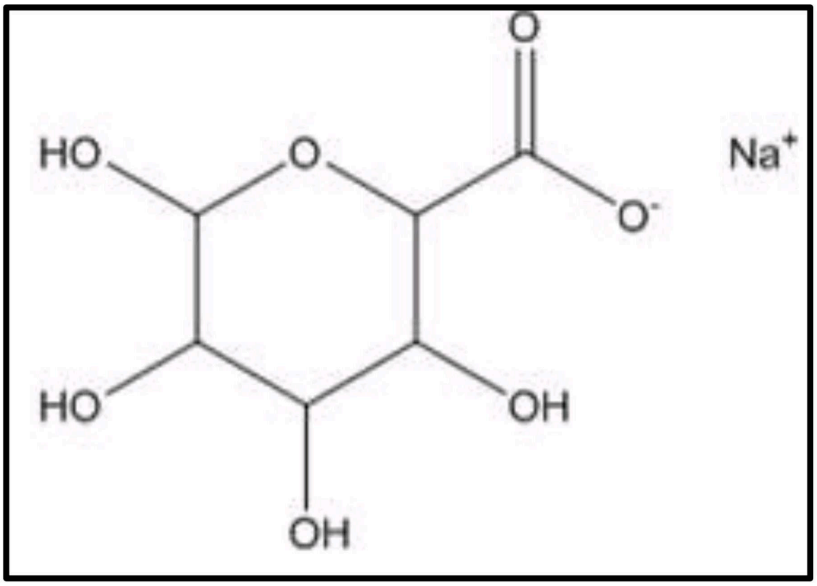

Figure 1.2 Structure of sodium alginate

Above important, these findings provided evidence that the therapeutic efficacy of capecitabine might be enhanced by a sustained release drug delivery system that can deliver a concentration above the minimal effective dose. When compared to system delivery for reducing the adverse effect, a local delivery system loaded with capecitabine for preventing colon cancer from returning after surgery may also have advantages.

Numerous techniques could be used to achieve the sustained release of capecitabine for this purpose, including spray drying microspheres or emulsion-solvent extraction, emulsion-solvent evaporation of nanospheres, and two-stage polyelectrolyte complexation of shell-core enteric coated microcarriers [35]. Among these technologies, ionotropic gelation method was frequently employed to provide long-term sustained release over the course of weeks, months, or even

years, which might significantly lower overall dose and frequency of administration, improve therapeutic outcomes, and minimize adverse effects [46].

1.14 Mechanisms of Ionotropic Gelation

Chemically covalent:

Covalent crosslinking, which develops robust chemical networks, is used in the chemical crosslinking process to produce microspheres. The main flaw is that the majority of chemical cross-linkers do not guarantee biocompatibility. Calcium chloride ($CaCl_2$) is undoubtedly the one that receives the most attention among them; it is frequently utilized as a crosslinking agent for a number of biopolymers. Among them, cellulose, gellan gum, sodium alginate, and chitosan can be recognized. For instance, polymer and calcium chloride solutions can be combined with an oil and surfactant mixture to create polymer microspheres [47].

pH-Induced:

Gelation that is pH-Induced can be produced by altering the pH of polymer solutions. Each drop of a polymer solution gels upon contact with an acidic or alkaline crosslinking medium. The shell is created during the early stage. The process of gelation is then continued by ions diffusing through the shell. [48].

Temperature-Induced:

Thermotropic or cryo-gelation are further terms for temperature-induced sol-gel transition. This technique makes use of the polymer chains' propensity to associate into a more orientated form in response to temperature, such as coil to helix and then double helix. Most of the process happens once the temperature is lowered. These helices combine to form a double helix, which subsequently gives rise to a gel network [49].

Non-Solvent:

NIPS, also known as a coagulation process or immersion precipitation, is a type of non-solvent induced phase separation. This procedure involves pressing a polymer solution in a particular solvent into a gelling bath that also contains a non-solvent. After that, the polymer's solubility suddenly drops, leading to phase separation. The polymer chains form a distinct 3D network with the non-solvent. Generally speaking, the addition of non-solvent causes the polysaccharide macromolecules to decrease. If the polymer concentration is higher than the loading concentration, its structure does not entirely collapse. There are shown schematic examples of the gelation techniques stated [50].

1.15 Importants of controlled release dosage form

Controlled release systems are promising methods to maintain the bioactive properties of molecules like polyphenols and to increase their bioavailability because these active properties must be applied to the body frequently to benefit from them due to their short half-lives and quick expulsion from the body [51]. Controlled release systems are made to avoid overdosing on the loaded dose when using conventional methods, to maintain a steady concentration of the active ingredient, or to prevent insufficiency [52].

In numerous industries, including farming, pharmacy, food engineering, medicine, and chemistry, controlled release systems are used to lessen the toxicity of medications and prevent negative effects. They are used in fertilization to manage pesticide effect zones, prevent overdosing, assure more effective use of agricultural lands, manage soil nutrient levels, and mitigate the negative effects of chemical fertilizers [53].

The active ingredient is disseminated in the particles at a molecular or macroscopic level in microspheres, which are structures made up of a continuous phase of one or more miscible polymers and have a particle size range of 1-1000 μm [54]. A technique called microencapsulation involves containing a bioactive

chemical or substances in a polymer matrix. This allows the encapsulated molecules to reach the targeted area without losing or deteriorating many of their bioactive features, such as their antioxidative action. Controlled dose forms have consistently proven to be superior to traditional or quick release versions. Microspheres have recently been tasked with regulating medications, vaccinations, antibiotics, and hormones [55].

In this study, formulations containing gum odina, a natural polymer, were utilised to create capecitabine-containing microspheres using the ionic gelation method. $CaCl_2$ was used as a complexing agent, and microsphere release tests were carried out. Analysis using SEM, DSC, TGA, AFM, NMR, XRD, and FTIR was used to describe the microspheres. HT29 cell line, Swiss albino mouse model, and DPPH technique were used, respectively, to examine antioxidant activity and anticancer activity.

CHAPTER 2

AIMS AND OBJECTIVES

2 Aims and Objective

Colon cancer is the fourth most prevalent cause of cancer-related death and the third most frequently diagnosed malignancy globally. More than 2.3 million new cases of colon cancer will be diagnosed globally, and the illness will claim 1.2 million lives. In many industrialized nations, particularly in Western countries, there has been a sharp rise in both colon cancer incidence and death as a result of changes in people's customary lifestyles and diets. Herein, to minimize this problem, we developed gum odina – sodium alginate based capecitabine loaded microsphere for effective delivery of drug to colon cancer cells with a lower dose and less systemic side effects.

The medicine capecitabine has been used extensively to treat colon cancer, but due to its short plasma half-life of only 0.85 hours and fast body clearance, it must be administered often. Additionally, the high dose of 1250 mg/m^2 that must be administered twice daily causes the most frequent overdose toxicities, such as dermatitis, bone marrow depression, cardiotoxicity, diarrhoea, nausea, and vomiting.

The term oral colon targeting system refers to a system that should control the release of therapeutic drugs taken orally until they reach the colon or cecum. Because normal cells in the upper GIT are not destroyed, local action can be applied to the sick area. This strategy reduces the drug's toxic or unpleasant effects while also enhancing its therapeutic efficacy. Most conventional drug delivery methods that target the colon failed, because, they are unable to

successfully transport the medication to the desired location in the anticipated concentration. The most difficult part of the therapy is creating a delivery system that is safe and effective for the colon.

Utilizing natural polymers in the creation of various drug delivery systems has drawn a lot of research interest over the past few decades. There are many benefits to using natural polymers, including their availability, affordability, biodegradability, and biocompatibility. One of the polyanionic polysaccharides that the FDA has classified as generally regarded as safe (GRAS) is alginate. It does have certain drawbacks, though, like an unregulated hydration rate, which might be diminished by altering the solubility through cross-linking or complexation. For the colon targeting of capecitabine, gum odina polymer was combined with alginate and gum odina to circumvent this disadvantage. Another intriguing strategy that will provide a new dimension to drug administration is the creation of polyelectrolyte complexes between gum odina and alginate. As far as we are aware, there are currently no reports on the one-step synthesis of gum odina - alginate microspheres with calcium for the delivery of functional ingredients. This has encouraged us to investigate the feasibility of creating capecitabine-targeted gum odina -calcium-alginate microsphere using a one-step approach without the need of any other harmful crosslinking agents.

The main objective of the thesis work is as follows

- To develop natural polymer gum odina and sodium alginate based capecitabine loaded microsphere by varying the concentration of gum odina and sodium alginate.
- Optimization of formulated microsphere by percentage yield, entrapment efficiency, swelling index, particle size, and *in vitro* drug release kinetic study and characterization of optimized formulation by using several instrumentation analysis like DSC, TGA, SEM, AFM, XRD and FTIR.
- Evaluation of biological characterizations of optimized microsphere through antioxidant property, hemolysis potentiality and thrombogenicity, moisture content, moisture uptake study, degradation study and accelerated stability study of optimized formulation by following ICH guideline and *in vitro* cell viability and ROS production of experimental formulation using HT29 colon cancer cell line.
- Evaluation of acute toxicity of gum odina in a rat model and therapeutic efficacy and antiproliferative activity of prepared microsphere through *in vivo* study using mice model.

CHAPTER 3

EXPERIMENTAL SECTION

3 Experimental Section

3.1 Materials used in formulation of microspheres

From August to October, gum odina (GO) exudate was collected and purified using a technique that has before been described[43]. In this investigation, GO that had been purified was employed to create microspheres. Capecitabine, sodium alginate (SA), calcium chloride were bought from Merck Specialties Private Limited, India. Deionized water (pH = 6 to 6.4) was used for all analysis purposes.

3.1.1 Collection, refinement, and measurement of the carboxyl group number of gum odina

Odina wodier, Roxb., an Anacardiaceae tropical deciduous plant from Maheshtola South 24 Parganas District in West Bengal, India, was used to make gum odina. The purification of gum odina was carried out using an already de et al. described technique [18]. In order to fully swell the sample, the crude gum odina was left in deionized water (pH of 6 to 6.4) overnight at temperature of 37˚ C. The viscous solution was then allowed to swirl continuously for up to 6 hours at room temperature using a mechanical stirrer (REMI Lab Stirrer, India). To obtain a clear solution, the brown homogenized viscous solution was filtered through muslin fabric after standing for 12 hours at room temperature (37˚ C).Thermo Scientific Heraeus Biofuge Stratos Centrifuge, Osterode, Germany, centrifuged the solution for 15 minutes at 1500 rpm. White precipitate was produced after this solution was gradually added to 100% ethanol. The precipitate was further refined using a mixture of dry ether and pure ethanol. The next day,

the purified gum odina was left to dry at room temperature(37˚C). Powdered dried, purified gum odina was kept in a desiccator for further use. By back titrating with sodium hydroxide, hydrochloric acid (HCl), and phenolphthalein as indicators, the carboxyl group of gum odina was calculated [19]. Three separate measurements of the carboxyl group in gum odina revealed a 27.86 g/L carboxyl group concentration.

3.2 Materials used in physicochemical and biological evaluations of prepared microsphere

Dipotassium hydrogen phosphate, potassium dihydrogen phosphate, sodium hydroxide pellet, sodium chloride, hydrochloric acid, DPPH (2, 2-diphenyl-1-picrylhydrazyl) were purchased from Merck Specialties Private Limited, India.

3.3 Cell culture media and reagents for *in vitro* colon cancer study

For an *in vitro* cell line research of formed microspheres, HT29 colon cancer cell line was purchased from National Centre for Cell Science (NCCS), Pune. Fetal Bovine Serum (FBS) and Dublbecco's Modified Eagle's medium (DMEM) were acquired from Gibco, Invitrogen Germany. From Promocell GMBH in Germany, MTT (3-dimethylthiazole-2,5-diphenyl tetrazolium bromide) was purchased.

3.4 Reagents used for *in vivo* anticancer study

Hematoxyline, eosin, phenol, chloroform, formaldehyde, dipotassium hydrogen phosphate, sodium hydroxide were purchased from Himedia Laboratories Pvt. Ltd. (Mumbai, India). DMH (1,2 -dimethylhydrazine), DSS (Dextran sodium

sulphate) and all other chemicals were purchased from Merck Specialties Private Limited, India.

3.5 Preparation of capecitabine-loaded gum odina-sodium alginate composite microspheres by ionotropic gelation method

Ionic gelation process was used to create capecitabine-loaded gum odina-sodium alginate composite microspheres. Calcium chloride was used as a crosslinking agent. The concentrations of capecitabine, the volume ratio of polymer to crosslinker, the flow rate, pH, light, salts, stirring time, stirring speed, sonication time, sonication power, and cryoprotectant during the ionotropic gelation process were modified to create a series of formulations. Capecitabine was accurately weighed out and added to polymeric matrix of different ratio of gum odina – sodium alginate while being continuously stirred for up to 10 minutes using a REMI Lab Stirrer from India. In all of the formulations, such as F1, F2, F3, F4, F5, and F6, listed in Table 3-1, the ratio of the drug and polymer mixes was taken to be 1:2. After preparation of the homogeneous mixture, it was added dropwise into calcium chloride solution at several concentrations (2.5%, 5%, 7.5%) via a 26 gauge needle using a syringe under continuous stirring (REMI Lab Stirrer, India) for 15 minutes at 50 rpm. The microsphere was then filtered using membrane filters with particle sizes of 0.45 μm, rinsed in water two to three times to remove any excess calcium chloride, and dried for up to six hours at 40°C. The dried microspheres were stored in a desiccator for further use. The best formulation among all the formulated microspheres was optimized based on

entrapment efficiency, swelling study, microspheres size, and drug release kinetics. The optimized formulation was further subjected to several physicochemical and biological evaluations. Antitumor efficacy of optimized formulation was assessed by *in vitro* and *in vivo* studies [56].

Table 3-1 Composition of formulated microspheres

Formulation Code	GO:SA	Calcium chloride (% w/v)
F1	1:2	2.50
F2	1:2	5.00
F3	1:2	7.50
F4	1:3	2.50
F5	1:3	5.00
F6	1:3	7.50

3.6 Optimization of formulated microsphere

Several formulations were developed by varying ratios of the polymeric mixture (GO- SA) and crosslinking agent (calcium chloride) (Table 3-1) and these were subjected to physicochemical evaluation like entrapment efficiency, swelling

study, microspheres size, and drug release kinetics to optimize the best formulation [57].

3.6.1 Optimization parameters

3.6.1.1 Drug entrapment efficiency and percentage yield of microspheres

Formulated dry microspheres approx. 20 mg were added to the mortar and pestled to test the effectiveness of drug entrapment. Crushed microsphere powder was added to phosphate buffer (pH 7.4), allowed to dissolve, and then kept at 40°C overnight. After that samples were sonicated in bath sonicator at frequency of 20 kHz (Digital Ultrasonic Cleaner, Equitron PVT. LTD., India) for 15 minutes and the absorbance of collected supernatant was analyzed by using a UV spectrophotometer (Shimadzu, Japan) at 276 nm. The formula below was used to compute the percentage of encapsulation efficiency [57] .

$$\text{Percentage of drug entrapment efficiency} = \frac{Actual\ drug\ content}{Theoratical\ drug\ content} \times 100 \ldots (1)$$

The percentage yield of microspheres was calculated using the following formula

$$\text{Percentage yield} = \frac{Total\ mass\ of\ microsphere}{\text{Total added solid component}} \times 100 \ldots (2)$$

3.6.1.2 Microspheres size

The mean particle size of microspheres was determined according to the following methodology as mentioned by Rastogi et al.[58] using an optical microscope (Olympus India Private Ltd.). A stage micrometer was traditionally used to calibrate the ocular micrometer [46].

3.6.1.3 Swelling study

A swelling analysis of all generated microspheres was conducted in order to evaluate the optimized microsphere's medication release pattern. Briefly, 20 mL of each of two petriplates containing pre-weight dried all produced microspheres (W_d) were added together with phosphate buffer (pH 7.4). Then, the petri plates were set aside for 24 hours. After using tissue paper to dry the surface of the microspheres, the swollen microspheres (W_s) were taken out of the petriplates and precisely weighed [59]. The following equation was used to obtain the swelling index's percentage:

$$\text{Swelling index (\%)} = \frac{(W_s - W_d)}{W_d} \times 100 \ldots (3)$$

W_s stands for the weight of swelling microspheres, while W_d stands for the weight of drying microspheres.

3.6.1.4 *In vitro* release kinetics study

The *in vitro* drug release profile of capecitabine from microspheres in 0.1 N HCl (pH 1.2) and phosphate buffer (pH 7.4) was measured using a USP type 1 dissolution apparatus (Campbell Electronics, India) while stirring continuously at 50 rpm. Exact weighted dried microspheres containing capecitabine were allowed to soak for up to two hours in 900 ml of 0.1 N HCl (pH 1.2). It was then maintained in a phosphate buffer (pH 7.4) for the following six hours. To keep the sink condition, the 1 ml aliquot samples were removed and replaced with new dissolving media. The samples were correctly diluted and filtered, and a UV-VIS spectrophotometer (Shimadzu, Japan) set at 276 nm was used to determine the

drug concentrations. To forecast the drug release kinetics, the *in vitro* drug release data were plotted in a variety of kinetic models, including zero order, first order, Higuchi, and Korsemeyer - Peppas [59].

3.7 Physiochemical characterization of an optimized microsphere

3.7.1 Micromeritics studies of optimized microspheres

Micromeritics studies of optimized microspheres were performed as earlier described method [60].

3.7.1.1 Angle of repose

The fixed funnel approach was used to estimate the optimized formulation's angle of repose using the following equation.

$\theta = tan^{-1} (h/r)$..... (4)

Where, θ is angle of repose, r is the radius, and h is the height.

Bulk density and tapped density

To precisely compute bulk density and tapped density, dried microspheres were placed in a 100 mL graduated cylinder, and the final volume was recorded. Bulk density (D_b) was then calculated. After that, the cylinder was mechanically tapped 100 times to determine the tapped volume and determine the tapped density (D_t).

Carr's index

Carr index and Hausner ratio were calculated using following equations:

Carr index = $(D_t - D_b) \times 100 / D_t$ ..... (5)

Hausner ratio = (D_t / D_b)..... (6)

3.7.2 Surface morphology analysis (SEM)

Using a ZEISS EVO-18 scanning electron microscope, the surface morphology and microstructure of a capecitabine-loaded optimized microsphere (F6) at a distance of 15 cm from the sample and under ambient conditions. On a metallic stub covered in double-sided tape, a sample of the improved formulation was applied, and the platinum was then added using an auto fine coater [61].

3.7.3 Atomic force microscopy (AFM)

The surface topography of the optimized microsphere was measured by atomic force microscopy (AFM) by dimension Icon, Bruker, Karlsruhe, Germany. On the mica sheet's surface with a 20 mm diameter, the sample solution of the optimized microsphere was spread out and left to air dry overnight. Using a silicon nitride probe, a sample solution of F6 was scanned at a resonance frequency of 150–350 kHz with a constant force of 0.4 N/m. Software called Pico View 1.12 was used to analyze AFM pictures [43].

3.7.4 Fourier Transform Infrared (FTIR) Spectroscopy

FTIR was used to examine any potential chemical interactions between the microsphere's component parts. The FTIR spectra of the optimized microsphere (F6) and each of its component parts (gum odina, sodium alginate, and capecitabine) was examined in the region of 4000 - 500 cm^{-1} with a resolution of 4 cm^{-1} and a scan speed of 1 cm/s using a Shimadzu 8400S FTIR spectrometer. Optimized microsphere powder sample combined with KBr to form pellets using

a hydraulic pellet press. Following that, the pellet was kept in the FTIR and crushed to obtain the samples FTIR spectra. Both the blank and drug-loaded microspheres were acquired with FTIR spectra of the individual microsphere components [62].

3.7.5 X-ray diffraction (XRD) study

Utilizing an Ultima III theta-theta gonio x-ray diffractometer filled with a K-beta filter and Cu as a radiation source, an X-ray diffraction (XRD) investigation was used to determine the crystallinity pattern of capecitabine. Each sample's XRD pattern was measured throughout a 5° to 60° scanning range. The X-ray tube was operated at 40 kV tube voltages and 30 mA tube current with Cu as the radiation source [62].

3.7.6 Thermal analysis

The Perkin Elmer instrument was utilized to assess the physical state of the improved formulation and capecitabine using differential scanning calorimetry (DSC) and thermogravimetric analysis (TGA). As a sample's physical and chemical state changes with temperature, DSC is used to determine enthalpy changes of its component parts. The sample's weight loss with steadily rising temperature was investigated using TGA. A powder sample weighing between 0.5 and 2 mg was placed within an aluminum pane, sealed, and subjected to a nitrogen purge at a rate of 30 mL per minute while being heated up by 20°C per minute for analysis[63].

The thermal kinetic study was performed for the formulated microsphere using the Coats–Redfern integral method to calculate activation energy (Ea).

Coats–Redfern model: $\ln\left[\frac{g(\alpha)}{T\text{^}2(K)}\right] = \ln\left[\frac{AR}{\beta Ea}\right]\left(1-\frac{2RT}{Ea}\right)-\frac{Ea}{RT}$ …….. (7)

Where the response mechanism for various kinetic functions is represented by g (α). The heating speed (°C/min) is. The gas constant, R, is regarded as having a value of 0.008321 kJ/mol. The frequency factor (min^{-1}) is K and A[40].

Thermodynamic study

The temperature at which the adsorption process was more impulsive was identified using a thermodynamic evaluation. Gibbs free energy (*G*) using Eq. (8), entropy (*S*), and enthalpy (*H*) were the parameters computed[64].

$$\Delta G = \Delta H - T\Delta S \ldots (8)$$

3.7.7 *In vitro* biodegradation study

A physiological media of PBS 7.4 with 0.2% (w/v) lysozyme was used to hold dried microspheres (W_0) for 28 days at 37°C [62]. Every 7 days, sample (W_t) was removed, washed with deionized water, and dried. The study was performed in accordance with Das et al., 2021[63] with some modifications to study the biodegradability and morphological stability.

$$\text{Degradation (\%)} = \frac{(W_0 - W_t)}{W_t} \times 100 \ldots (9)$$

The rate constant of optimized formulation was estimated might be fitted to a first order kinetic equation.

where C_t is the product concentration, or the degree of hydrolysis at that moment *t*. C_∞ is the concentration that corresponds to the end point and represents the total amount of digested starch., and *k* is a first order rate constant and ln ($\frac{dc}{dt}$) is the logarithm of slope [65]. Differentiation of the given equation gives

$$Ct = C\infty\ (1 - e^{-Kt})$$

This equation might be expressed in logarithmic form as follows:

$$ln\ (\frac{dc}{dt}) = ln\ (C\infty\ k) - kt$$

3.7.8 Moisture content study

The moisture content of the optimized microsphere (F6) was assessed using the technique reported by Wang et al. in 2020. About 250 mg of a dried sample of the (W_0) optimized microsphere were put in a desiccator using silica gel. Preweighed samples were used, and optimum microsphere weight (W_t) measurements were made every day until a constant weight was noticed. The following equation was used to calculate the moisture content [66].

$$\text{Moisture Content (\%)} = \frac{(W_0 - W_t)}{W_t} \times 100 \ldots (10)$$

3.7.9 Moisture uptake capacity of optimized microsphere

In order to assess the bulkiness of the microsphere caused by the presence of hydrophilic components, moisture uptake capacity was performed. Using a

saturated sodium chloride solution, microspheres were precisely weighed and deposited in a desiccator at a relative humidity (RH) of 75% and at 45℃ temperature. Periodically, the microspheres were removed and weighed to ensure a steady weight [67]. The standard deviation was calculated after the studies were completed in triplicate.

The percentage of moisture uptake was calculated by the following equation

$$\text{Moisture uptake capacity (\%)} = \frac{(W_0 - W_t)}{W_t} \times 100 \ldots.(11)$$

Where, W_0 is the initial weight of microsphere and W_t is the final weight of microsphere.

3.7.10 Antioxidant activity (DPPH assay)

The improved formulation (F6)'s DPPH radical scavenging activity was assessed using the Das et al., 2021 technique. Antioxidant release is influenced by oxidative stress. Free radicals and ROS (reactive oxygen species) produced by oxygen may cause cell death, which is crucial for preventing colon cancer. In a 96-well plate containing 100 mg of dried prepared microsphere was incubated for 8 hours at room temperature in a dark area with 4 ml of an ethanolic DPPH solution. Molecular Devices' Spectra Max microtitreplate reader was used to measure the solution's absorbance at 517 nm (A_S) [63]. The control experiment's absorbance was calculated as *Ac*.

Percentage of DPPH radical scavenging activity was estimated according to the following equation

The percentage of free radical scavenging activity (%)

$$= \frac{(A_C - A_S)}{A_C} \times 100 \ldots (12)$$

3.7.11 Haemolysis potentiality and thrombogenicity

According to the procedure described by Das et al., the formed microsphere's capacity for hemolysis was examined. Briefly, microspheres were immersed for up to 72 hours in a polypropylene tube containing 7 ml of pH 7.4 phosphate buffer saline. After incubation, PBS was removed from the sample and 1 ml of recently drawn citrate blood was added. After three hours of incubation, the tube was allowed to centrifuge (REMI RM-12C) at 2000 rpm for 15 min. After that, the supernatant was gathered to gauge the absorbance at 540 nm [63].

The Haemolysis potential (%) was obtained by Equation.

$$\text{Haemolysis potentiality (\%)} = \frac{A_{Sample} - A_{Negative\ control}}{A_{Positive\ control} - A_{Negative\ control}} \times 100 \ldots..(13)$$

Where, $A_{Sample,}$ $A_{Positive\ \ control}$ and $A_{Negative\ \ control}$ represented as absorbance of samples, absorbance of positive control and absorbance of negative control respectively.

To assess the formulation microspheres' impact on erythrocytes, coagulation, and the complement system, thrombogenecity was assessed. Before the experiment,

formulations were soaked in the PBS solution for 48 hours at 37°C. The samples were taken out of the PBS solution after incubation and replaced with anticoagulated blood. The blood clotting test was started by adding 0.02 ml of 10 M $CaCl_2$ solution, and after 45 minutes, the process was halted by adding 5 ml of water. The blood clots were preserved by adding 5 ml of a 36% formaldehyde solution, followed by tissue paper drying, and then weighing [63]. Triplicate measurements were made and the mean ± SD was recorded.

3.7.12 Stability of capecitabine loaded microspheres in simulated gastrointestinal fluids

The physical stability of the microsphere was tested using simulated stomach fluid (SGF, pH 1.2), intestinal fluid (SIF, pH 7.4), and colonic fluid (SCF, pH 6.8). In order to predict the stability research of the microsphere, 1 mL of the formulation was added to 9 mL of simulated gastrointestinal fluid and incubated for up to 2 hours in the case of SGF, 4 hours in the event of SIF, and 8 hours in the case of SCF. The mean particle size (micrometer) and outward appearance of the microsphere were assessed after the incubation period in each simulated media was complete, and these results were compared to the initial measurements taken before incubation [68].

3.8 Accelerated stability study of formulated microsphere

In order to assess the product's stability, the accelerated stability analysis of the optimized microsphere was carried out in accordance with the International

Conference on Harmonization (ICH). The accelerated stability investigation was conducted utilizing a stability chamber (THERMOLAB, Humidity Chamber) for optimized microspheres (F6) for up to six months at 40 ± 2°C and 75 % RH 5%. The improved microsphere's (F6) physicochemical stability was assessed utilizing a number of physicochemical criteria, including entrapment effectiveness, *in vitro* drug release studies, FTIR, DSC, and TGA [40]. To check the stability of the microsphere during storage, samples were taken out of the stability chamber at regular intervals. The assumed stability study plan design was shown in Table 3-2.

Table 3-2 Represents the parameters found during the stability analysis.

Points	Analysis
1	The entrapment efficiency
2	*In vitro* drug release
3	FTIR analysis
4	Thermal analysis (DSC/TGA)
5	X-ray diffraction study
6	SEM study

Table 3-3 Design of the accelerated stability study plan with the point of analysis

ICH conditions	Time period (Days)					
	0	**14**	**30**	**60**	**90**	**180**
40 ± 2°C and 75 % RH 5%	1-8	1-5	1-5	1-5	1-5	1-5

3.8.1 Drug entrapment efficiency and percentage yield

Optimized microsphere (F6) were stored under accelerated stability condition up to 6 months to detect the changes of entrapment efficiency according to ICH guidelines. The crushed powder of microspheres was dissolved in phosphate buffer pH 7.4 and kept overnight at 40°C. After that samples were sonicated (Digital Ultrasonic Cleaner, Equitron PVT. LTD., India) for 15 minutes and the absorbance of collected supernatant was analyzed by using a UV spectrophotometer (Shimadzu, Japan) at 276 nm [62]. The percentage of encapsulation efficiency was calculated by the following formula.

Percentage of drug entrapment efficiency = $\frac{Actual\ drug\ content}{Theoratical\ drug\ content} \times 100 \ldots$ (14)

3.8.2 *In vitro* release study

The *in vitro* drug release study of F6 kept under accelerated stability condition (40 ± 2 °C and 75 % RH 5%) was performed by USP type 1 dissolution apparatus. Using a buffer solution with a pH of 7.4, which mimics the pH of colon conditions, the release behavior of capecitabine from microspheres was investigated at 37°C. A common procedure involved adding samples one at a time to the buffer solution, then shaking the mixtures in the dark. Approximately 5 mL of the supernatant were removed and replaced with an equal volume of new buffer at a predetermined period. At 276 nm, the solution's absorbances were examined [62].

3.8.3 Fourier transform infrared spectroscopy (FTIR)

The FTIR study of F6 was evaluated before and after accelerated stability to find out the stability of drug within polymeric matrix. Using Shimadzu 8400S FTIR spectrometer and KBr plates, FTIR measurements were made in the 4000-400 cm^{-1} scan range [69] .

3.8.4 (DSC and TGA) Thermal analysis

Optimized microspheres (F6) were analyzed before and after completion of 6 months accelerated stability study using TGA and DSC equipment, Perkin Elmer Instrument, to obtain phase transition and weight loss preview of capecitabine

loaded optimized microsphere. Both the reference pan and the sample pan were tarred before loading the sample.

Both the sample and the reference pans were left empty after tarring. A nitrogen environment with a flow rate of 10 mL/min was introduced into the furnace after loading, and it was heated from ambient temperature to 450°C with a heat flow rate of 10°C/min [63].

3.8.5 X-ray diffraction (XRD)

Ultima III theta – theta gonio was used for the XRD investigation of F6 in order to examine the samples' structure and phase detection before and after the stability study. Cu-K radiation acting at 40 kV and 30 mA was used to irradiate the samples. At a temperature of 25°C, the diffraction patterns were acquired over an angular range of 5° to 60° with a step size of 0.05° and a dwell period of 12 s per increment [63].

3.8.6 SEM (Scanning electron microscopy)

Surface morphology has been studied using the ZEISS EVO-18 scanning electron microscope examination at 15 kV. The dried samples were sputtered with platinum and coated for 120 seconds in an argon environment prior to inspection of microsphere during 6 months storage under accelerated stability condition [62].

3.9 *In vitro* cell line study

3.9.1 Cell lines and culture

The National Centre for Cell Science in Pune, India, was where the HT29 colon cancer cell was purchased. The cells were grown in 25 cm^2 flasks of Dulbecco's modified Eagle's media supplemented with 10% fetal bovine serum (FBS), penicillin (100 U/ml), and streptomycin (100U/ml), all at 37°C in a humidified incubator with 5% CO_2. The prepared microsphere was sown over the HT29 cells in a 96-well plate for the *in vitro* biocompatibility assay. For the purpose of determining the IC50 value, cell viability, and ROS investigations, the cells were washed three to four times with PBS for 30 minutes and twice with FBS-containing DMEM [70].

3.9.2 Cell viability

In 96-well plates, 1×10^5 cells were planted, and the cells were then left to incubate for 24 hours. In the space of 2, 6, 8, 12, and 24 hours, respectively, the drug, a blank formulation, and an optimized formulation were added. Cell viability was assessed using the MTT test (3-dimethylthiazole-2,5diphenyltetrazolium bromide) after 24 hours of treatment. With various amounts of the drug, polymer, and produced microspheres at various times, a viability assay was conducted. After a 24-hour incubation period, the culture medium was taken out and subjected to a 4-hour MTT solution treatment to promote the development of formazan crystals. The formazan crystal was solubilized by gently shaking the

plates with 100 L of MTT solubilization solution DMSO and the cell after the incubation period. The optical density of the supernatant was observed spectrophotometrically at 570 nm [71]. The percentage of cell viability was measured according to the following equation:

$$\frac{Absorbance\ of\ test\ sample}{Absorbance\ of\ control} \times 100 \ldots\ldots(15)$$

The outcomes were viewed as IC50 values, which were derived by graphical representation using Graph Pad Prism InStat 3.1 software. All of the experiments were carried out in a triplicate manner.

3.9.3 Measurement of reactive oxygen species (ROS)

HT29 cell ROS generation was measured using the chemical 2′, 7′-dichlorofluorescein diacetate (DCFDA). For 48 hours, cells at a density of 1×10^5 were incubated in 96-well plates. Following incubation, cells were given free capecitabine and a formulation containing capecitabine for a maximum of 48 hours. Following trypsin-aided cell separation, cells were then rinsed in phosphate buffer solution and treated with 10 M DCFDA for 60 minutes at 37°C with 5% CO_2. A spectrofluorimeter (PerkinElmer, USA) was used to measure the generation of ROS at wavelengths of 485 nm for excitation and 530 nm for emission [72].

3.10 Animals study

The male Wistar rats (8 weeks old, weighing 200–250 g) and Swiss albino mice (6–8 weeks old) used in the animal investigations were acquired from

Chakraborty Enterprise. The Institutional Animal Ethics Committee (IAEC) of Jadavpur University in India (Ref No. JU/IAEC-22/05) approved the protocol for the Department of Pharmaceutical Technology at Jadavpur University in Kolkata, where all animals were acclimated to the laboratory environment for a week prior to dosing. The animals were fed pellet food, given access to water, and kept in a climate-controlled environment with a 12-hour light cycle, a relative humidity of 50–15 percent, and a temperature of 25 ± 2°C. To lessen the pain and suffering of animals, every attempt was made [40].

3.10.1 Acute toxicity study of gum odina

The goal of the acute toxicity study was to determine the maximum safe dose of gum odina. For 14 days, gum odina 2000 mg/Kg was administered. Before administering gum odina, the animals were fasted for a whole night. Following the recommendations of the Organization for Economic Co-operation and Development (OECD), this study was conducted on male wistar rats. All of the study's animals were kept under observation for 14 days to look for the beginning of clinical signs of toxicity, mortality, and behavioral abnormalities, as well as alterations in their physical appearance, signs of injury, pain, and symptoms of illness. Bodyweight measurements were taken before and after treatment. The animals were sacrificed 14 days after the medication was administered. Following the studies, blood samples from a cardiac puncture were collected into vials that contained anticoagulant. Hematological and biochemical analyses were performed on the blood that was drawn. The liver, heart, and kidneys were all

collected, preserved in 10% formalin, and paraffin-embedded. Tissues were cut after paraffin embedding, slides were made with hematoxylin and eosin staining, and they were then examined using an optical microscope (Magnus microscope, Chennai) to look for any noticeable morphological alterations [73].

3.10.2 Pharmacokinetic study

Swiss albino mice were divided (n=6) into two groups to determine the oral bioavailability of a single dose of capecitabine and capecitabine-loaded microspheres (30 mg/kg body weight). Blood samples were taken at various time intervals following the completion of the dosage, including 2, 4, 8, 12, 24, and 48 hours. Colon tissue was also removed, and samples were maintained at 80 °C until future use. In PBS 7.4, colon tissues were weighed and homogenized. A cardiac puncture was used to extract about 0.5 cc of blood into EDTA tubes. Serum was extracted from the blood and stored at -20°C before to analysis. Blood was allowed to centrifuge at 5000 rpm for 10 minutes. The serum was put into a container and subjected to HPLC analysis (Cyberlabs, Millbury, USA) [74]. The pharmacokinetic parameters including peak serum concentration (C_{max}), biological half-life ($t_{½}$), and area under curve (AUC) were measured. The values were expressed as mean ± SD.

3.10.3 DMH+DSS induced colon cancer in mice model

The animals were split up into four groups at random. Group I acted as a vehicle control group and was made up of the control group (n=3). Group II, often known as the positive control group, had six participants and received DMH and DSS at

a dose of 20 mg/kg body weight. After administering DMH for five weeks, 3% DSS was added to drinking water for one week, followed by another two weeks of monitoring. Group III (n = 6) began receiving DMH + DSS at the beginning of the first remission cycle and continued until the completion of the research. They also got capecitabine (30 mg/kg body weight; orally). Orally, DMH + DSS and the suspension of the optimized formulation were given to Group IV (n = 6) for up to 48 hours at a dose of 30 mg/kg body weight of the animals for up to 4 weeks [75].

3.10.4 Histopathological examination

When the therapy phase was through, the colon was removed and saline-flushed. After being cut longitudinally on a 5 m thickness, the tissues were saline-washed. These colonic sections were embedded in paraffin after being fixed in a 10% formalin solution for up to 24 hours. Then, a segment of colonic tissue was deparaffinized with ethanol and xylene, stained with hematoxylin and eosin, and subjected to histological examinations using a Magnus microscope (Chennai) to assess the existence of adenoma, polyps, hyperplasia, and colonic tissue architecture [76].

3.10.5 *In Vivo* antitumor efficacy study

Swiss albino mice were used to compare the antitumor effectiveness of capecitabine and a capecitabine loaded gum odina- sodium alginate-based

optimized formulation. For the experimental animals, changes in body weights and food intake were tracked on a weekly basis. Following a 8-week course of DMH and DSS, two groups of rats received separate 4-week courses of capecitabine and a capecitabine-loaded optimal formulation. The animals were slaughtered after four weeks, and the colon was removed and cleaned with PBS. Slide calipers were used to quantify the volumes of colon tumors. Animals receiving formulations after DMH+DSS therapy and all animals' body weight changes over the course of the trial were tracked in order to assess changes in body weight during that time and to assess the progression and regression of the tumor [77].

$$\text{Tumor volume } (mm^3) = \text{length (mm)} \times [\text{width (mm)}]^2/2 \ldots\ldots (16)$$

3.10.6 Tumor marker detection test

The tumor marker test relied on a monoclonal antibody directed against an antigen from a colon cancer cell line that had undergone metastasis. The retro-orbital plexus was used to obtain the blood sample, and centrifugation was used to obtain the serum. Using an electrochemiluminescence immunoassay equipment (Roch Modular E170 electrochemiluminescence), the blood levels of CA19-9 and CA125 were measured to examine cancer before and after treatment. For CA19-9 and CA125, the reference range was 0 to 35 kU/L respectively [78].

CHAPTER 4

RESULTS AND DISCUSSION

4 Results and Discussion

4.1 The development of microspheres

The intermolecular cross-linking between the negatively charged carboxyl group of alginic acid and gum odina and the divalent calcium chloride caused microspheres to form instantly when the polymeric mixture of sodium alginate and gum odina was introduced gradually into $CaCl_2$ solution. Capecitabine-containing freshly made formulations had a spherical, translucent, white, and elastic look. However, after they dried, the produced microspheres shrank, grew denser, and hardened; this is remarkably similar to the outcome shown in the earlier work using mucoadhesive alginate beads by Sinha et al., 2018 [36].

4.2 Percentage yield and drug entrapment efficiency

The variation in capecitabine yield between batches, which ranges from 61.29% to 86.66%, (Figure 4.1 a) may be the result of polymer agglomeration that occurs when it sticks to the beaker wall and stirrer blades during the creation of microspheres [79]. The amount of total drug actually entrapped in the microsphere was used to express drug entrapment efficiency. Due to variations in microsphere composition, the drug entrapment efficiency of various formulations ranges from 21.44 ± 0.87% to 45.91 ± 2.58% (Figure 4.1 b) [62]. It was discovered that an increase in sodium alginate concentration considerably improves drug entrapment efficiency ($p < 0.05$). This happened as a result of the

polymeric matrix's internal structure, which was extremely dense and prevented drug migration into the crosslinking solution. Once more, drug entrapment effectiveness rose with increasing cross-linking agent concentration, which stiffened the polymeric microspheres' outer layer and decreased drug leakage into the exterior phase [80].

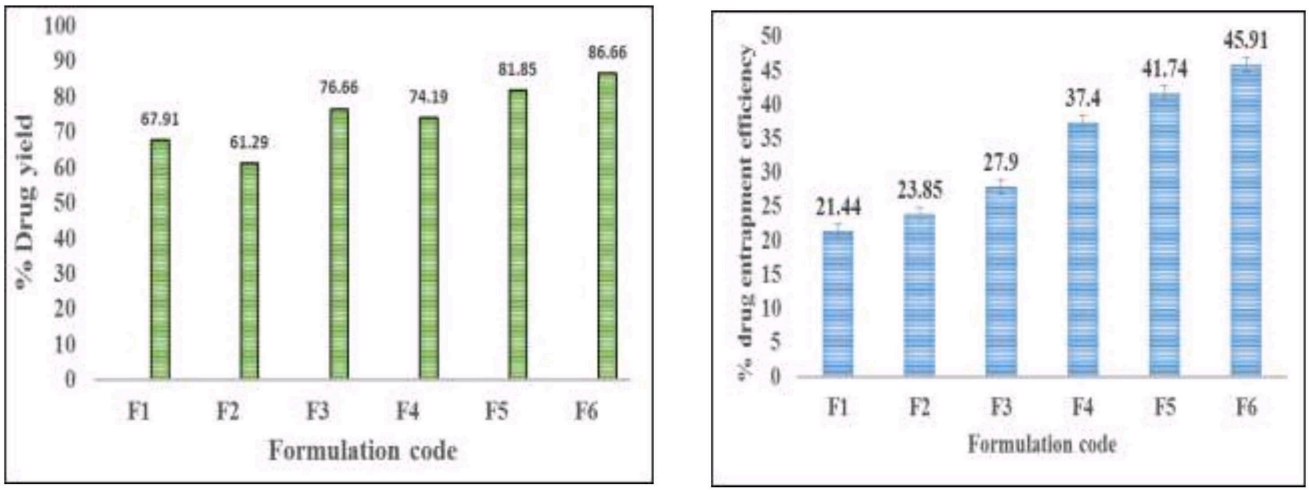

Figure 4.1 (a) % Drug yield and (b) % drug entrapment efficiency of F1, F2, F3, F4, F5 and F6.

4.3 Microsphere size

A key factor in determining drug release, biodistribution, cellular uptake, and formulation stability is microsphere size. All microspheres (F1, F2, F3, F4, F5, and F6) had particle diameters that ranged from 279.66 µm to 568.33 µm (Figure 4.2). With an increase in sodium alginate concentration in the formulations, a substantial ($p < 0.05$) increase in particle diameter was seen. The creation of a microsphere with a greater diameter may be caused by a polymeric mixture that

has become more viscous and, as a result, flows through the needle less freely. In comparison to smaller ones, larger microspheres have a higher propensity to aggregate, which leads to sedimentation. Again, during the formulation of the microspheres, smooth, spherical microspheres were produced with increasing calcium chloride and sodium alginate concentrations. Variations in the availability of binding sites for the crosslinking agent may be to blame for the outcome. Additionally, a calcium chloride solution that was too concentrated caused a decrease in the average size of the microspheres. This can be because a stronger cross-linking agent caused the polymeric gel to shrink [80].

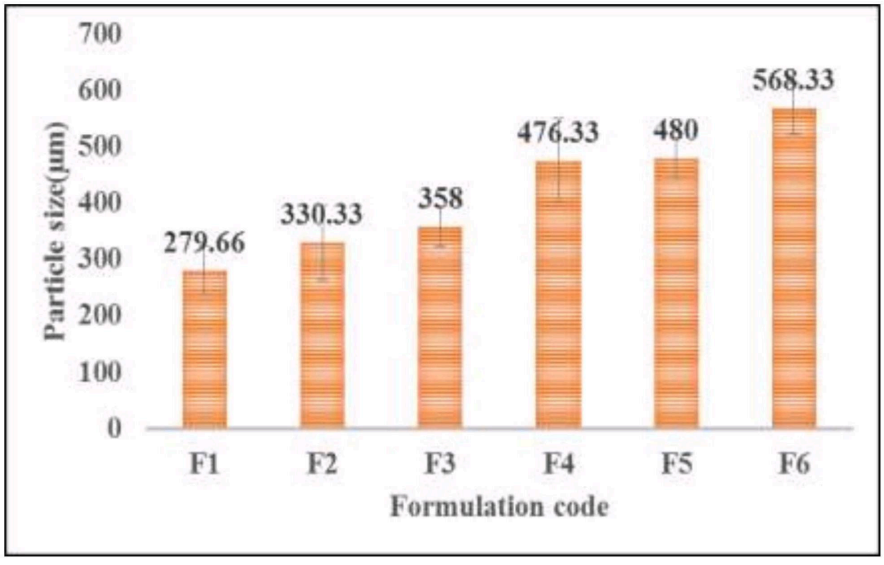

Figure 4.2 Particle size (µm) of F1, F2, F3, F4, F5 and F6.

4.4 Swelling Study

The swelling behavior of capecitabine-loaded optimized formulations were examined in 0.1 N HCl (pH 1.2) and phosphate buffer (pH 7.4). The shrinkage of alginate caused the swelling index of synthesized microspheres to be at its lowest at acidic pH, but the erosion of the polymer matrix caused the swelling index to be at its highest in phosphate buffer pH 7.4. Microspheres swelling properties were assessed in terms of an equilibrium swelling state. The outcome also showed that swelling properties were depending on the cross-linking agent concentration. It was discovered that the swelling index rose significantly ($P< 0.05$) along with the decrease in crooslinking agent concentration for formulations F1, F2, F4, and F5. Due to the stiff polymeric matrix and fewer surface pores with diameter of 2 to 6 μm open to water penetration, the formulations (F3 and F6) with calcium chloride concentrations greater than 5% had modest swelling indices [81].

4.5 *In vitro* release study

The research of *in vitro* drug release from formulated microspheres (F1 to F6) was carried out in 0.1 N HCl, (pH 1.2) for the first 2 hours, and in phosphate buffer, (pH 7.4) for the following 6 hours (Figure 4.3 (a) and (b)). Because calcium alginate is poorly soluble and shrinks at an acidic pH, the rate of drug release from formed microspheres was lowest in the physiological environment of the stomach. In phosphate buffer pH 7.4, a faster drug release from microspheres was observed, which may be related to a higher microsphere

swelling rate. The concentration of the crosslinking agent ($CaCl_2$) was also shown to affect how quickly capecitabine released from microspheres. For instance, formulation F1 with a 1:2 polymeric mixture ratio showed an initial drug release of 52.62 ± 4.16% after two hours, whereas formulation F6 with a 1:3 polymeric mixture ratio revealed an initial drug release of 36.732 ± 12.06% at two hours [36]. The findings show that as polymer concentration rises, medication release eventually slows down significantly ($p< 0.05$). In the case of microspheres made of gum odina-alginate that contain more sodium alginate, a viscous gel structure may emerge, slowing the pace of swelling and the release of the medication from the polymeric matrix. The Korsemeyer-Peppas model was used to assess the release exponent data (n) of several formulations. The findings showed that formulations F1 and F2 followed fickian transport mechanism, while formulations F3, F4, F5, and F6 followed nonfickian (anomalous transport) type ($1< n < 0.5$) (Table 4-1). In contrast to fickian release, which only followed the diffusion mechanism, abnormal transport refers to the combination of diffusion and erosion-controlled rate release [82]. According to experimental investigations, formulation F6 had the best drug release control, had an average swelling index, and had the maximum entrapment efficiency. F6 was chosen as an improved formulation to conduct additional essential studies.

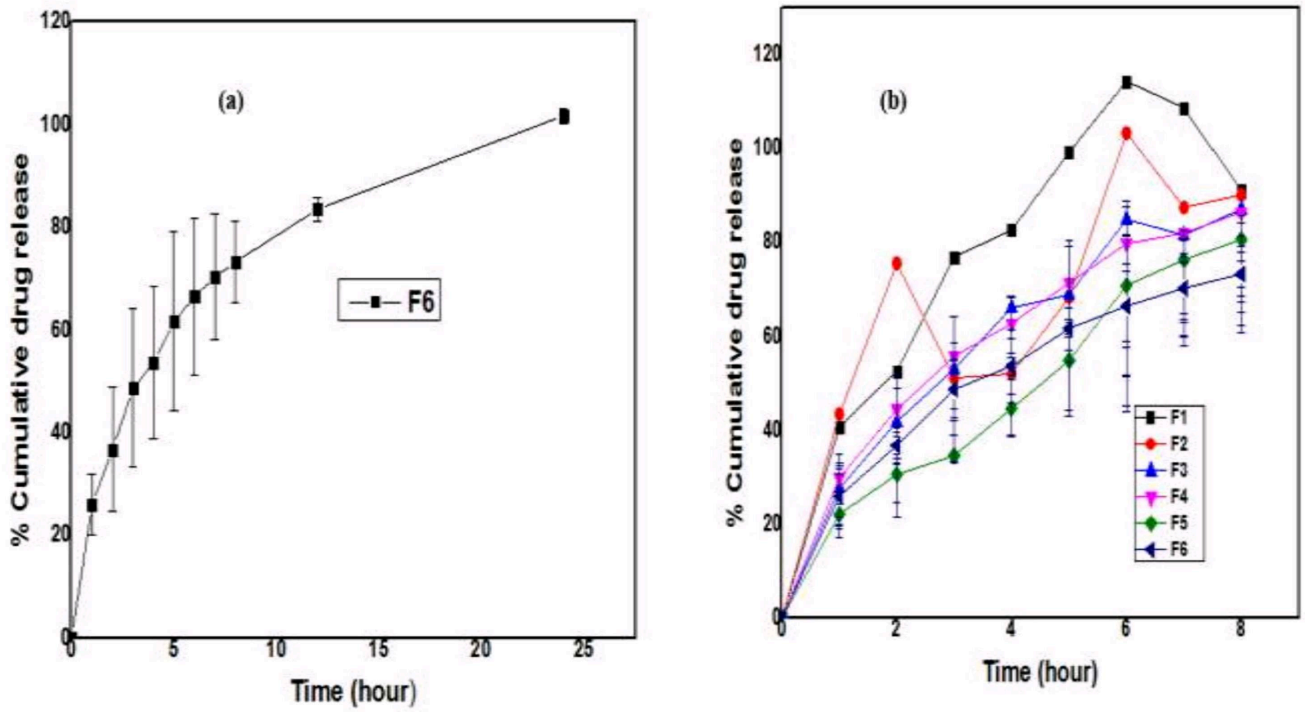

Figure 4.3 *In vitro* release pattern of (a) capecitabine from F6 at 24 hours and (b) capecitabine from F1, F2, F3, F4, F5 and F6 at 8 hours. Data are represented as Mean ± SD.

Table 4-1 Release profile of capecitabine from different formulation showing the R^2 value in different kinetics model

Formulation code	Correlation Coefficients (R^2Value)			Model of Best Fit	Korsemeyer- Peppas Model		
	Zero order	First order	Higuchi		Correlation coefficient (R^2 value)	Release exponent (n)	Release Mechanism
F_1	0.780	0.484	0.915	Higuchi	0.894	0.487	Fickian
F_2	0.687	0.444	0.797	Higuchi	0.551	0.330	Fickian
F_3	0.909	0.540	0.985	Higuchi	0.985	0.567	Non-Fickian
F_4	0.902	0.520	0.994	Higuchi	0.978	0.516	Non-Fickian
F_5	0.948	0.618	0.974	Higuchi	0.957	0.660	Non-Fickian
F_6	0.898	0.526	0.996	Higuchi	0.993	0.510	Non-Fickian

4.6 Surface morphology

Figure 4.4 (a and b) depicts the surface morphology of the F6 microsphere as seen using a scanning electron microscope (SEM) at various magnifications. The microsphere appeared spherical in the SEM images and had a rough surface with pores. The instantaneous coagulation that took place during the contact of the polymeric mixture with the calcium ions gave rise to the microspheres spherical

shape [62]. The porous structure may also be the result of the polymeric matrix shrinking. The water uptake, swelling, and release mechanisms benefit from the microspheres porous structure. The simultaneous synthesis of the matrix consisting of a polymer-blend could be to blame for the presence of some polymeric debris on the surface of the microsphere. The absence of capecitabine crystal on the microspheres surface may be due to the drugs full dispersion within the polymeric matrix. The physical condition of the medication within the created microsphere may have had a significant impact on the kinetics of the drug release [83].

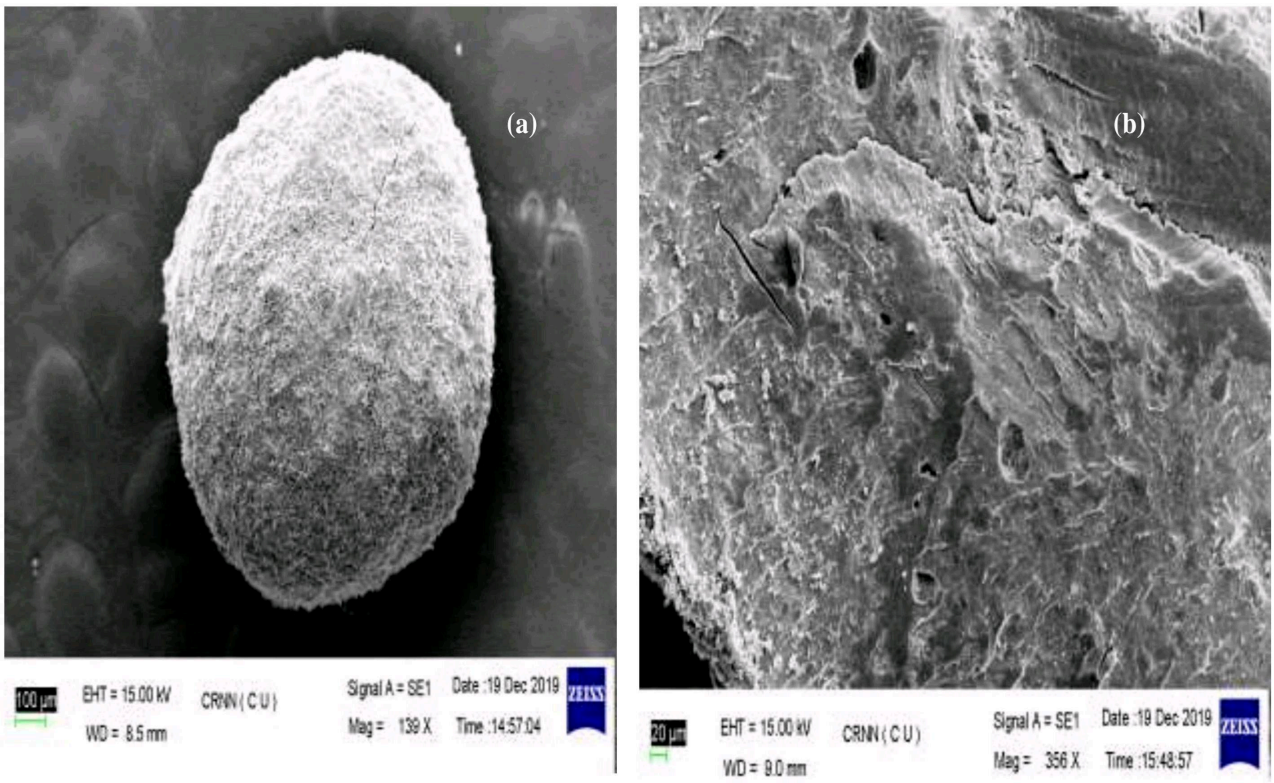

Figure 4.4 SEM images of (a) spherical microsphere (F6) and (b) pores on the microspheres surface

4.7 AFM study

The presence of the crosslinker (calcium chloride) may be responsible for the smooth, spherical surface and lack of a significant number of cervices or fissures seen in Figure 4.5 of the AFM topography images of the improved formulation [84]. AFM data also showed incredibly small particles that formed microsized clusters with amplitude values of 200Mv and a maximum height of 1m. On the other hand, the crosslinking agent decreased the matrix's porosity, normalized the surface of the microspheres, and customized the matrix's characteristics.The regulated release of the medication molecule from the microsphere to the targeted organ is likely a result of the reduction in fractures and porosity to some extent [85].

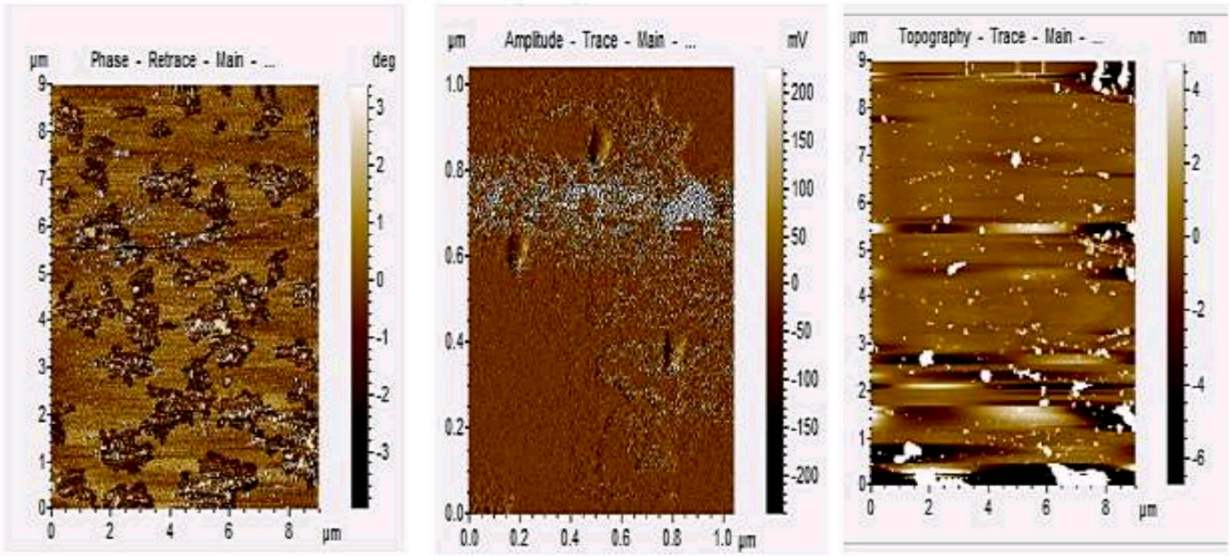

Figure 4.5 Atomic force microscopy images of F6.

4.8 FTIR spectra

Figure 4.6 displays the FTIR spectra of sodium alginate, gum odina, capecitabine, and the optimized formulation (F6). The band for the symmetric and asymmetric C-O stretching vibrations of the COO anions, respectively, occurred in the sodium alginate FTIR spectrum (Figure 4.6 a), and a large band appeared due to the OH stretching vibrations at 3441 cm^{-1}[20]. The distinctive band at 3304, 2920, and 1598 cm^{-1} in the case of gum odina (Figure 4.6 b) showed that the -OH, CH, and COO (asymmetric) were being stretched. Peaks were seen at 1413.50 cm^{-1} (CH_2 bending), 1050–1015 cm^{-1} (C–C stretching), and 1413.50–1415 cm^{-1} (OH–bending) [43]. The characteristic peaks of the pure medication capecitabine (Figure 4.6 c) were OH stretching, NH stretching, CH stretching, aldehyde group (CHO) vibrations, and CO carbonyl group of stretching vibrations, respectively. These peaks were located at wavenumbers of 3520 cm^{-1}, 3215 cm^{-1}, 2958 cm^{-1}, 2861 cm^{-1}, and 1716 cm^{-1}. Peaks at 1502, 1245, 1042, and 1202 cm^{-1} displayed NO and CN bending vibrations, respectively. C-F stretching vibrations and the tetrahydrofuran rings existence, respectively [36]. The fact that the sodium alginate, gum odina, and capecitabine characteristic peaks in the FTIR spectrum of F6 (Figure 4.6 d) did not significantly shift suggested that mixing drug molecules with other formulating agents did not significantly alter the individual characteristics of the components[62]. Since the chemical makeup of the drug was preserved during microsphere formulation, it can be deduced from the FTIR

data that there was no potential chemical interaction between the drug candidate and polymeric mixture. As a result, the microsphere formulation is sufficient to deliver the target molecule to colon for prevention therapy.

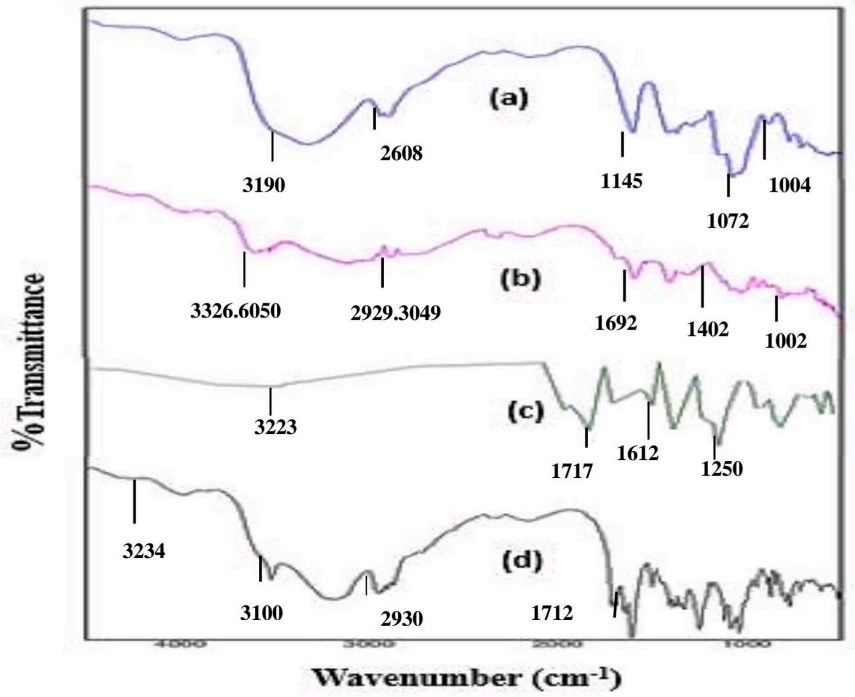

Figure 4.6 FTIR spectra of (a) gum odina, (b) sodium alginate, (c) capecitabine and (d) F6

4.9 X-ray diffraction (XRD)

Figure 4.7 (a and b) shows the X-ray diffraction pattern of the drug and drug-loaded microsphere (F6). Capecitabine showed crystalline characteristics with strong, dramatic peaks at 2θ of 5°, 20°, and 25° [86]. The absence of the drugs distinctive crystalline peaks in formulation (F6) may be the result of capecitabine

gradually becoming amorphous after being trapped inside a polymeric matrix. Capecitabine's hygroscopicity, dissolving rate, solubility, and bioavailability all increased dramatically when the drug's crystalline form was changed to an amorphous one at the desired side of action (the colon) [87]. Further, the XRD results were analysed and interplanner spacing (d), interchain separation (r), microstrain (ε), dislocation density (δ), distoration parameters (g) have been calculated and found to be which can be can be comparable to be which can be comparable to standars of the excipients used in drug delivery systems represented in Table 4-2

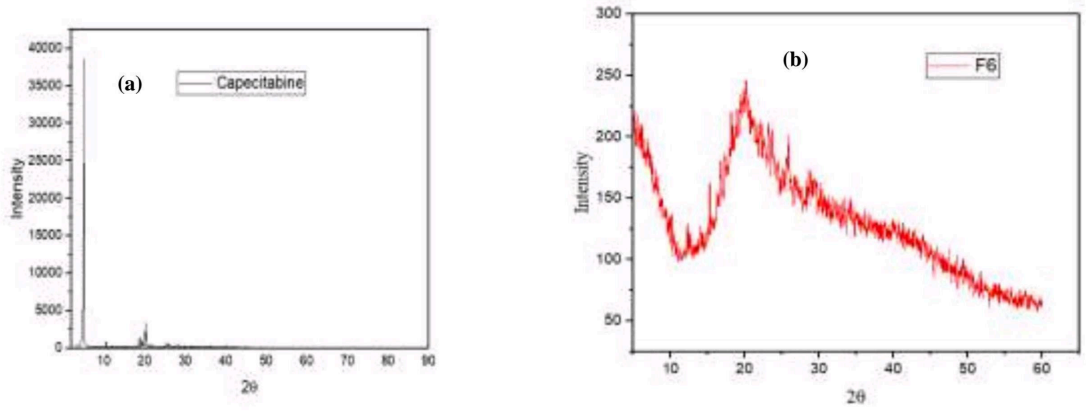

Figure 4.7 X-ray diffraction study of (a) capecitabine and (b) F6

Table 4-2 XRD interplanner spacing (d), interchain separation (r), microstrain (ε), dislocation density (δ), distoration parameters (g)

Formulation Code	Crystallinity size D (nm)	Interplaner spacing d (Å)	Interchain separation r (Å)	Distoration parameters g (%)	Dislocation density δ (nm^{-2})	Crystallinity index CI (%)	Microstrain ε (10^{-3})
F6	0.2477	4.435	5.54	0.99	16.28	16.65	1.38

4.10 Thermal analysis

The shape and appearance of capecitabine and capecitabine-loaded microsphere were analyzed using DSC studies. The sharp endothermic peak of capecitabine showed at 121.9 °C and it was corresponding to the melting point of capecitabine (105–120 °C) [33]. But, this peak was absent in gum odina and sodium alginate-based formulation, this might be due to the drug's total entrapment in the polymeric matrix and the drug's transformation from crystalline to amorphous state (Figure 4.8 (a) and (b)). Capecitabine and formulated microsphere were evaluated by performing TGA studies which represented the weight loss of the sample for temperature (TGA thermogram of capecitabine showed 7.23 % weight loss at 132.21°C which was raised to 29.38% at 178.04°C, 53.57% at 289.39°C and 75.78% at 493.74°C. In the case of Capecitabine loaded formulated

microsphere exhibited weight loss of 7.45% at 87.63°C that was raised gradually with successive rises in temperature i.e. 23%, 46%, and 70% at temperatures 239.10, 302.67, and 402.43°C, respectively (Figure 4.9 (c) and (d))[86]. This result displayed that total weight loss in the case of formulated microspheres was less than observed for capecitabine. Hence, capecitabine-loaded gum odina and sodium alginate-based polymeric matrix was proved to be more stable at higher temperatures as compared to free drugs [64]**.** The mechanical and thermal stability of the capecitabine-loaded optimized microsphere must be greater than that of the individual polymer components, and thermal kinetic analysis may be a reliable method of verifying this. TGA analysis was used to determine the activation energy of the improved formulation at various heating speeds. The TGA curve's peak form and location differed from those of the free drug, which may be due to calcium chloride-assisted crosslinking. By multiplying the slope value by the gas constant (R = 8.314 J/mol K) and activation energy was found. For optimized formulation, the activation energy is graphically depicted as a function of conversion degree (α). The optimized formulation's Ea value (55 KJ/mol) started out at its maximum and fell as increased, reaching a minimum at 0.6 before increasing further [64]. Due to optimized formulation's strongly crosslinked structure, which prevented random decomposition in favor of organized decomposition with rising values, this observation was made. optimized formultion's fixed increment and varied activation energy pattern at each value suggested that they were more thermally and mechanically stable. The

change in energy within a system under a constant pressure is revealed by enthalpy. Independent of the path, enthalpy change depends on the internal state. the ΔH value -24.1106 KJ/mol produced in a capecitabine-loaded, optimized microsphere at a heating rate of 30 k min^{-1}. Where endothermic reactions take place, the enthalpy changes that occur during thermal deterioration are negative. An entropy increase reveals the degradation happens in a spontaneous manner. The 5FU encapsulation method based on chitosan was used to characterize this phenomenon, and Krimidost, S. et al[64]. showed that at temperatures above 25 °C, the spontaneity of the process decreased. As a result, 25 °C was selected as the temperature at which to continue evaluating the gum odina- sodium alginate based polymeric matrix's ability to be used as a material for the encapsulation of capecitabine. Based on the observation that a stable monolayer of the drug formed on the surface of the biomaterial at this temperature, this was thought to be the most spontaneous mechanism [116].

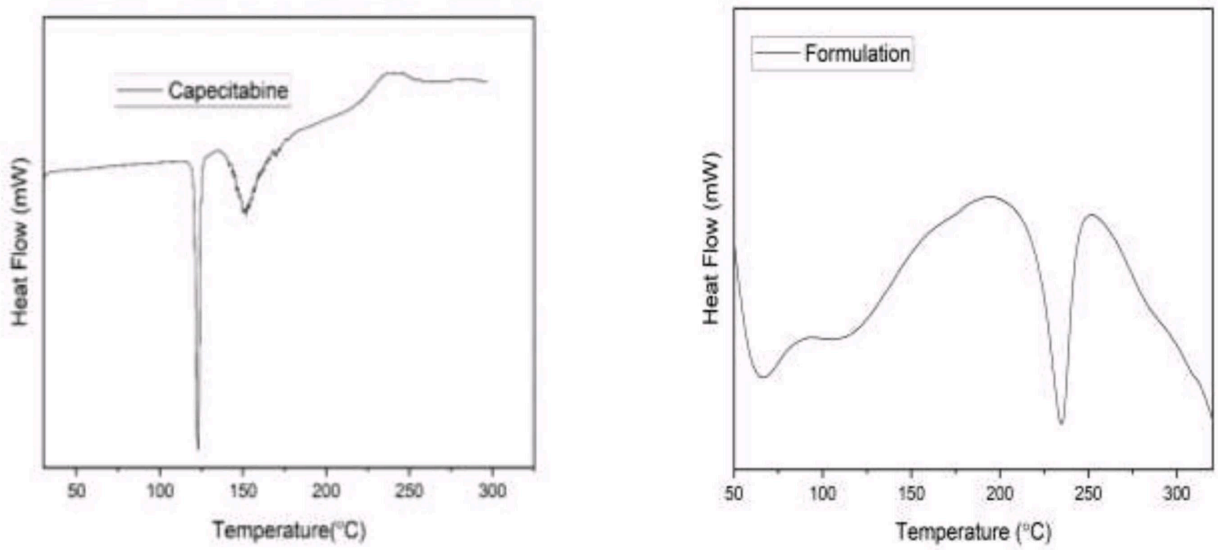

Figure 4.8 DSC of (a) capecitabine and (b) F6.

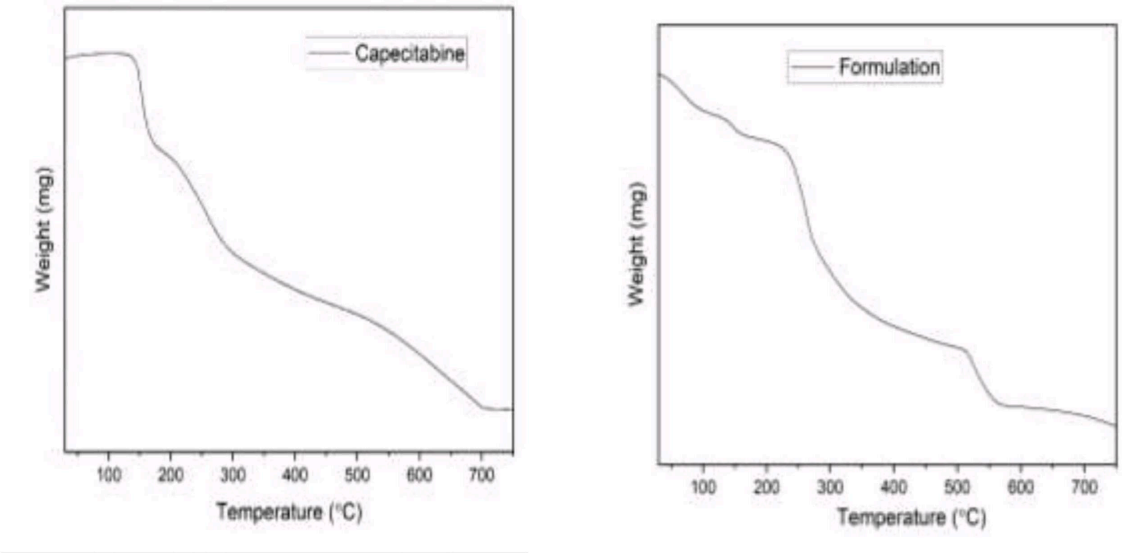

Figure 4.9 TGA of (c) capecitabine and (d) F6.

4.11 *In vitro* biodegradation study

After incubation in PBS 7.4, an *in vitro* biodegradation investigation of the optimized microsphere was conducted to determine morphological stability and biodegradation. After 7, 14, and 28 days, respectively, the formulation F6 showed degradation of 11 ± 0.74%, 22.45± 0.023%, and 35.55 ± 0.20% (Figure 4.10). The results indicated that the optimized microsphere in PBS 7.4 degraded during a regulated period of time up to 28 days [63]. Due to the microspheres wide surface area and porous structure, which allows it to absorb liquid and swell while also causing the outside polymer matrix to deteriorate, the decreased weight of the microsphere at PBS may have been caused by biodegradation of the polymeric matrix (gum odina, sodium alginate). The results of an *in vitro* biodegradation investigation showed that the amount of crosslinking agent in the polymeric mixture tends to slow down the deterioration of the microspheres by preventing their rapid erosion [62]. Biodegradation of the microsphere at the colon's location (pH of about 7.4) is confirmed by the constant deterioration at pH 7.4 [88]. As a result, polymeric microspheres made of gum odina-sodium alginate and loaded with capecitabine are widely used as effective biodegradable formulations for colon-targeted drug delivery systems. The formed microsphere had a degradation rate constant of 0.0083 min^{-1} and a degradation percentage of 48.03% up to 24 hours. First-order kinetics were followed by the biodegradation curve [89]. The crosslinking agent concentration in the polymeric mixture, which

tends to slow down the quick erosion of the microspheres and hence delay their release, has caused the rate of degradation to occur in a steady way.

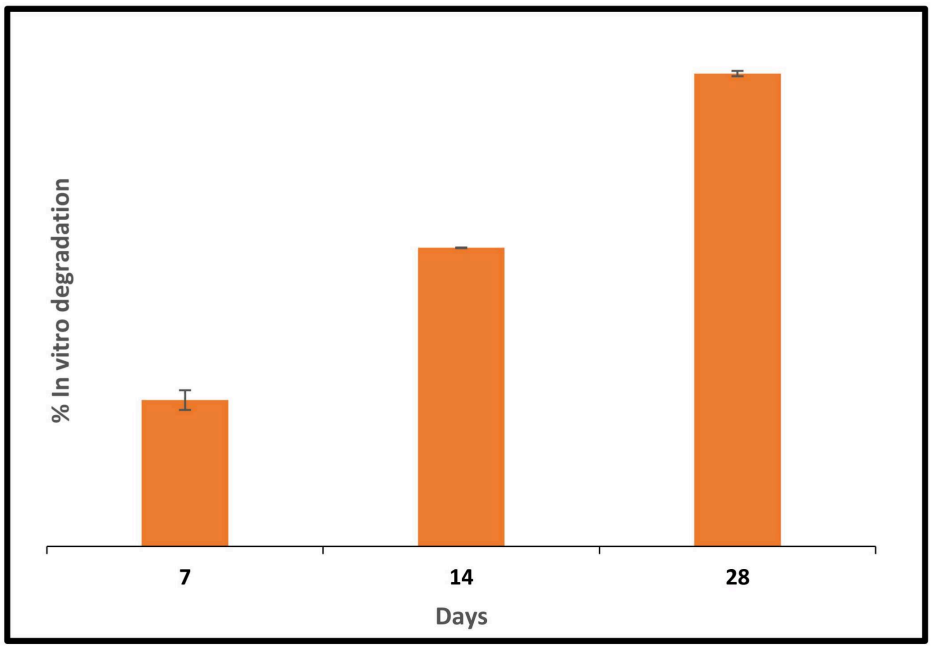

Figure 4.10 The *in vitro* biodegradation activity of F6 at varying time intervals.

4.12 Study of moisture content

The optimized microsphere (F6) displayed a moisture content (%) of 9.92 ± 5.38%.According to Sander et al., [90] the moisture content of microspheres is typically under 10%. The formulation's high moisture content causes particle agglomeration, which lowers the stability of the microsphere and its active ingredients.Since water was used in this work as a medium for chemical reactions, ordinarily low moisture contents should be extremely desirable since they may prevent drug degradation, hinder interparticle cohesiveness, and preserve long-term stability [63].A specific level of moisture content in the

microspheres can keep them from becoming dry and brittle and can also increase their stability.Gum odina and sodium alginate, which are hydrophilic formulating ingredients, may have had a substantial impact by moistening the microspheres and preventing them from breaking [62]. De et al., previously revealed that gum odina has a low moisture content value [43], indicating that it may have use as a carrier for medications that are sensitive to moisture. Additionally, the presence of sufficient water molecules on the surface of the microspheres enabled improved flow and wetting characteristics of the particles, which in turn accelerated the process of medication dissolution [91].

4.13 Moisture uptake study

A crucial factor in the investigation of drug targeting for the prevention of colon cancer is the evaluation of the water uptake of formed optimized microspheres. Increasing the levels of water uptake in optimized microsphere upto 22.37% in six hours. This outcome was attributable to capecitabine's sustained release from the polymeric matrix over a protracted period of time [67]. This protracted release pattern of capecitabine from a polymeric matrix may have been made possible by the development of a compact wall, which slows the drug's quick decomposition from the matrix. The two polymers might establish a bond and be cross-linked using calcium chloride to create the compact wall [92]. The degradation of capecitabine-loaded gum odina and sodium alginate-based microsphere occurred at a pH of 7.4 PBS rather than 0.1(N) HCl, according to a swelling investigation

of an improved formulation. This suggests that the improved water uptake capacity at the highest pH value may be due to enhanced formulation [93]. Similar results were seen in the water uptake behavior of the semi-interpenetrating gelatin-DNA polymer network at various pH levels, as reported by Liu et al [94].

4.14 Antioxidants (DPPH test)

DPPH scavenging activity was used to gauge the improved microsphere's antioxidant capacity. After 2, 4, 6, and 8 hours, the DPPH assay of F6 revealed scavenging rates of 40.58 ± 1.46%, 46.16 ± 0.16%, 83.51 ± 0.44%, and 88.13 ± 0.771%, respectively (Figure 4.11) [40]. Data were presented as the mean SD of three independent measurements. Microsphere's anti-oxidant action may be a result of formulation elements such gum odina[69] and sodium alginate[95]. According to Das et al.,[96] an excess of oxidative stress results from a lack of antioxidant systems. Numerous pathogenic conditions, such as inflammatory disorders, cancer, and cardiovascular diseases, have been linked to oxidative stress. Antioxidants help prevent chemotherapy by decreasing the growth of cancer [62].

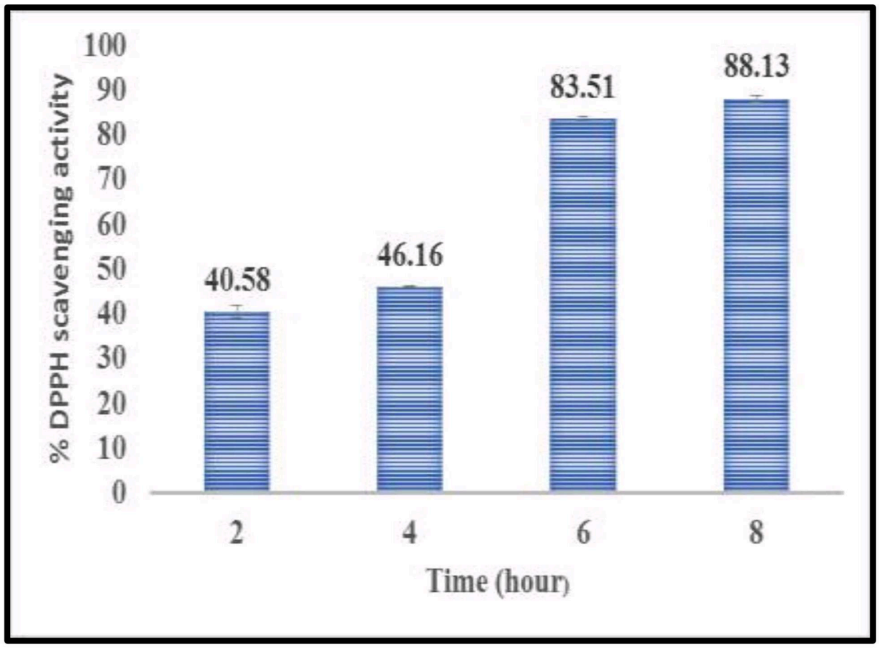

Figure 4.11 The antioxidant activity of F6 at varying time intervals. Values were represented as mean ± SD in triplicate.

4.15 Haemolysis potentiality and thrombogenicity

According to ISO specification 10993-32002, 4.55± 0.92%, which is regarded as a safe number for a biocompatible material, was determined as F6's hemolysis potentiality. The hemolysis potential value of 4.2 ± 0.2% of a gum odina-gelatin based antimicrobial loaded biodegradable spongy scaffold was already reported by Das et al. to be pretty similar to the hemolysis potentiality of F6. Therefore, these manufactured microspheres are regarded as suitable for use in drug delivery systems. The polymeric matrix displayed a thrombose percentage of 63.92 ± 7.24%, indicating that it is not thrombogenic [63]. Because the thrombus formation is slower and smaller than the control, our results suggested that this microsphere might be categorized as non-thrombogenic material [97].

4.16 Capecitabine-loaded microspheres capacity to remain stable in simulated gastrointestinal fluids

To determine the potential value of an improved formulation for delivering capecitabine to the colon, a stability investigation of the capecitabine-loaded microsphere in the stimulated gastrointestinal fluid was conducted. At the end of the storage time, the improved formulation's physical characteristics and particle size had somewhat changed. No appreciable difference ($P>0.05$) in particle size between the optimized microsphere and the formulation's pre-storage particle size (496.8 ± 1.35 μm) was seen when the microsphere was incubated in gastrointestinal fluids [98]. After being incubated in simulated gastrointestinal fluids, the optimized formulation's physical characteristics and particle size showed little changes, suggesting that the formulations may be stabilized gastrointestinal fluids.

4.17 Stability study

The entrapment efficiency of the optimized formulation (F6) after 6 months was found to be 42.92 ± 1.30%, which might be similar to the value of the freshly prepared formulation (49.5 ± 2.58%). No significant difference ($p > 0.05$) in drug entrapment efficiency was observed between the freshly prepared microsphere and the 6 months storage-formulated. The result of the percentage cumulative drug release (Figure 4.12 (a) and (b)) of capecitabine from freshly prepared microspheres was 73.27 ± 7.97%, and after 6 months' storage, microspheres

exhibited mostly similar results with a small amount of variance (87.49 ± 6.74%) [62]. This variation might have occurred due to the formation of fractures or voids on the surface of the microsphere. From this result, it could be predicted that the elevated temperature does not affect the integrity of the microsphere.

From the FTIR analysis study, we might conclude that the optimized formulation during the storage period of 6 months did not exhibit any shifting or disappearance of the characteristic peak. In the FTIR study, peaks of capecitabine were observed at a wavenumber of 3520 cm^{-1}, 3215 cm^{-1}, 2958 cm^{-1}, and 2861 cm^{-1}, and at 1716 cm^{-1}, which indicated OH stretching, NH stretching, CH stretching, aldehyde group (CHO) vibrations, and CO carbonyl group stretching vibrations, respectively, which was similar to our previous study of capecitabine-loaded biopolymeric vehicles for the treatment of colon cancer. Peaks at 1502 cm-^{1}, 1245 cm^{-1}, 1042 cm^{-1}, and 1202 cm^{-1} showed NO bending vibrations and CN bending vibrations. C-F stretching vibrations as well as the presence of tetrahydrofuran rings. Optimized formulation under storage conditions showed various characteristic peaks of capecitabine at 1245 cm^{-1}, 1042 cm^{-1}, and 1202 cm^{-1} due to the presence of NO bending vibrations and CN bending vibrations. C-F stretching vibrations that might be completely similar to the peaks of freshly formulated microspheres (Figure 4.13 (c) and (d)), which presented the stability of drug molecules within microspheres under storage conditions [62].

The shape and appearance of the capecitabine-loaded microsphere were analyzed before and after 6 months using DSC studies. The sharp endothermic peak of the capecitabine-loaded formulation did not exhibit a peak at 121.9 °C, and it corresponded to the melting point of capecitabine (105 –120 °C). But, this peak was absent in gum odina and sodium alginate-based formulations before and after the 6-month storage period. This might be due to the complete entrapment of the drug in the polymeric matrix and the conversion of the crystalline form to an amorphous state (Figure 4.14 (e) and (f)) [62].

In the case of TGA analysis, there was a slight shifting of the TGA curve observed in the optimized formulation (F6) before and after storage, which might have occurred due to the presence of moisture. In the TGA curve of capecitabine, this first stage of thermal degradation and weight loss occurred at 137 °C, and about 7.5% of it might be water evaporation, which was raised to 43% at 174.35°C, 54% at 302 °C, and 75% at 694°C. In the case of optimized formulation F6, after storage conditions, initial weight loss was 7.96% at 219°C (Figure 4.15 (g) and (h)), which was enhanced steadily with successive increases in temperature, i.e., 21.82%, and 60% at temperatures 515 and 567.86°C, which might be almost analogous to the freshly prepared microsphere. Hence, in the case of total weight loss in optimized formulation before and after storage conditions, 60% was above 567.86 °C, which was very low in the case of capecitabine. This result revealed that after the encapsulation of capecitabine into a polymeric matrix, thermal

stability increased before and after storage conditions by shifting the denaturation temperature to a higher value [99]. Hazra et al. have already reported that capecitabine exhibited sharp, intense peaks at 2θ of 5°, 20°, and 25°, indicating the crystalline nature of the drug. The XRD study of figure 4.16 ((i) and (j)) showed that the prepared microsphere did not display crystalline peaks of the drug before and after 6 months of the formulation. Despite the above studies, the analysis of surface morphology played a key role in the stability study as drugs tend to convert from an amorphous to crystalline nature in the formulation during storage conditions, which probably obstructs the *in vitro* drug release pattern [62]. SEM photographs Figure 4.17 (k) of the microsphere having a spherical shape and a rough surface with pores. The microsphere's porous structure makes it ideal for mechanisms that cause water to be absorbed, swell, and be released. The absence of capecitabine crystals on the microsphere's surface may be due to the capecitabine being evenly distributed throughout the polymeric matrix. In terms of drug release kinetics, the physical condition of the drug in the formed microsphere may be quite important. From SEM study we concluded that there was no confirmation of crystals of drugs either in freshly prepared F6 or formulations stored under storage conditions for up to 6 months [62].

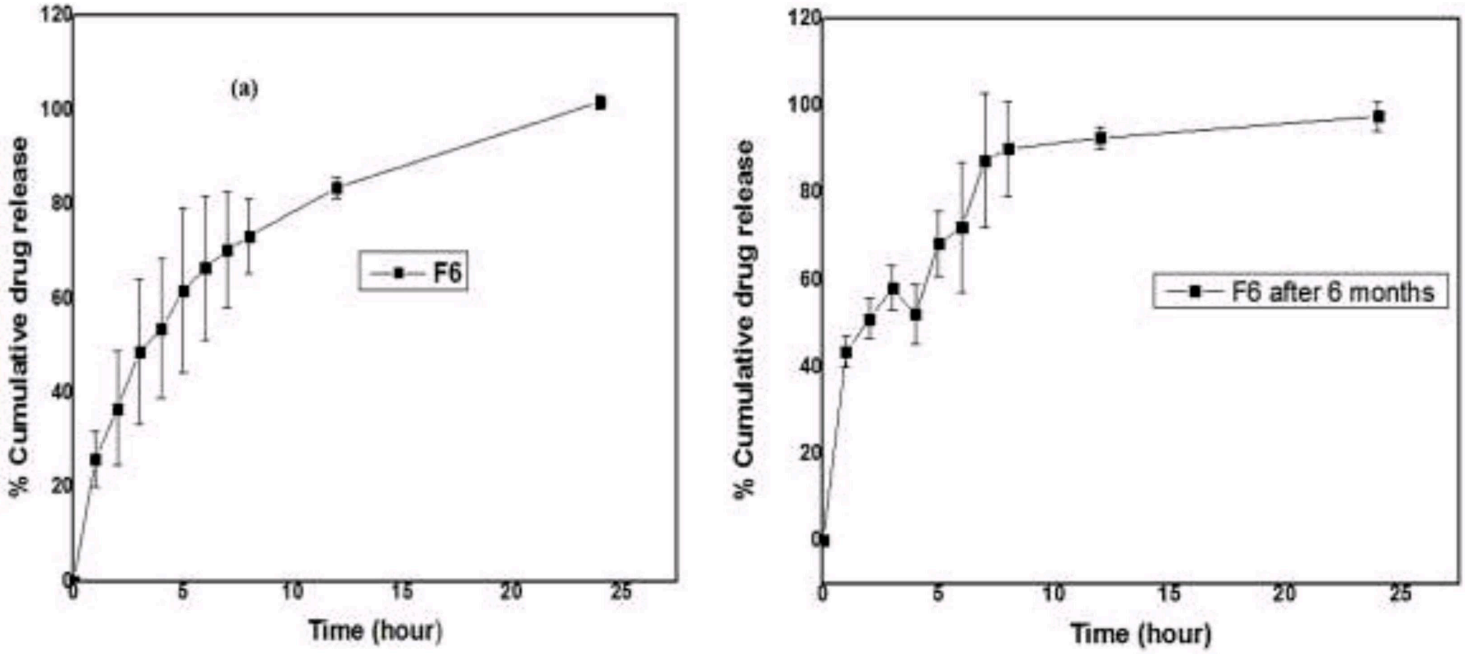

Figure 4.12 (a) *In vitro* drug release profile of (a) capecitabine at initial day and (b) after 6 months storage.

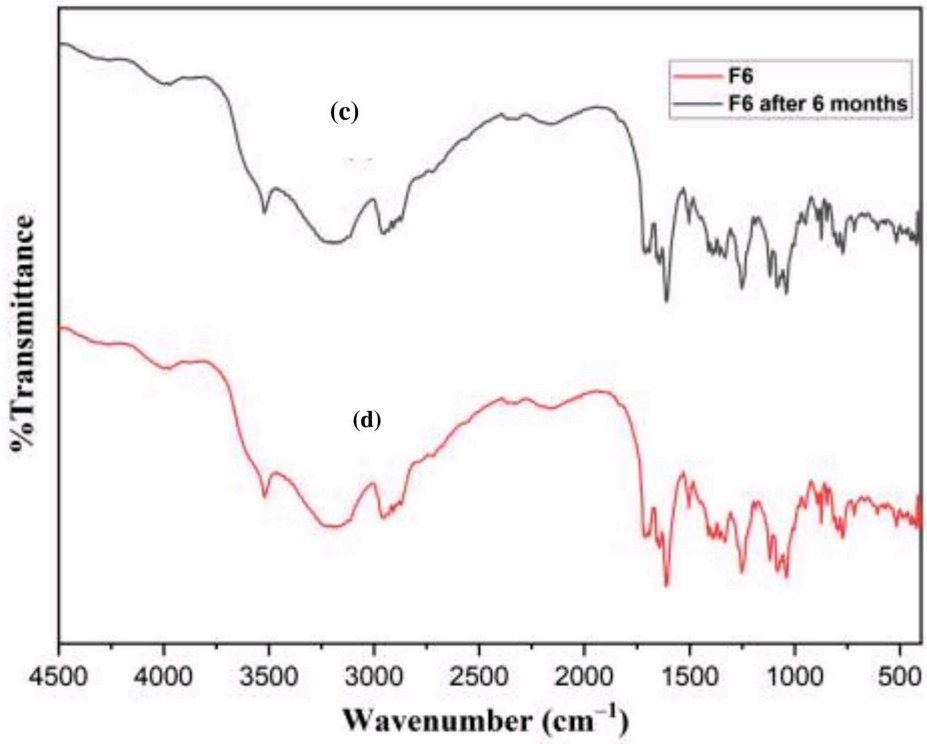

Figure 4.13 The FTIR results demonstrate the existence of characteristic peaks of (c) capecitabine of 6 months stored in F6 as (d) similar to the freshly prepared microsphere.

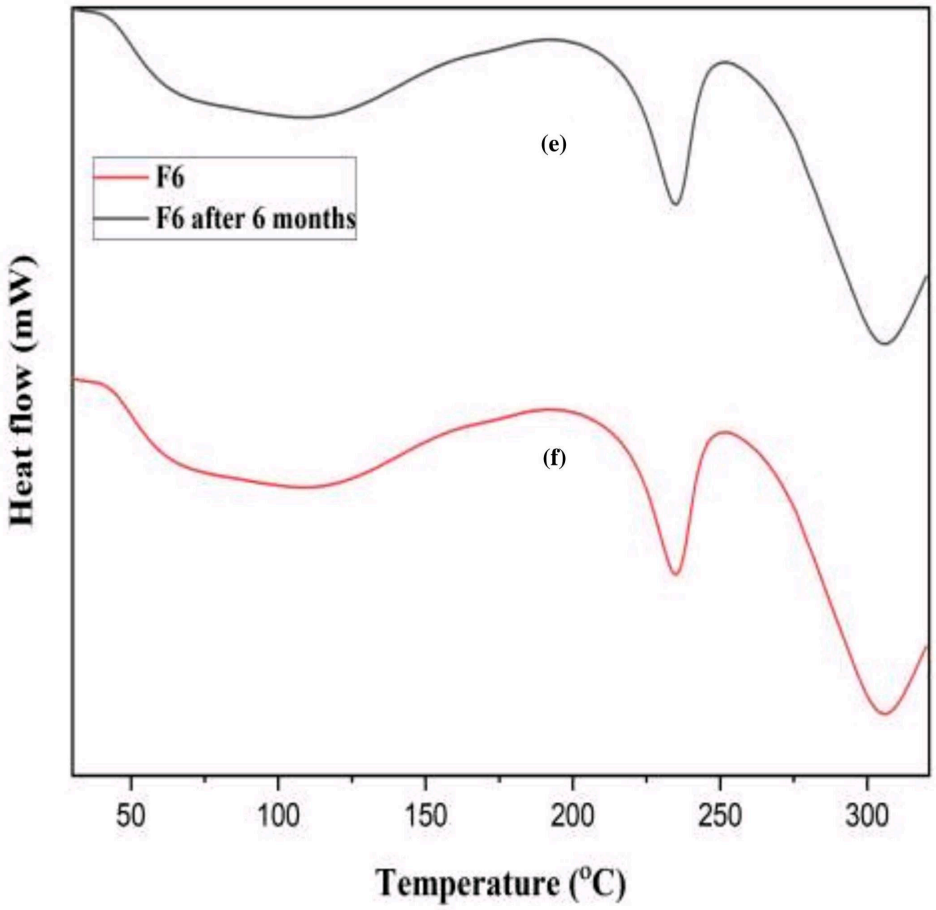

Figure 4.14 The DSC thermogram of (e) F6 at the initial period and (f) F6 after 6 months of storage

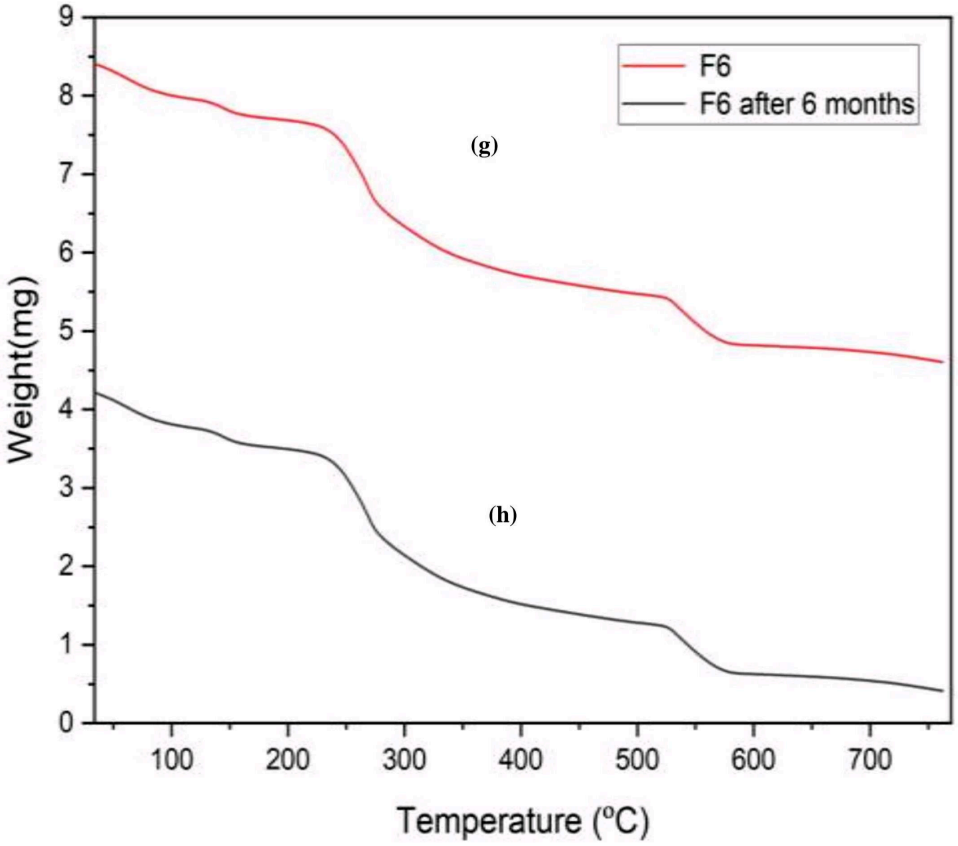

Figure 4.15 The TGA thermogram of (g) F6 at initial period and (h) F6 after 6 months storage

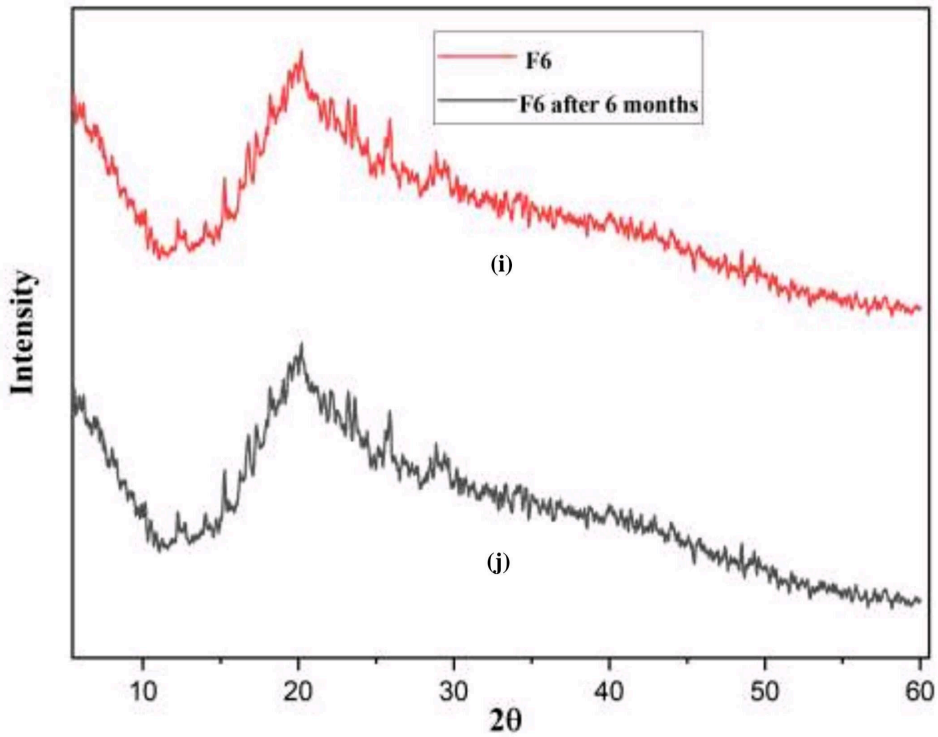

Figure 4.16 XRD diffraction study of (i) F6 at 0 months and (j) after 6 months storage

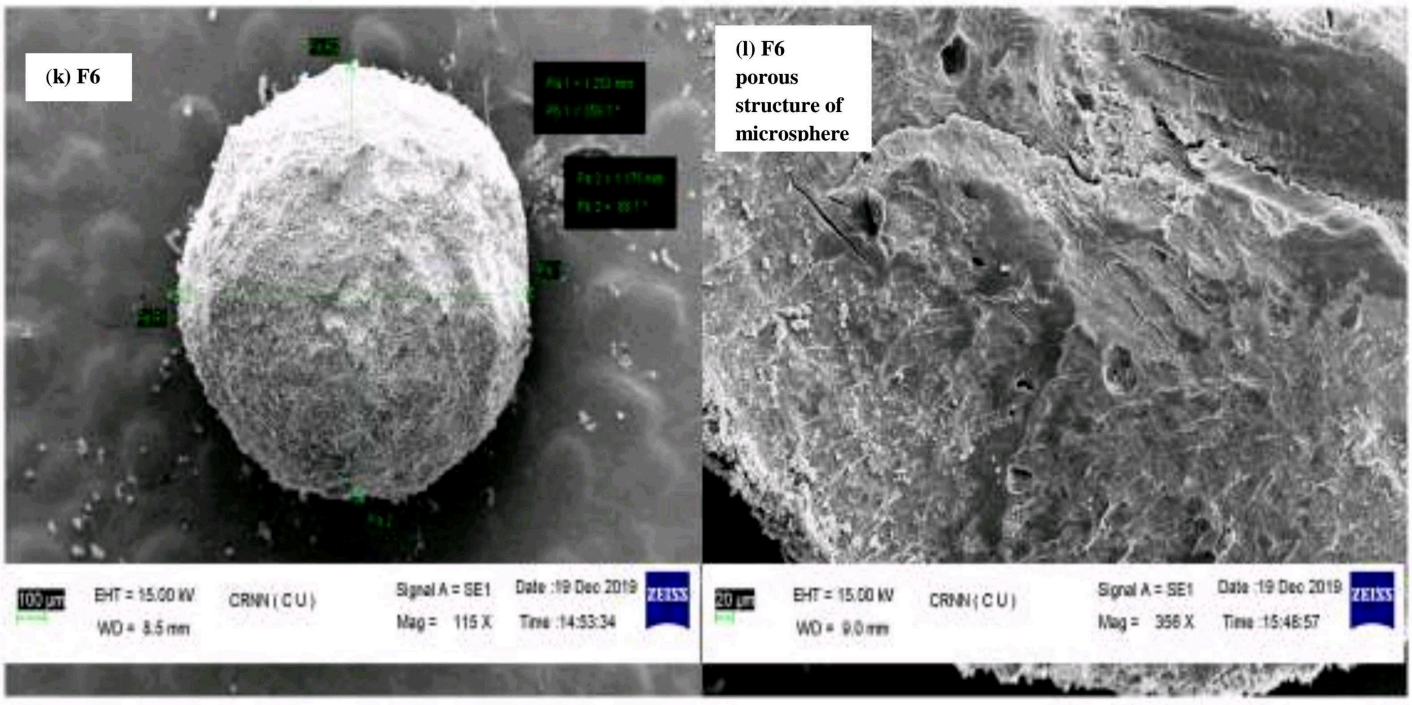

Figure 4.17 SEM study shows the morphological stability of the F6 microsphere. The SEM image of (k) freshly formulated F6 and (l) porous structure of microsphere

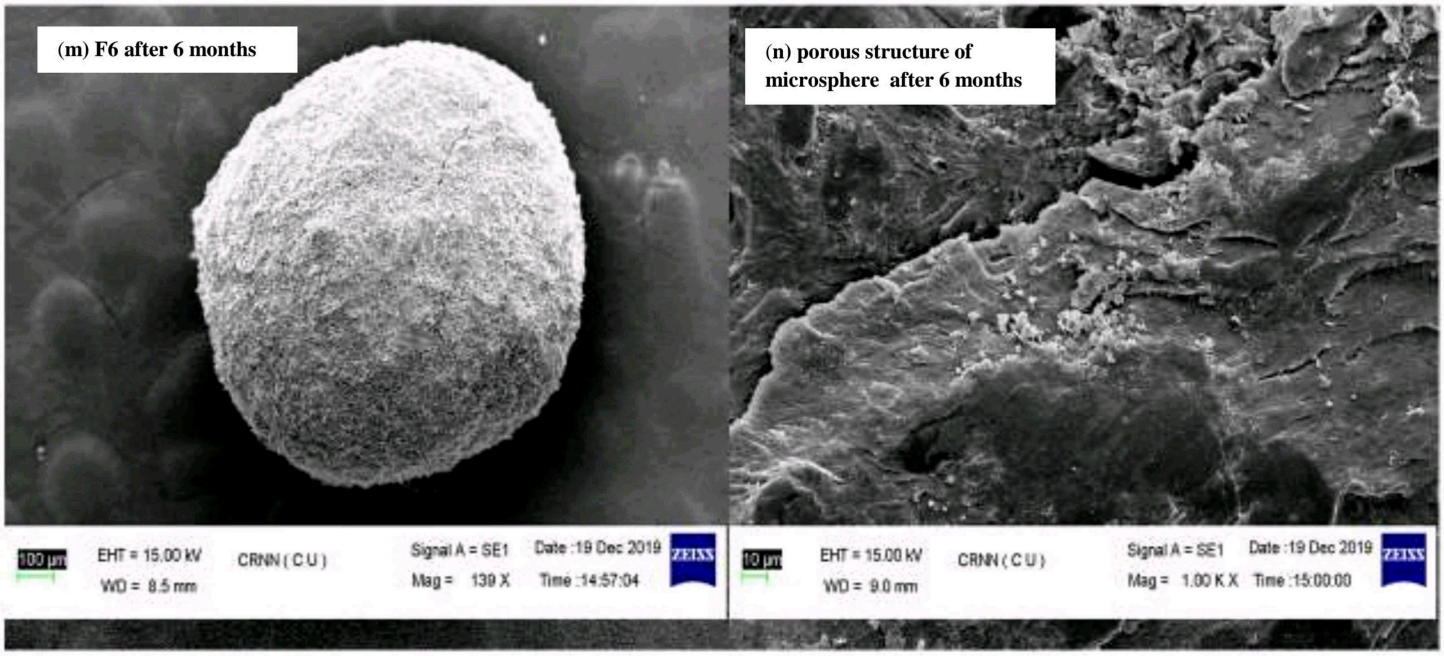

Figure 4.18 SEM study shows the morphological stability of the F6 microsphere. The SEM image of (m) formulated F6 after 6 months storage and (n) porous structure of F6 after 6 months storage period

4.18 *In vitro* cell line study

4.18.1 *In vitro* cytotoxicity

The MTT assay was used to test the *in vitro* cytotoxicity of pure drug, blank microsphere, and drug-loaded microsphere. The results demonstrate that the blank microsphere exhibit a higher level of cell viability, indicating that they are safe to employ as a drug delivery system (Figure 4.19). Within two hours, the pure medication caused a high level of cell death and decreased the cell viability upto 83.42 ± 0.15 % [100].The improved GO - SA microspheres significantly reduced cytotoxicity up to 6 hours. This outcome suggested that GO-SA microspheres had decreased cytotoxicity prior to entering the colon. This shows that the colon was the target and not the stomach area when capecitabine was released. Additionally, there was a significant decrease in cell viability after 6 hours, showing strong cytotoxicity that was under control for up to 24 hours in the colon region [36]. The outcome is consistent with GO-based alginate polymers that promote cell adhesion and proliferation. Additionally, GO-SA microspheres offer a negatively charged carrier system that sticks better to the positively charged proteins found in the colonic mucosa's injured tissues. Inhibiting HT29 tumor cell proliferation using GO-SA microspheres results in a longer-lasting induction of apoptosis, lasting until the decomposition of the polymer matrix [62]. As a result, it was determined that adding GO to SA,

particularly in formulations with significantly more GO, may have greater potential as a carrier for treating colon cancer.

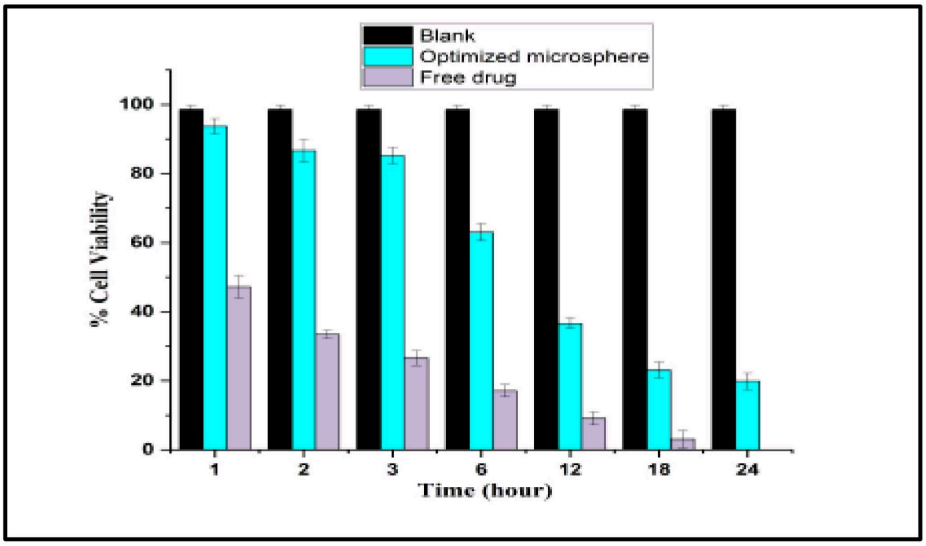

Figure 4.19 *In vitro* cytotoxicity profile of blank, optimized formulation and free drug

4.18.2 *In vitro* antiproliferative activity

We looked into *in vitro* antiproliferative activity of blank, capecitabine and capecitabine loaded microsphere over a range of concentrations (0–50 μM) in HT-29 cell line represented in Table 4-2. A lower IC50 value for the HT29 cell line was discovered for capecitabine. As a result, there were differences between the results obtained using capecitabine and capecitabine-loaded microsphere on HT29 cells. HT-29 cells were most lethal to the improved formulation, as indicated in Table 4-2, at a concentration of 11.47±14.96 μM after 24 hours of incubation. In the case of the blank microsphere, there was no discernible cytotoxicity. In comparison to the free medication, the improved formulation's

potential cytotoxicity toward human colon cancer cells is shown by its IC50 value on HT29 cells [101]. The degree of uptake by colorectal cancer cells may be related to the cytotoxic pattern of every microsphere and free drug, which is a potential explanation. The results also revealed that significant anticancer activity was achieved for all capecitabine loaded formulations as compared to free drug and control group on cancer cell line.

Table 4-3 Comparison of IC50 values among free Drug (capecitabine), capecitabine loaded microspheres, and blank microsphere in colon cancer cell. Data are represented as Mean ± SD.

Sample	HT29
Capecitabine	17.13 ± 27.22 µM
Capecitabine loaded optimized formulaton	11.47±14.96 µM
Blank microspheres	26.417 ± 19.25 µM

4.14.3 Measurement of reactive oxygen species (ROS)

Capecitabine and capecitabine loaded optimized formulation at IC50 concentration were used to study ROS generation in HT29 cell line by DCFDA assay. Capecitabine loaded optimized formulation (F6) showed much higher ROS

producing abilities in HT29 cell line than free drug capecitabine represented in Figure 4.20 [102]. Additionally, MTT assay explore that capecitabine loaded optimized formulation showed more active to kill the cancer cells at lower IC50 concentration as compared to free drug. Furthermore, gum odina and sodium alginate, exhibited a strong antioxidant properties which might be accelerate its effect on ROS production and cytotoxicity was monitored. It can be seen from the Figure 4.20, that HT29 cancer cells with 4 µM optimized formulation, showing in reducing the activity of cancer cells as indicated direct involvement of ROS production in colon cancer cell line HT29 [103].

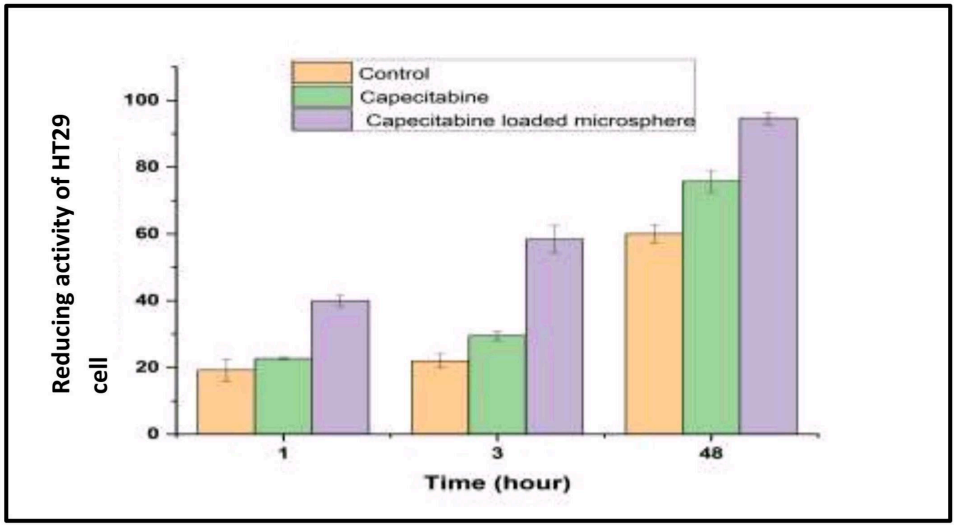

Figure 4.20 The intracellular effects of ROS production by control, capecitbine and capecitabine loaded microsphere in HT29 cells

4.19 *In vivo* study

4.19.1 Acute toxicity study of gum odina

Male Wistar rats were subjected to acute toxicity testing to investigate the potential impact of gum odina on hematological parameters, biochemical parameters, visual examination, and the histology of critical organs. There were no behavioral abnormalities, acute toxicological effects, or significant weight loss observed in any of the therapy groups. The average body weights of rats at 1, 7, and 14 days were found to be 196.05 ± 13.43, 200.74 ± 82.71, and 241.4 ± 4.82 g, respectively [104]. Additionally, all the treatment groups showed normal urea, serum creatinine, and liver function of the liver like ALT, AST, total protein, total bilirubin hemoglobin counts, platelet counts, total red blood cell counts, differential white blood cell counts, etc., with no significant variance ($p < 0.05$) as compared to control groups of animals represented in Table 4 -3.

Microscopic evaluation of the histology of rat kidneys (Figure 4.21 b) exhibited slight morphological changes, including a lessening of glomerulus cells (black star) and an extension of the bowman space (black arrow), found in gum odina-treated groups as compared with control groups. In the case of the control group, rats (Figure 4.21 a) did not exhibit any kind of necroscopy or abnormal morphological changes in the kidney (glomeruli, tubules, interstitium, and blood vessels) [105]. Results suggested that histological assessment of kidneys revealed

a minor variant in the morphology of kidneys in 2000 mg/kg body weight-treated rats. Alternatively, biochemical parameters of renal function in all rats treated showed no significant changes. Hence, based on the biochemical and histological results of the kidneys, it might be concluded that gum odina did not display adequate nephrotoxicity to cause a variation in the functions of the kidneys. Histology of the liver sections of control rats (Figure 4.21 c) did not show any histologic abnormalities in conjunction with well-maintained hepatic cells and visible central veins. Rats treated with 2000 mg/kg of gum odina were exposed to certain alterations in the histology of the liver (Figure 4.21 d), like slight dilation of sinusoids and atrophy of hepatic cords (black arrow), moderate hepatocytes, and some binucleated cells (black star) [106]. Most of the bioactive compounds were exhibited in the liver and metabolized to other compounds, which may or may not be hepatotoxic to the mice. However, 2000 mg/kg body weight of gum odina in mice models showed a remarkably significant elevation of ALT, AST, creatinine, and urea, which are probably good indicators of liver and kidney functions. Therefore, the moderate variations presented on histology of the liver sections are not attributed to the toxic effect of the gum odina. Comparing treated groups to control groups, the histological cross-section of the treated groups hearts revealed regularly arranged and conserved polarity of myocytes organized in muscular bundles, with no signs of heart necrosis or haemorrhage (Figure 4.21 e) [107]. The study revealed that upon oral administration of gum odina in mouse models, there were no adverse effects

exhibited, and hence, they might be safe for potential use as a polymer for the development of oral formulations.

Several hematological and serum biochemical parameters and the histopathological images of the vital organs like the liver, kidney, and heart did not show any significant difference between the test and control groups. Further in the experiment, the mortality of the animals was zero, which suggested the LD50 value of gum odina was set at 2000 mg/kg of body weight [108]. Hence, gum odina was categorized under "category 5" with "zero toxicity," indicating safety for drug delivery through the oral route.

Table 4-4 Hematological and biochemical parameters in male Wistar rat treated for 14 days with gum odina (mean ± SD, n=6)

Parameters (Unit)	Control	Treatment
White blood cells	8.5 ± 1.10 $10^3/mm^3$	8.31 ± 0.38 $10^3/mm^3$
Hemoglobin	12.24 ± 0.05 g/dL	10.62 ± 0.71 g/dL
Total red blood cells	4.81 ± 0.53 $10^6/mm^3$	5.166 ± 1.088 $10^6/mm^3$
Mean corpuscular volume	41.34 ± 4.15 fL	46.34 ± 4.15 fL

Mean corpuscular hemoglobin	20.80 ± 9.38 pg/cell	20.12± 1.34 pg/cell
ALT	44.56 ± 4.53 mg/dl	42.16 ± 1.45 mg/dl
AST	0.54 ± 0.05 mg/dl	0.59 ± 0.028 mg/dl
Total protein	35.8 ± 2.97 IU/L	35.84 ± 1.61 IU/L
Total bilirubin	103 ± 46.76 IU/L	110 .45 ± 4.87 IU/L

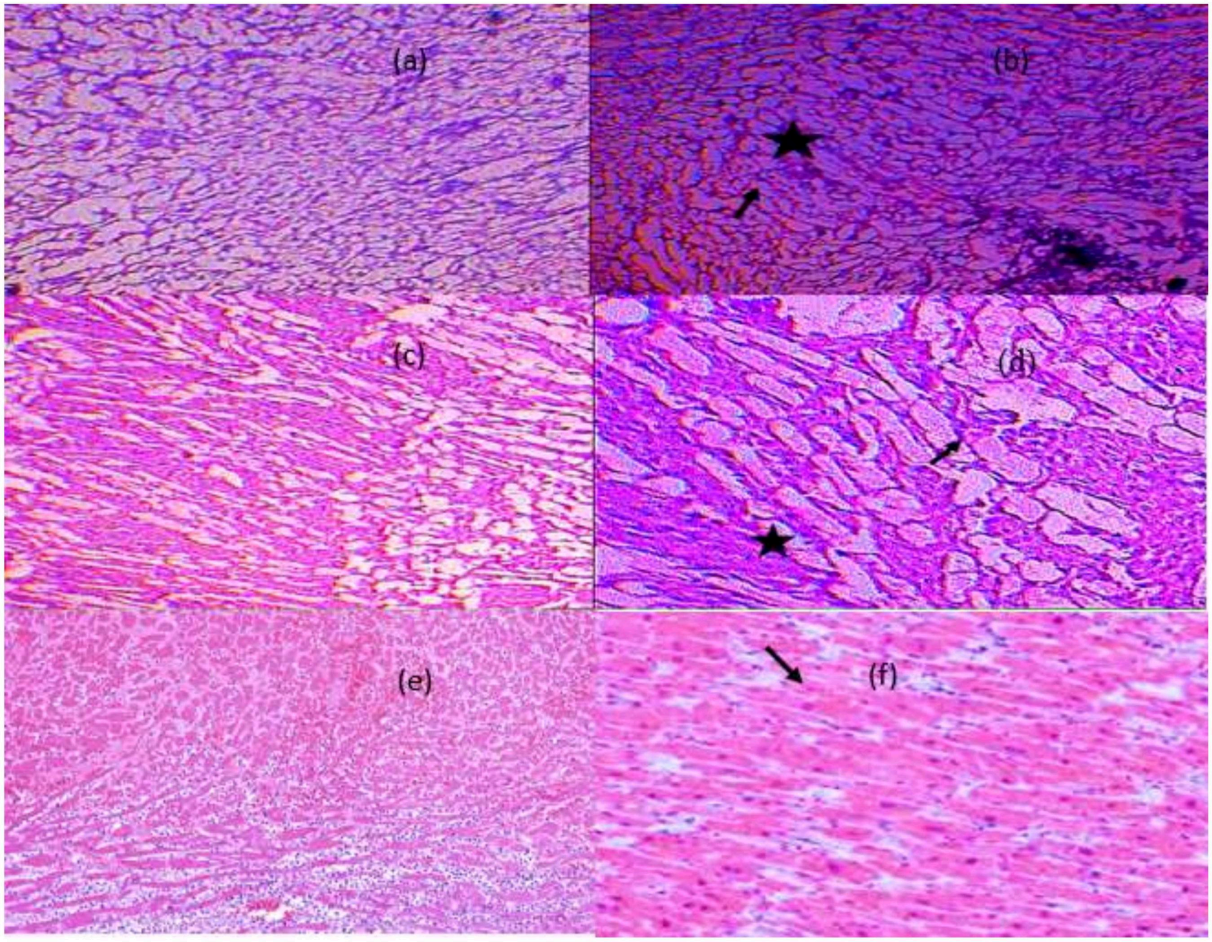

Figure 4.21 (a) Histopathological examination of kidney on controlled male rats and (b) treated rats. (c) histopathological examination of the liver on controlled

male rats and (d) treated rats and (e) histopathological examination of the heart on controlled male rats and (f) treated rats.

4.19.2. Pharmacokinetic studies

An *in vivo* pharmacokinetic study was performed on optimized formulation F6, which was compared with the standard drug capecitabine at an orally administered dose equivalent to 30 mg/kg body weight of mice in two study groups I and II, respectively (Table 4-3) [103]. The plasma concentration of the capecitabine-loaded optimized formulation showed a value of 24%, which is higher as compared to capecitabine administration. Significant changes in $t_{1/2}$ and AUC total values were also detected in the case of F6 as compared to free drug access, and the $t_{1/2}$ value of the optimized formulation suggested that drug release from microspheres occurs after reaching the colon. According to the pharmacokinetic data, capecitabine loaded microspheres were shown to have the greatest C_{max} of medication in the colon. AUC values, delayed biological $t_{1/2}$ values, and low elimination rate constants all pointed to the distinct advantage of optimized formulation based treatment over free drug capecitabine treatment in terms of the bioavailability of capecitabine in colon tissue and plasma [109]. These results showed that the rate of drug absorption followed in a sustained manner in the systemic circulation, satisfying one of the objectives of controlled release formulation. The value of area under the curve (AUC) indicated the extent of absorption, which was considerably greater for formulation F6, suggesting a

prolonged duration of action above the free drug, signifying that the capecitabine-encapsulated optimized formulation might fruitfully control the release of capecitabine [110].

Table 4-5 Pharmacokinetic parameters of capecitabine and capecitabine loaded microsphere treated with different groups of mice. Data are representd ± SD.

Pharmacokinetic parameters	*In-vivo* pharmacokinetic data of free capecitabine	*In-vivo* pharmacokinetic data of capecitabine loaded optimized formulation
C_{max} (ng/mL)	30.64 ± 2.85	51.16 ± 5.68
AUC_{0-t} (ng h/mL)	62.79 ± 48.36	102.32 ± 11.37
$AUC_{0-infinity}$ (ng h/mL)	324.08 ± 68.29	350.5 ± 1.06
AUC total (ng h/mL)	386.87 ± 18.77	454. 32 ± 11.37
$t_{1/2}$ (h)	5.27 ± 0.66	11.38 ± 0.45

4.19.3. Histopathological changes in colon carcinoma tissue before and after treatment of capecitabine-loaded microsphere

The diagnosis of various stages of colorectal cancer depends greatly on histopathological characteristics. The term colon cancer refers to cancers that start in the colon or rectum. Hematoxylin and eosin histopathological staining of

colorectal cancer tissue shows various tumor grades of colorectal carcinoma. The most common type of colorectal cancer that begins in the epithelial cells lining the colon's mucosa layer are adenocarcinomas. Oncogenes and tumor suppressor genes begin to undergo genomic changes as the lesion grows [101]. Oncogenes and tumor suppressor genes begin to undergo genomic changes as the lesion grows. The serrated pathway of colorectal cancer development may account for the development of colorectal cancer in hyperplastic polyps, according to mounting data. The histopathology study of colon tissue was viewed under a light microscope at several magnifications to explore the histological morphology of colonic mucosa. As seen in Figure 4.22, colonic cells largely generated an adenoma or polyp after being treated with DMH+DSS at the various time periods, which gradually might reach the uncontrolled cell division stage before its infiltration into the next layer, i.e., submucosa. The adenoma-carcinoma sequence may be broken by this pre-existing adenomatous precursor (polyps) in the colon interfering with the natural processes that control epithelial renewal. When they are further advanced, they may enter blood vessels, spread to other tissues, and eventually develop metastasis. The colon of the control group (Figure 4.22 a) showed normal mucosa and submucosal layers and normal colonic architecture without apparent abnormality in colonic cells. In DMH+ DSS-induced group (Figure 4.22 b and c) showed clear degeneration of tubular glands in the mucosal and submucosal layer, aberrant crypts, and growth of polyps on the lining of colon cancer cells [111]. The adenoma-carcinoma sequence may be broken by this pre-

existing adenomatous precursor (polyps) in the colon interfering with the natural processes that control epithelial renewal. When they are further advanced, they may enter blood vessels, spread to other tissues, and eventually develop metastasis. Mice treated with the standard drug capecitabine exhibited hyperplastic crypts with cell infiltration and a slight change in the muscular layer architecture. Mice treated with optimized formulation exhibited a reduced incidence of polyps and showed normal crypts as compared to cancer-induced mice. This result showed that optimized formulation was well tolerated in a healthy colon and did not harm or significantly alter the histology of the colonic tissues [112]. Along with the submucosal and muscular layers, which were both structured properly, the epithelial layer was also present. Additionally, this shows that optimized formulation was not harmful to the healthy colon (4.22 d).

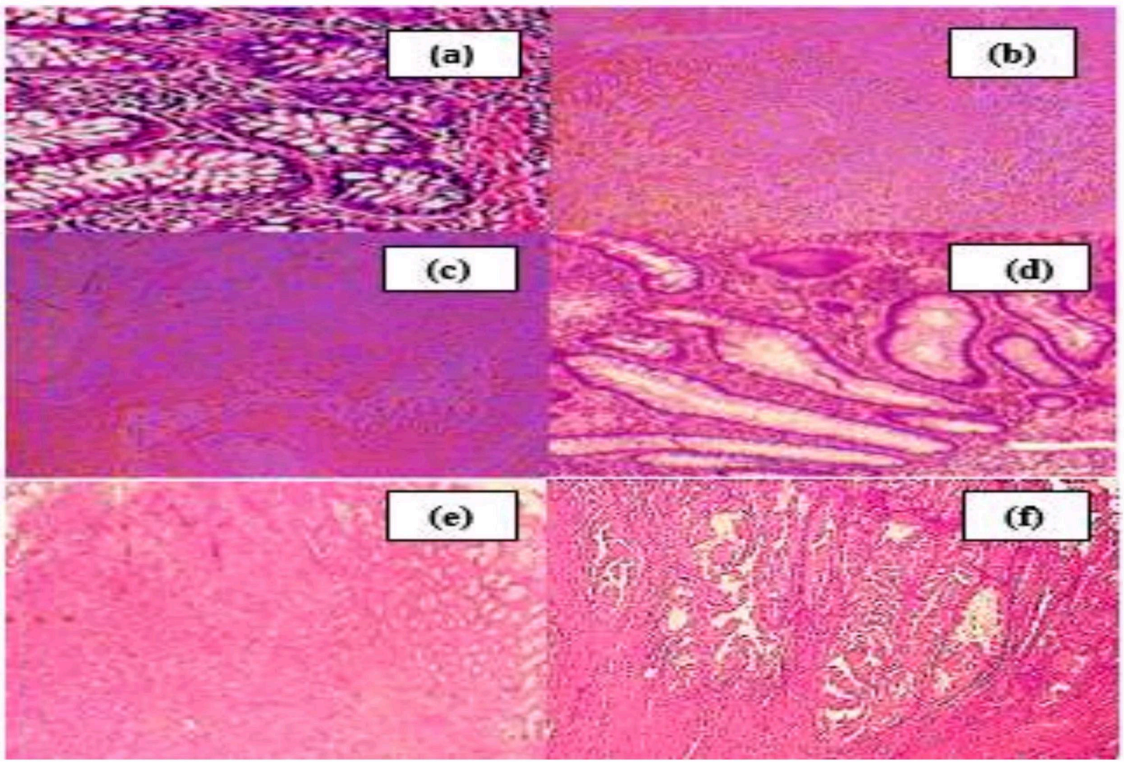

Figure 4.22 Histopathological morphology of (a) normal colonic tissue, (b), (c) and (e) exhibiting different grades of cancer progression, (d) carcinogen-treated mice received optimized capecitabine loaded microsphere and (f) carcinogen-treated mice treated with standard drug.

4.19.4 *In Vivo* Antitumor Efficacy Study

Animals taking DMH + DSS alone were seen to gradually lose body weight (184.7 ± 1.83 gm), and this was followed by a variety of behavioral changes, including decreased food intake, slower locomotion, increased resting, and a propensity for infrequent outbursts of anger. With the addition of capecitabine, capecitabine loaded optimized formulation, the body weight began to rise. The animals treated with optimized formulation showed the greatest improvement. Moreover, optimized formulation (F6) treated groups exhibited statistical ($p < 0.05$) enhancement in weight growth compared to carcinogen-treated rats [103]. A group of mice were slaughtered and their colon tissues were extracted after receiving DMH therapy for 8 weeks. Different-sized tumors in the tissues were discovered, and the majority of them were mostly visible under a microscope (Table 4 - 5) To establish a general idea of the average tumor volume, their volumes were measured [101]. It was challenging to determine the weights of the majority of the tumors because they were often so tiny and intertwined with colonic epithelium. We sacrificed a different group of mice and looked at changes in the tumor morphology after the mice had been given capecitabine and

optimized formulation treatment for 4 weeks. The volumes of the isolated tumors were calculated. The tumor volume was found to be 13.16 ± 7.36 mm^3 for the DMH-treated colorectal cancer mice, whereas volumes of 8 ± 6.59 mm^3 and 5.21 ± 2.79 mm^3 were found in the case of capecitabine and capecitabine loaded optimized formulation respectively [113].

Table 4 -6 Tumor volume and body weight of different experimental mice

Group	**Initial body weight** (gm)	**Final body weight** (gm)	**Tumor Volume** mm^3
DMH	163.9 ± 7.83 gm	184.7 ± 1.83 gm	13.16 ± 7.36 mm^3
Capecitabine	182.5 ± 6.27gm	204.3 ± 6.02 gm	8.37 ± 6.59mm^3
Capecitabine loaded formulation	171.7 ± 17.82gm	214 ± 7.14 gm	5.21 ± 2.79 mm^3

4.19.5 Tumor marker detection test

Serum concentrations of CA 19-9 and CA 125 played an important role in the clinical purpose of detecting the degree of angiogenesis, the presence of endothelial cells, and cellular proliferation. We first evaluated the sensitivity of individual markers, followed by CA 19-9 and CA 125, whose displayed values were 33.4 U/mL and 29 U/mL on cancer-induced mice [114]. These results

suggested that these tumor markers revealed a positive correlation with the advancement of tumor stages. In addition, the increase of such indicators as CA19-9 and CA125 was also influenced by lymph node metastasis, vascular invasion, nerve infiltration and vascularization or angiogenesis. In treated mice, CA 19-9 and CA 125 values were obtained at 1.05 U/mL and 0.27 U/L, respectively. CA 19-9 and CA 125 have proven to be useful in monitoring the effect of therapy and are pertinent prognostic tools for clinical use . This has given evidence of the successful development of our formulation for the treatment of colorectal carcinoma. These results clearly express that serum CA 19-9 and CA 125 tests are probably most applicable for colon cancer diagnosis, postoperative surveillance, and the monitoring of treatment effective [115].

The above results indicate that capecitabine-loaded microspheres might be related to the increased cellular availability of the drugs in the tumor due to the polymeric matrix of gum odina and sodium alginate, which enhance permeation and retention of drugs; however, a thorough comparison with the respective free drug capecitabine-treated groups and pharmacokinetic studies would be applicable to confirm this hypothesis.

CHAPTER 5

CONCLUSION

5 Conclusion

One of the most significant health issues in the world today is cancer and its implications. Facilitating an efficient site-based chemotherapy drug administration to protect healthy organs from harmful cytotoxic reactions brought on by chemotherapy is a significant obstacle in oncotherapy. Scientists have created unique drug delivery systems in response to the growing need for more effective cancer treatments and the desire to reduce the negative effects of chemotherapy procedures. Different carriers have been developed that can encapsulate and deliver the anti-cancer drug to the targeted tumors in a stimuli-sensitive manner, overcoming the limitations of conventional drug delivery systems such as uncontrollable drug release, short half-life, and high cytotoxicity. Microspheres have reportedly been used in oncological treatments to enhance drug delivery to tumors and anti-cancer efficacy. These microspheres improve the bioavailability, reduce the pharmacological toxicity of the drugs under study, and increase the sensitivity and specificity of chemotherapeutic treatments.

Despite having serious systemic adverse effects, capecitabine is the medication of choice has been used to treat a variety of cancers, particularly breast and colon cancer. In the therapeutic application of capecitabine for the treatment of colon cancer, preventing the drug molecules from degrading or being successfully delivered to the target region of the colon are key challenges. Taking into account

these ideas, we developed pH-sensitive, controlled-release microspheres made of gum odina and sodium alginate and calcium chloride used as a crosslinker that were evaluated for *in vitro* and *in vivo* efficacies. The microspheres were monodispersed, microsized, and contained fewer agglomerative particles. Studies on swelling indicated that they might be used as a smart pH-sensitive drug delivery vehicle because they demonstrated high swelling percentages, drug loading, and subsequent drug release at higher pH, i.e. 7.4. In comparison to free capecitabine, the capecitabine-loaded core-shell microspheres shown superior physicochemical stability under the simulated colon scenario. This suggests that core-shell microspheres made of gum odina and sodium alginate could effectively protect capecitabine degradation from the digestive fluids. According to the SEM findings, the microsphere exhibited spherical shape, superior porosity and pore size might be facilated water uptake, swelling and release mechanism. The hemolysis tests showed that the formed microspheres had a high blood compatibility, which is encouraging for their potential to be used in biomedicine. The aforementioned findings also showed that developed optimized microspheres were more thermally stable than their component parts individually. Additionally, the microsphere demonstrated great encapsulation efficiency, prolonged release patterns, preferable hemocompatibility, and increased cytotoxicity on HT29 colon cancer cells. The intracellular absorption of capecitabine-loaded microsphere by HT 29 cells was revealed to be time-dependent. A colon cancer-bearing Swiss albino mouse model in *in vivo* research has shown that

capecitabine-loaded gum odina-sodium alginate based microspheres were more effective at stifling tumor growth than free capecitabine and that this method did not produce any harmful side effects. The formulated microsphere was found to be safe and non-toxic to living tissues after toxicity testing using hematological, biochemical and histological analysis. These results suggest that the pH-responsive carrier system could decrease dose frequency and increase capecitabine efficacy in cancer therapy. The system's safety, non-toxicity, and biocompatibility were demonstrated by toxicity profiling. The pharmacokinetic analysis showed enhanced bioavailability, and the GI distribution showed that the colon had a localized capecitabine concentration that was higher than the IC50 of capecitabine for colon cancer cell lines. After receiving therapy with microspheres, biochemical markers significantly change, with a considerable decrease in tumor volume was noticed. By improving therapeutic outcomes and reducing the amount of anti-cancer medications, this approach may eventually result in fewer adverse effects for the patient.The current finding is promising and supports the conduct of thorough preclinical research using capecitabine-loaded microspheres as a requirement for conceivably moving further into human applications.

CHAPTER 6

REFERENCES

References

[1] R. Siegel, C. DeSantis, A. Jemal, Colorectal cancer statistics, 2014, CA: A Cancer Journal for Clinicians 64 (2014) 104–117. https://doi.org/10.3322/caac.21220.

[2] Y. Riadi, O. Afzal, M.H. Geesi, W.H. Almalki, T. Singh, Baicalin-Loaded Lipid–Polymer Hybrid Nanoparticles Inhibiting the Proliferation of Human Colon Cancer: Pharmacokinetics and In Vivo Evaluation, Polymers 15 (2023) 598. https://doi.org/10.3390/polym15030598.

[3] H.-T. Arkenau, U. Graeven, S. Kubicka, A. Grothey, C. Englisch-Fritz, A. Kretzschmar, R. Greil, W. Freier, T. Seufferlein, A. Hinke, H.-J. Schmoll, W. Schmiegel, R. Porschen, AIO Colorectal Study Group, Oxaliplatin in combination with 5-fluorouracil/leucovorin or capecitabine in elderly patients with metastatic colorectal cancer, Clin Colorectal Cancer 7 (2008) 60–64. https://doi.org/10.3816/ccc.2008.n.009.

[4] A. Banerjee, S. Pathak, V.D. Subramanium, D. G., R. Murugesan, R.S. Verma, Strategies for targeted drug delivery in treatment of colon cancer: current trends and future perspectives, Drug Discovery Today 22 (2017) 1224–1232. https://doi.org/10.1016/j.drudis.2017.05.006.

[5] H. Idrees, S.Z.J. Zaidi, A. Sabir, R.U. Khan, X. Zhang, S. Hassan, A Review of Biodegradable Natural Polymer-Based Nanoparticles for Drug Delivery Applications, Nanomaterials 10 (2020) 1970. https://doi.org/10.3390/nano10101970.

[6] D. Mitra, A. Basu, B. Das, A.K. Jena, A. De, M. Das, S. Bhattacharya, A. Samanta, Gum odina: an emerging gut modulating approach in colorectal cancer prevention, RSC Advances 7 (2017) 29129–29142.

[7] M. Nurmik, P. Ullmann, F. Rodriguez, S. Haan, E. Letellier, In search of definitions: Cancer-associated fibroblasts and their markers, International Journal of Cancer 146 (2020) 895–905. https://doi.org/10.1002/ijc.32193.

[8] B. Scallon, A. Cai, N. Solowski, A. Rosenberg, X.-Y. Song, D. Shealy, C. Wagner, Binding and Functional Comparisons of Two Types of Tumor Necrosis Factor Antagonists, J Pharmacol Exp Ther 301 (2002) 418–426. https://doi.org/10.1124/jpet.301.2.418.

[9] E. Jullumstrø, A. Wibe, S. Lydersen, T.-H. Edna, Colon cancer incidence, presentation, treatment and outcomes over 25 years, Colorectal Disease 13 (2011) 512–518. https://doi.org/10.1111/j.1463-1318.2010.02191.x.

[10] M. Teeuwssen, R. Fodde, Cell Heterogeneity and Phenotypic Plasticity in Metastasis Formation: The Case of Colon Cancer, Cancers 11 (2019) 1368. https://doi.org/10.3390/cancers11091368.

[11] T. Veen, A. Kanani, D. Lea, K. Søreide, Clinical trials of neoadjuvant immune checkpoint inhibitors for early-stage operable colon and rectal cancer, Cancer Immunol Immunother 72 (2023) 3135–3147. https://doi.org/10.1007/s00262-023-03480-w.

[12] T. Nawa, J. Kato, H. Kawamoto, H. Okada, H. Yamamoto, H. Kohno, H. Endo, Y. Shiratori, Differences between right- and left-sided colon cancer in patient characteristics, cancer morphology and histology, Journal of Gastroenterology and Hepatology 23 (2008) 418–423. https://doi.org/10.1111/j.1440-1746.2007.04923.x.

[13] Y. Yuan, K. Zheng, L. Zhou, F. Chen, S. Zhang, H. Lu, J. Lu, C. Shao, R. Meng, W. Zhang, X. Gao, F. Shen, Predictive value of modified MRI-based split scar sign (mrSSS) score for pathological complete response after neoadjuvant chemoradiotherapy for patients with rectal cancer, Int J Colorectal Dis 38 (2023) 40. https://doi.org/10.1007/s00384-023-04330-y.

[14] J. He, M. He, J.-H. Tang, X.-H. Wang, Anastomotic leak risk factors following colon cancer resection: a systematic review and meta-analysis, Langenbecks Arch Surg 408 (2023) 252. https://doi.org/10.1007/s00423-023-02989-z.

[15] R. Hüneburg, K. Bucksch, F. Schmeißer, D. Heling, T. Marwitz, S. Aretz, D.J. Kaczmarek, G. Kristiansen, O. Hommerding, C.P. Strassburg, C. Engel, J. Nattermann, Real-time use of artificial intelligence (CADEYE) in colorectal cancer surveillance of patients with Lynch syndrome—A randomized controlled pilot trial (CADLY), United European Gastroenterology Journal 11 (2023) 60–68. https://doi.org/10.1002/ueg2.12354.

[16] Y.J. Ha, Y.J. Shin, K.H. Tak, J.L. Park, J.H. Kim, J.L. Lee, Y.S. Yoon, C.W. Kim, S.Y. Kim, J.C. Kim, Reduced expression of alanyl aminopeptidase is a robust biomarker of non-familial adenomatous polyposis and non-hereditary nonpolyposis colorectal cancer syndrome early-onset colorectal cancer, Cancer Medicine 12 (2023) 10091–10104. https://doi.org/10.1002/cam4.5675.

[17] M. Nielsen, H. Morreau, H.F.A. Vasen, F.J. Hes, MUTYH-associated polyposis (MAP), Critical Reviews in Oncology/Hematology 79 (2011) 1–16. https://doi.org/10.1016/j.critrevonc.2010.05.011.

[18] De, A., Malpani, D., Das, B., Mitra, D. and Samanta, A., 2020. Characterization of an arabinogalactan isolated from gum exudate of Odina wodier Roxb.: Rheology, AFM, Raman and CD spectroscopy. *Carbohydrate polymers*, *250*, p.116950.

[19] M.L. Slattery, J.D. Potter, G.D. Friedman, K.-N. Ma, S. Edwards, Tobacco use and colon cancer, International Journal of Cancer 70 (1997) 259–264. https://doi.org/10.1002/(SICI)1097-0215(19970127)70:3<259::AID-IJC2>3.0.CO;2-W.

[20] D.C. Gibson, J.D. Prochaska, X. Yu, S. Kaul, An examination between census tract unhealthy food availability and colorectal cancer incidence, Cancer Epidemiology 67 (2020) 101761. https://doi.org/10.1016/j.canep.2020.101761.

[21] A. Tarasiuk, P. Mosińska, J. Fichna, The mechanisms linking obesity to colon cancer: An overview, Obesity Research & Clinical Practice 12 (2018) 251–259. https://doi.org/10.1016/j.orcp.2018.01.005.

[22] T. Jess, J. Simonsen, K.T. Jørgensen, B.V. Pedersen, N.M. Nielsen, M. Frisch, Decreasing Risk of Colorectal Cancer in Patients With Inflammatory Bowel Disease Over 30 Years, Gastroenterology 143 (2012) 375-381.e1. https://doi.org/10.1053/j.gastro.2012.04.016.

[23] V.F. Sai, F. Velayos, J. Neuhaus, A.C. Westphalen, Colonoscopy after CT Diagnosis of Diverticulitis to Exclude Colon Cancer: A Systematic Literature Review, Radiology 263 (2012) 383–390. https://doi.org/10.1148/radiol.12111869.

[24] V. Kloten, N. Rüchel, N.O. Brüchle, J. Gasthaus, N. Freudenmacher, F. Steib, J. Mijnes, J. Eschenbruch, M. Binnebösel, R. Knüchel, E. Dahl, Liquid biopsy in colon cancer: comparison of different circulating DNA extraction systems following absolute quantification of KRAS mutations using Intplex allele-specific PCR, Oncotarget 8 (2017) 86253–86263. https://doi.org/10.18632/oncotarget.21134.

[25] T. Lang, R. Zhu, X. Zhu, W. Yan, Y. Li, Y. Zhai, T. Wu, X. Huang, Q. Yin, Y. Li, Combining gut microbiota modulation and chemotherapy by capecitabine-loaded prebiotic nanoparticle improves

colorectal cancer therapy, Nat Commun 14 (2023) 4746. https://doi.org/10.1038/s41467-023-40439-y.

[26] R.B. Corcoran, T. André, C.E. Atreya, J.H.M. Schellens, T. Yoshino, J.C. Bendell, A. Hollebecque, A.J. McRee, S. Siena, G. Middleton, K. Muro, M.S. Gordon, J. Tabernero, R. Yaeger, P.J. O'Dwyer, Y. Humblet, F. De Vos, A.S. Jung, J.C. Brase, S. Jaeger, S. Bettinger, B. Mookerjee, F. Rangwala, E. Van Cutsem, Combined BRAF, EGFR, and MEK Inhibition in Patients with BRAFV600E-Mutant Colorectal Cancer, Cancer Discovery 8 (2018) 428–443. https://doi.org/10.1158/2159-8290.CD-17-1226.

[27] A. Mangerich, C.G. Knutson, N.M. Parry, S. Muthupalani, W. Ye, E. Prestwich, L. Cui, J.L. McFaline, M. Mobley, Z. Ge, K. Taghizadeh, J.S. Wishnok, G.N. Wogan, J.G. Fox, S.R. Tannenbaum, P.C. Dedon, Infection-induced colitis in mice causes dynamic and tissue-specific changes in stress response and DNA damage leading to colon cancer, Proceedings of the National Academy of Sciences 109 (2012) E1820–E1829. https://doi.org/10.1073/pnas.1207829109.

[28] I. Mármol, J. Quero, M.J. Rodríguez-Yoldi, E. Cerrada, Gold as a Possible Alternative to Platinum-Based Chemotherapy for Colon Cancer Treatment, Cancers 11 (2019) 780. https://doi.org/10.3390/cancers11060780.

[29] R. Costi, F. Leonardi, D. Zanoni, V. Violi, L. Roncoroni, Palliative care and end-stage colorectal cancer management: The surgeon meets the oncologist, World J Gastroenterol 20 (2014) 7602–7621. https://doi.org/10.3748/wjg.v20.i24.7602.

[30] N.A. Johdi, N.F. Sukor, Colorectal Cancer Immunotherapy: Options and Strategies, Frontiers in Immunology 11 (2020). https://www.frontiersin.org/articles/10.3389/fimmu.2020.01624 (accessed September 15, 2023).

[31] Z. Yu, X. Li, J. Duan, X.-D. Yang, Targeted Treatment of Colon Cancer with Aptamer-Guided Albumin Nanoparticles Loaded with Docetaxel, International Journal of Nanomedicine 15 (2020) 6737–6748. https://doi.org/10.2147/IJN.S267177.

[32] M.G. Haddock, Intraoperative radiation therapy for colon and rectal cancers: a clinical review, Radiation Oncology 12 (2017) 11. https://doi.org/10.1186/s13014-016-0752-1.

[33] N. Dudhipala, G. Puchchakayala, Capecitabine lipid nanoparticles for anti-colon cancer activity in 1,2-dimethylhydrazine-induced colon cancer: preparation, cytotoxic, pharmacokinetic, and pathological evaluation, Drug Development and Industrial Pharmacy 44 (2018) 1572–1582. https://doi.org/10.1080/03639045.2018.1445264.

[34] C.M. Walko, C. Lindley, Capecitabine: A review, Clinical Therapeutics 27 (2005) 23–44. https://doi.org/10.1016/j.clinthera.2005.01.005.

[35] B.S.G. Prasad, V.R.M. Gupta, N. Devanna, K. Jayasurya, MICROSPHERES AS DRUG DELIVERY SYSTEM – A REVIEW, 5 (2014).

[36] P. Sinha, U. Udhumansha, G. Rathnam, M. Ganesh, H.T. Jang, Capecitabine encapsulated chitosan succinate-sodium alginate macromolecular complex beads for colon cancer targeted delivery: in vitro evaluation, International Journal of Biological Macromolecules 117 (2018) 840–850. https://doi.org/10.1016/j.ijbiomac.2018.05.181.

[37] K. Chaturvedi, K. Ganguly, U.A. More, K.R. Reddy, T. Dugge, B. Naik, T.M. Aminabhavi, M.N. Noolvi, Sodium alginate in drug delivery and biomedical areas, in: Natural Polysaccharides in Drug Delivery and Biomedical Applications, Elsevier, 2019: pp. 59–100.

[38] S. Jana, M.K. Trivedi, R.M. Tallapragada, A. Branton, D. Trivedi, G. Nayak, R. Mishra, Characterization of physicochemical and thermal properties of chitosan and sodium alginate after biofield treatment, Pharmaceutica Analytica Acta 6 (2015).

[39] A. Samanta, A. De, M.S. Hasnain, H. Bera, A.K. Nayak, Gum odina as pharmaceutical excipient, in: Natural Polysaccharides in Drug Delivery and Biomedical Applications, Elsevier, 2019: pp. 327–337.

[40] S. Das, T.K. Dey, A. De, A. Banerjee, S. Chakraborty, B. Das, A.K. Mukhopadhyay, B. Mukherjee, A. Samanta, Antimicrobial loaded gum odina - gelatin based biomimetic spongy scaffold for accelerated wound healing with complete cutaneous texture, International Journal of Pharmaceutics 606 (2021) 120892. https://doi.org/10.1016/j.ijpharm.2021.120892.

[41] R.P. Sarathi, S. Amalesh, M. Manabendra, R. Bappaditya, M. Abhishek, Designing Novel pH-Induced Chitosan–Gum Odina Complex Coacervates for Colon Targeting, (2013).

[42] S.C. Dinda, B. Mukharjee, Gum cordia-A new tablet binder and emulsifier, Acta Pharmaceutica Sciencia 51 (2009).

[43] A. De, D. Malpani, B. Das, D. Mitra, A. Samanta, Characterization of an arabinogalactan isolated from gum exudate of Odina wodier Roxb.: Rheology, AFM, Raman and CD spectroscopy, Carbohydrate Polymers 250 (2020) 116950.

[44] A.K. Jena, A.K. Nayak, A. De, D. Mitra, A. Samanta, Development of lamivudine containing multiple emulsions stabilized by gum odina, Future Journal of Pharmaceutical Sciences 4 (2018) 71–79.

[45] D. Mitra, A.K. Jena, A. De, M. Das, B. Das, A. Samanta, Prebiotic potential of gum odina and its impact on gut ecology: in vitro and in vivo assessments, Food & Function 7 (2016) 3064–3072.

[46] D. Agarwal, M.S. Ranawat, C.S. Chauhan, R. Kamble, FORMULATION AND CHARECTERISATION OF COLON TARGETED pH DEPENDENT MICROSPHERES OF CAPECITABINE FOR COLORECTAL CANCER, Journal of Drug Delivery and Therapeutics 3 (2013) 215–222. https://doi.org/10.22270/jddt.v3i6.747.

[47] W. Fan, W. Yan, Z. Xu, H. Ni, Formation mechanism of monodisperse, low molecular weight chitosan nanoparticles by ionic gelation technique, Colloids and Surfaces B: Biointerfaces 90 (2012) 21–27.

[48] F. Pati, B. Adhikari, S. Dhara, Development of chitosan–tripolyphosphate fibers through pH dependent ionotropic gelation, Carbohydrate Research 346 (2011) 2582–2588.

[49] P. Gadziński, A. Froelich, B. Jadach, M. Wojty\lko, A. Tatarek, A. Bia\lek, J. Krysztofiak, M. Gackowski, F. Otto, T. Osma\lek, Ionotropic Gelation and Chemical Crosslinking as Methods for Fabrication of Modified-Release Gellan Gum-Based Drug Delivery Systems, Pharmaceutics 15 (2023) 108.

[50] S. Kunjachan, S. Jose, T. Lammers, Understanding the mechanism of ionic gelation for synthesis of chitosan nanoparticles using qualitative techniques, Asian Journal of Pharmaceutics (AJP) 4 (2010).

[51] M.M. Talukdar, J. Plaizier-Vercammen, Evaluation of xanthan cum as a hydrophilic matrix for controlled-release dosage form preparations, Drug Development and Industrial Pharmacy 19 (1993) 1037–1046.

[52] B. Ankit, R.P.S. Rathore, Y.S. Tanwar, S. Gupta, G. Bhaduka, Oral sustained release dosage form: an opportunity to prolong the release of drug, IJARPB 3 (2013) 7–14.

[53] P. Vega-Vásquez, N.S. Mosier, J. Irudayaraj, Nanoscale drug delivery systems: from medicine to agriculture, Frontiers in Bioengineering and Biotechnology 8 (2020) 79.

[54] J. Singh, T. Garg, G. Rath, A.K. Goyal, Advances in nanotechnology-based carrier systems for targeted delivery of bioactive drug molecules with special emphasis on immunotherapy in drug resistant tuberculosis–a critical review, Drug Delivery 23 (2016) 1676–1698.

[55] H. Singh, G. Sharma, Recent Development of Novel Drug Delivery of Herbal Drugs, RPS Pharmacy and Pharmacology Reports (2023) rqad028.

[56] B. Ibrahim, O.Y. Mady, M.M. Tambuwala, Y.A. Haggag, pH-sensitive nanoparticles containing 5-fluorouracil and leucovorin as an improved anti-cancer option for colon cancer, Nanomedicine 17 (2022) 367–381.

[57] M. Nagpal, D.K. Maheshwari, P. Rakha, H. Dureja, S. Goyal, G. Dhingra, Formulation development and evaluation of alginate microspheres of ibuprofen, Journal of Young Pharmacists 4 (2012) 13–16.

[58] R. Rastogi, Y. Sultana, M. Aqil, A. Ali, S. Kumar, K. Chuttani, A.K. Mishra, Alginate microspheres of isoniazid for oral sustained drug delivery, International Journal of Pharmaceutics 334 (2007) 71–77.

[59] M.Z. Ahmad, S. Akhter, I. Ahmad, A. Singh, M. Anwar, M. Shamim, F.J. Ahmad, In vitro and in vivo evaluation of Assam Bora rice starch-based bioadhesive microsphere as a drug carrier for colon targeting, Expert Opinion on Drug Delivery 9 (2012) 141–149.

[60] A. Tayyab, A. Mahmood, H. Ijaz, R.M. Sarfraz, N. Zafar, Z. Danish, Formulation and optimization of captopril-loaded microspheres based compressed tablets: in vitro evaluation, International Journal of Polymeric Materials and Polymeric Biomaterials 71 (2022) 233–245.

[61] M.M. Badran, A.H. Alomrani, G.I. Harisa, A.E. Ashour, A. Kumar, A.E. Yassin, Novel docetaxel chitosan-coated PLGA/PCL nanoparticles with magnified cytotoxicity and bioavailability, Biomedicine & Pharmacotherapy 106 (2018) 1461–1468.

[62] A. Hazra, D. Sanyal, A. De, S. Chatterjee, K. Chattopadhyay, A. Samanta, Development and in vitro characterization of capecitabine loaded biopolymeric vehicle for the treatment of colon cancer, Journal of Applied Polymer Science 139 (2022) e52374. https://doi.org/10.1002/app.52374.

[63] S. Das, A. De, B. Das, B. Mukherjee, A. Samanta, Development of gum odina-gelatin based antimicrobial loaded biodegradable spongy scaffold: A promising wound care tool, Journal of Applied Polymer Science 138 (2021) 50057.

[64] S. Karimidost, E. Moniri, M. Miralinaghi, Thermodynamic and kinetic studies sorption of 5-fluorouracil onto single walled carbon nanotubes modified by chitosan, Korean Journal of Chemical Engineering 36 (2019) 1115–1123.

[65] C.M. Agrawal, J.S. McKinney, D. Lanctot, K.A. Athanasiou, Effects of fluid flow on the in vitro degradation kinetics of biodegradable scaffolds for tissue engineering, Biomaterials 21 (2000) 2443–2452.

[66] K.S. Soppirnath, T.M. Aminabhavi, Water transport and drug release study from cross-linked polyacrylamide grafted guar gum hydrogel microspheres for the controlled release application, European Journal of Pharmaceutics and Biopharmaceutics 53 (2002) 87–98.

[67] H.-L. Yu, Z.-Q. Feng, J.-J. Zhang, Y.-H. Wang, D.-J. Ding, Y.-Y. Gao, W.-F. Zhang, The evaluation of proanthocyanidins/chitosan/lecithin microspheres as sustained drug delivery system, BioMed Research International 2018 (2018).

[68] S.A. Agnihotri, T.M. Aminabhavi, Novel interpenetrating network chitosan-poly (ethylene oxide-g-acrylamide) hydrogel microspheres for the controlled release of capecitabine, International Journal of Pharmaceutics 324 (2006) 103–115.

[69] A. De, B. Das, D. Mitra, A.K. Sen, A. Samanta, Exploration of an arabinogalactan isolated from Odina wodier Roxb.: Physicochemical, compositional characterisations and functional attributes, Polymers for Advanced Technologies 31 (2020) 1814–1826.

[70] L. Baricault, G. Denariaz, J.-J. Houri, C. Bouley, C. Sapin, G. Trugnan, Use of HT-29, a cultured human colon cancer cell line, to study the effect of fermented milks on colon cancer cell growth and differentiation, Carcinogenesis 16 (1995) 245–252.

[71] K. Ho, L.S. Yazan, N. Ismail, M. Ismail, Apoptosis and cell cycle arrest of human colorectal cancer cell line HT-29 induced by vanillin, Cancer Epidemiology 33 (2009) 155–160.

[72] D. Figueroa, M. Asaduzzaman, F. Young, Real time monitoring and quantification of reactive oxygen species in breast cancer cell line MCF-7 by 2′, 7′–dichlorofluorescin diacetate (DCFDA) assay, Journal of Pharmacological and Toxicological Methods 94 (2018) 26–33.

[73] K.A. Ketuly, Acute toxicity study and wound healing potential of Gynura procumbens leaf extract in rats, Journal of Medicinal Plants Research 5 (2011) 2551–2558.

[74] C. Ge, X. Huang, S. Zhang, M. Yuan, Z. Tan, C. Xu, Q. Jie, J. Zhang, J. Zou, Y. Zhu, In vitro co-culture systems of hepatic and intestinal cells for cellular pharmacokinetic and pharmacodynamic studies of capecitabine against colorectal cancer, Cancer Cell International 23 (2023) 14.

[75] S. Kumar, N. Agnihotri, Piperlongumine, a piper alkaloid targets Ras/PI3K/Akt/mTOR signaling axis to inhibit tumor cell growth and proliferation in DMH/DSS induced experimental colon cancer, Biomedicine & Pharmacotherapy 109 (2019) 1462–1477. https://doi.org/10.1016/j.biopha.2018.10.182.

[76] N. Kumar, M. Sharma, V.P. Singh, C. Madan, S. Mehandia, An empirical study of handcrafted and dense feature extraction techniques for lung and colon cancer classification from histopathological images, Biomedical Signal Processing and Control 75 (2022) 103596.

[77] B.E. Huber, E.A. Austin, S.S. Good, V.C. Knick, S. Tibbels, C.A. Richards, In vivo antitumor activity of 5-fluorocytosine on human colorectal carcinoma cells genetically modified to express cytosine deaminase, Cancer Research 53 (1993) 4619–4626.

[78] F. Fazli Khalaf, M. Asadi Gharabaghi, M. Balibegloo, H. Davari, S. Afshar, B. Jahanbin, Pleural CEA, CA-15-3, CYFRA 21-1, CA-19-9, CA-125 discriminating malignant from benign pleural effusions: Diagnostic cancer biomarkers, The International Journal of Biological Markers (2023) 03936155231158661.

[79] C.V. Prajapati, R.P. Patel, B.G. Prajapati, Formulation, optimization and evaluation of sustained release microsphere of ketoprofen, Journal of Pharmacy & Bioallied Sciences 4 (2012) S101.

[80] S. Kakar, D. Batra, R. Singh, Preparation and evaluation of magnetic microspheres of mesalamine (5-aminosalicylic acid) for colon drug delivery, Journal of Acute Disease 2 (2013) 226–231.

[81] J. Zeng, C. Gu, Y. Zhuang, K. Lin, Y. Xie, X. Chen, Injectable hydrogel microspheres encapsulating extracellular vesicles derived from melatonin-stimulated NSCs promote neurogenesis and alleviate inflammation in spinal cord injury, Chemical Engineering Journal (2023) 144121.

[82] S. Noreen, S. Hasan, S.A. Ghumman, S. Anwar, H.Y. Gondal, F. Batool, S. Noureen, Formulation, Statistical Optimization, and *In Vivo* Pharmacodynamics of *Cydonia oblonga* Mucilage/Alginate Mucoadhesive Microspheres for the Delivery of Metformin HCl, ACS Omega 8 (2023) 5925–5938. https://doi.org/10.1021/acsomega.2c07789.

[83] Y. Xue, L. Xu, A. Wang, Y. Ma, W. Zhang, W. Ji, G. Leng, F. Zhou, W. Liu, X. Di, Studying spatial drug distribution in golf ball-shaped microspheres to understand drug release, Journal of Controlled Release 357 (2023) 196–209.

[84] S. Bhattacharya, S. Bonde, K. Hatware, S. Sharma, M.M. Anjum, R.K. Sahu, Physicochemical characterization, in vitro and in vivo evaluation of chitosan/carrageenan encumbered with Imatinib mesylate-polysarcosine nanoparticles for sustained drug release and enhanced colorectal cancer targeted therapy, International Journal of Biological Macromolecules (2023) 125529.

[85] M. Ekrami, M. Babaei, M. Fathi, S. Abbaszadeh, M. Nobakht, Ginger essential oil (Zingiber officinale) encapsulated in nanoliposome as innovative antioxidant and antipathogenic smart sustained-release system, Food Bioscience 53 (2023) 102796.

[86] U. Rehman, R.M. Sarfraz, A. Mahmood, T. Mahmood, N. Batool, B. Haroon, Y. Benguerba, Tamarind/β-CD-g-poly (MAA) pH responsive hydrogels for controlled delivery of Capecitabine: fabrication, characterization, toxicological and pharmacokinetic evaluation, J Polym Res 30 (2023) 41. https://doi.org/10.1007/s10965-022-03422-7.

[87] I. Ahmed, A. Mahmood, O.S. Qureshi, R.M. Sarfraz, H. Ijaz, M. Zaman, M.R. Akram, S. Usmani, Zulcaif, M. Malook, Development of tamarind gum/β-CD-co-poly (MAA) hydrogels for pH-driven

controlled delivery of capecitabine, Polym. Bull. (2023). https://doi.org/10.1007/s00289-023-04999-9.

[88] F.D. Pouya, R. Salehi, Y. Rasmi, F. Kheradmand, A. Fathi-Azarbayjani, Combination chemotherapy against colorectal cancer cells: Co-delivery of capecitabine and pioglitazone hydrochloride by polycaprolactone-polyethylene glycol carriers, Life Sciences (2023) 122083.

[89] M.Z. Ahmad, S. Akhter, M. Anwar, A. Kumar, M. Rahman, A.H. Talasaz, F.J. Ahmad, Colorectal cancer targeted Irinotecan-Assam Bora rice starch based microspheres: a mechanistic, pharmacokinetic and biochemical investigation, Drug Development and Industrial Pharmacy 39 (2013) 1936–1943. https://doi.org/10.3109/03639045.2012.719906.

[90] A. Sander, S. Tomas, D. Skansi, THE INFLUENCE OF AIR TEMPERATURE ON EFFECTIVE DIFFUSION COEFFICIENT OF MOISTURE IN THE FALLING RATE PERIOD, Drying Technology 16 (1998) 1487–1499. https://doi.org/10.1080/07373939808917472.

[91] E. Anwar, N. Farhana, Formulation and evaluation of phytosome-loaded maltodextrin-gum Arabic microsphere system for delivery of Camellia sinensis extract, Journal of Young Pharmacists 10 (2018) S56.

[92] W.F. Zhang, X.G. Chen, P.W. Li, Q.Z. He, H.Y. Zhou, Preparation and characterization of theophylline loaded chitosan/β-cyclodextrin microspheres, Journal of Materials Science: Materials in Medicine 19 (2008) 305–310.

[93] H. Cai, S. Sharma, W. Liu, W. Mu, W. Liu, X. Zhang, Y. Deng, Aerogel Microspheres from Natural Cellulose Nanofibrils and Their Application as Cell Culture Scaffold, Biomacromolecules 15 (2014) 2540–2547. https://doi.org/10.1021/bm5003976.

[94] S. Farris, K.M. Schaich, L. Liu, L. Piergiovanni, K.L. Yam, Development of polyion-complex hydrogels as an alternative approach for the production of bio-based polymers for food packaging applications: a review, Trends in Food Science & Technology 20 (2009) 316–332.

[95] C. Ruan, Y. Zhang, J. Wang, Y. Sun, X. Gao, G. Xiong, J. Liang, Preparation and antioxidant activity of sodium alginate and carboxymethyl cellulose edible films with epigallocatechin gallate, International Journal of Biological Macromolecules 134 (2019) 1038–1044.

[96] B. Das, A. De, M. Das, S. Das, A. Samanta, A new exploration of Dregea volubilis flowers: Focusing on antioxidant and antidiabetic properties, South African Journal of Botany 109 (2017) 16–24.

[97] G. Muhammad, M.T. Haseeb, M.A. Hussain, M.U. Ashraf, M. Farid-ul-Haq, M. Zaman, Stimuli-responsive/smart tablet formulations (under simulated physiological conditions) for oral drug delivery system based on glucuronoxylan polysaccharide, Drug Development and Industrial Pharmacy 46 (2020) 122–134. https://doi.org/10.1080/03639045.2019.1706551.

[98] N. Patel, J. Desai, P. Kumar, H.P. Thakkar, Development and In Vitro Characterization of Capecitabine-Loaded Alginate–Pectinate–Chitosan Beads for Colon Targeting, Journal of Macromolecular Science, Part B 55 (2016) 33–54. https://doi.org/10.1080/00222348.2015.1110551.

[99] G.K. Jena, C.N. Patra, P.K. Dixit, Cytotoxicity and pharmacokinetic studies of PLGA based capecitabine loaded nanoparticles, Indian Journal of Pharmaceutical Education and Research 54 (2020) 349–356.

[100] R. Nazari-Vanani, K. Karimian, N. Azarpira, H. Heli, Capecitabine-loaded nanoniosomes and evaluation of anticancer efficacy, Artificial Cells, Nanomedicine, and Biotechnology 47 (2019) 420–426. https://doi.org/10.1080/21691401.2018.1559179.

[101] D. Dutta, A. Chakraborty, B. Mukherjee, S. Gupta, Aptamer-Conjugated Apigenin Nanoparticles To Target Colorectal Carcinoma: A Promising Safe Alternative of Colorectal Cancer Chemotherapy, ACS Appl. Bio Mater. 1 (2018) 1538–1556. https://doi.org/10.1021/acsabm.8b00441.

[102] A. Sathiyaseelan, K. Saravanakumar, M.-H. Wang, Cerium oxide decorated 5-fluorouracil loaded chitosan nanoparticles for treatment of hepatocellular carcinoma, International Journal of Biological Macromolecules 216 (2022) 52–64.

[103] D. Dutta, A. Chakraborty, B. Mukherjee, S. Gupta, Aptamer-Conjugated Apigenin Nanoparticles To Target Colorectal Carcinoma: A Promising Safe Alternative of Colorectal Cancer Chemotherapy, ACS Appl. Bio Mater. 1 (2018) 1538–1556. https://doi.org/10.1021/acsabm.8b00441.

[104] J.S. Maziero, V.C. Thipe, S.O. Rogero, A.K. Cavalcante, K.C. Damasceno, M.B. Ormenio, G.A. Martini, J.G. Batista, W. Viveiros, K.K. Katti, A. Raphael Karikachery, D. Dhurvas Mohandoss, R.D. Dhurvas, M. Nappinnai, J.R. Rogero, A.B. Lugão, K.V. Katti, Species-Specific in vitro and in vivo Evaluation of Toxicity of Silver Nanoparticles Stabilized with Gum Arabic Protein, IJN Volume 15 (2020) 7359–7376. https://doi.org/10.2147/IJN.S250467.

[105] L. Xu, Y. Qiu, H. Xu, W. Ao, W. Lam, X. Yang, Acute and subacute toxicity studies on triptolide and triptolide-loaded polymeric micelles following intravenous administration in rodents, Food and Chemical Toxicology 57 (2013) 371–379.

[106] H. Ravi, R. Arunkumar, V. Baskaran, Chitosan-glycolipid nanogels loaded with anti-obese marine carotenoid fucoxanthin: Acute and sub-acute toxicity evaluation in rodent model, J Biomater Appl 30 (2015) 420–434. https://doi.org/10.1177/0885328215590753.

[107] B.C. Variya, A.K. Bakrania, P. Madan, S.S. Patel, Acute and 28-days repeated dose sub-acute toxicity study of gallic acid in albino mice, Regulatory Toxicology and Pharmacology 101 (2019) 71–78.

[108] C. Faggio, F. Fazio, S. Marafioti, F. Arfuso, G. Piccione, Oral administration of Gum Arabic: effects on haematological parameters and oxidative stress markers in Mugil cephalus, (2015). https://aquadocs.org/handle/1834/11832 (accessed October 3, 2023).

[109] A. Nawaz, T.W. Wong, Chitosan-carboxymethyl-5-fluorouracil-folate conjugate particles: microwave modulated uptake by skin and melanoma cells, Journal of Investigative Dermatology 138 (2018) 2412–2422.

[110] M.R. Abukhadra, N.M. Refay, A.M. El-Sherbeeny, M.A. El-Meligy, Insight into the Loading and Release Properties of MCM-48/Biopolymer Composites as Carriers for 5-Fluorouracil: Equilibrium Modeling and Pharmacokinetic Studies, ACS Omega 5 (2020) 11745–11755. https://doi.org/10.1021/acsomega.0c01078.

[111] R. Narayan, S. Gadag, S.P. Cheruku, A.M. Raichur, C.M. Day, S. Garg, S. Manandhar, K.S.R. Pai, A. Suresh, C.H. Mehta, Chitosan-glucuronic acid conjugate coated mesoporous silica nanoparticles: A smart pH-responsive and receptor-targeted system for colorectal cancer therapy, Carbohydrate Polymers 261 (2021) 117893.

[112] M. Upadhyay, S.K.R. Adena, H. Vardhan, S.K. Yadav, B. Mishra, Locust bean gum and sodium alginate based interpenetrating polymeric network microbeads encapsulating Capecitabine: Improved pharmacokinetics, cytotoxicity &in vivo antitumor activity, Materials Science and Engineering: C 104 (2019) 109958.

[113] P. Venkatesan, N. Puvvada, R. Dash, B.P. Kumar, D. Sarkar, B. Azab, A. Pathak, S.C. Kundu, P.B. Fisher, M. Mandal, The potential of celecoxib-loaded hydroxyapatite-chitosan nanocomposite for the treatment of colon cancer, Biomaterials 32 (2011) 3794–3806.

[114] S.R. Sinha, P. Prakash, R.K. Singh, D.K. Sinha, Assessment of tumor markers CA 19-9, CEA, CA 125, and CA 242 for the early diagnosis and prognosis prediction of gallbladder cancer, World Journal of Gastrointestinal Surgery 14 (2022) 1272.

[115] E. Somigliana, P. Vigano, A.S. Tirelli, I. Felicetta, E. Torresani, M. Vignali, A.M. Di Blasio, Use of the concomitant serum dosage of CA 125, CA 19-9 and interleukin-6 to detect the presence of endometriosis. Results from a series of reproductive age women undergoing laparoscopic surgery for benign gynaecological conditions, Human Reproduction 19 (2004) 1871–1876.

PUBLICATIONS

Received: 17 November 2021 | Revised: 12 January 2022 | Accepted: 5 February 2022

DOI: 10.1002/app.52374

RESEARCH ARTICLE

Applied Polymer SCIENCE WILEY

Development and in vitro characterization of capecitabine loaded biopolymeric vehicle for the treatment of colon cancer

Ahana Hazra[1] | **Dwipanjan Sanyal**[2] | **Arnab De**[1,3] | **Sohini Chatterjee**[1] | **Krishnananda Chattopadhyay**[2] | **Amalesh Samanta**[1]

[1]Division of Microbiology and Pharmaceutical Biotechnology, Department of Pharmaceutical Technology, Jadavpur University, Kolkata, India

[2]Protein Folding and Dynamics Group, Structural Biology and Bioinformatics Division, CSIR - Indian Institute of Chemical Biology, Kolkata, India

[3]School of Pharmacy, Sister Nivedita University, Kolkata, India

Correspondence
Amalesh Samanta, Division of Microbiology and Pharmaceutical Biotechnology, Department of Pharmaceutical Technology, Jadavpur University, 188 Raja S C Mullick Road, Kolkata 700032, India.
Email: asamanta61@yahoo.co.in and amalesh.samanta@jadavpuruniversity.in

Funding information
DST-INSPIRE; University Grants Commission RUSA

Abstract

The present study aims at developing and characterizing gum odina - sodium alginate based microsphere as a carrier for capecitabine. Microspheres with varying concentration of polymers (gum odina and sodium alginate) were formulated using calcium chloride as a cross-linker by ionotropic gelation technique. The formulated microspheres were optimized by entrapment efficiency, drug yield, particle size, swelling index, and in vitro drug release study. The optimized microsphere (F_6) was characterized in terms of SEM, AFM, FTIR, XRD, degradation study, moisture content study, and antioxidant activity. The F_6 was spherical in shape with a mean diameter of 568.33 ± 45.76 μm and drug entrapment efficiency of 45.91 ± 2.94%. In vitro dissolution study of optimized formulation exhibited negligible released in 0.1 N HCl (pH 1.2) and followed by 100% release in phosphate buffer (pH 7.4) within 24 h. In vitro cytotoxicity assay (MTT) of formulation F_6 on HT29 human colon cancer cell line indicated inhibition of the proliferation of tumor cell over a longer period of time. The overall experiment indicated that capecitabine loaded natural polymers based formulated microsphere could be a promising approach for the prevention of colon cancer.

KEYWORDS

capecitabine, colon cancer, gum odina, sodium alginate

1 | INTRODUCTION

Colon cancer is the most disastrous cancer and third most commonly diagnosed malignancy worldwide.[1] Incidence of colon cancer related death is mostly found in Europe, Asia, and South America due to changes of their habitual lifestyle and food habit.[2] In India every year more than 66,000 cases of colon cancer are also reported.[3] Many previous reports suggest that this malignancy mainly starts with the development of polyps, which can be benign or non-cancerous and later develop into cancerous lesions.[4] Both natural and synthetic drugs have been used as a chemotherapeutic agents for the treatment of colon cancer but however it causes public health problems like systemic accumulation of the drug, low therapeutic index, and unwanted side effects.[5] Hence, it is necessary to design prolong acting and targeted drug delivery system for the treatment of colon cancer to overcome the disadvantages of conventional chemotherapeutic approaches.

The oral route is the most convenient and preferred route than other routes due to less pain, reduced risk of

infection, needle stick injuries, and so forth.[6] But, apart from the aforementioned advantages, most of the conventional oral drug delivery system is unable to reach colon by avoiding the destruction in the upper gastrointestinal tract.[7] Thus, designing of safe and effective colon specific delivery system making a matter of concern for us.

Capecitabine is a prodrug of 5-flurouracil which was widely used as chemotherapeutic agent from several decades for the treatment of colon cancer. Excellent tolerability and intra- tumor drug concentration after preferential activation of capecitabine made it was a drug of choice for the treatment of colon cancer. But it has been not as effective as this drug has short plasma half-life <0.85 h that leads to rapid elimination from the body.[8] High dose (1250 mg) of capecitabine is needed twice per day leads to common over dose related toxicity like bone marrow depression, cardiotoxicity, diarrhea, nausea, vomiting, dermatitis, and so forth.[9] Hence, it is needed to develop such system that may deliver a chemotherapeutic agent to the tumor with retained therapeutic efficacy of drug. Microsphere based drug delivery systems may be the effective way of delivering the drug to the colonic region.[10]

From past few decades, natural polymers based various drug delivery systems were considered as significant approachable technique for the researchers.[11]Among various natural polymers sodium alginate has been widely used as a drug delivery matrix due to its nontoxic, biodegradable properties.[12] Alginate consist of (1,4)-linked β-D-mannuronic acid (M) and α-L-guluronic acid (G) residues. The G-blocks of sodium alginate participated in the formation ionotropic gelation with various multi-valentcations (Ca^{2+}, $Cd^{2+,}$ $Ba^{2+,}$ Zn^{2+}, Al^{3+}, and so forth).[13] Physiochemical properties of various drugs have been improved by incorporating within calcium alginate microsphere.[14] However, the drug release properties of ionotropically cross-linked calcium alginate microspheres exhibited several serious problems like poor entrapment efficiency, quick degradation and rapid burst release of drugs in the intestinal pH.[15] Gum odina is an anionic polysaccharides obtained from the bark of *Odina woider*, family Anacardiaceae.[16] It is a prebiotic which upon metabolism liberates lactic acid, acetic acid and other short chain organic the immune system by increasing IgA against any kind of infection in gut.[17]

Till date, no study has been found regarding the formation of polyelectrolyte complex between gum odina and sodium alginate with calcium ion for drug delivery at colonic region. In this context we developed and optimized capecitabine loaded microsphere consisting of gum odina – sodium alginate by various techniques likes entrapment efficiency, drug yield, in vitro drug release, swelling index, and particle size. We have studied the different physiochemical properties of optimized microsphere by using various advanced analytical tools such as Fourier transform infrared (FTIR) spectroscopy, surface morphology analysis by scanning electron microscopy (SEM), AFM study, X-ray diffraction (XRD), moisture content and degradation study, antioxidant activity (DPPH assay) and in vitro cytotoxicity against HT29 colon cancer cell line.

2 | EXPERIMENTAL

2.1 | Materials

All chemicals and reagents were used of analytical grade. Capecitabine, sodium alginate (216.12 g/mol), calcium chloride (110.98 g/mol), dipotassium hydrogen phosphate (174.2 g/mol), potassium dihydrogen phosphate (136.09 g/mol), sodium hydroxide pellet (40 g/mol), hydrochloric acid (36.458 g/mol), DPPH (2, 2-diphenyl-1-picrylhydrazyl) (394.32 g/mol) were purchased from Merck Specialities Private Limited, Mumbai. Dulbecco's Modified Eagle's Medium (DMEM REF 31600-034) was obtained from Gibco Life Technologies, India. Deionized water was used for all analyses.

2.2 | Methodologies

2.2.1 | Collection, purification, and quantification of carboxyl group number of gum odina

Gum odina was obtained from the barks of tropical deciduous plant *Odina wodier*, Roxb., of family Anacardiaceae, from Maheshtola South 24 Parganas District, West Bengal, India. Purification process of gum odina was performed according to earlier reported method.[18] Briefly, the crude gum odina was kept overnight in deionized water for complete swelling of the sample. Then viscous solution was allowed to stir continuously with a mechanical stirrer (REMI Lab Stirrer, India) upto 6 h at room temperature. The brown homogenized viscous solution was allowed to stand for 12 h at ambient temperature and passed through muslin cloth to get a clear solution. The solution was centrifuged (Thermo Scientific Heraeus Biofuge Stratos Centrifuge, Osterode, Germany) at 1500 rpm for 15 min. This solution was slowly added into absolute ethanol and white precipitate was obtained. The precipitate was further purified with combination of absolute ethanol and dry ether. After that purified gum odina was allowed to dry overnight at room temperature. Dried purified gum odina was powdered and stored in desiccator for further use.

Carboxyl group of gum odina was estimated by back titration method using sodium hydroxide, hydrochloric acid (HCl) and phenolphthalein as an indicator.[19] The carboxyl group of gum odina was measured three times and it was found that carboxyl group content of 27.86 g/L in gum odina.

2.2.2 | Preparation of capecitabine loaded gum odina-sodium alginate composite microspheres

Capecitabine loaded gum odina-sodium alginate composite microspheres were prepared by ionic gelation technique[20] using calcium chloride as a crosslinking agent. Briefly, aqueous slurry of sodium alginate and gum odina was prepared separately. Polymeric mixtures (1% concentration of gum odina, 3% concentration of sodium alginate) were well mixed on magnetic stirrer (REMI Lab Stirrer, India) at 1000 rpm up to 10 min. Drug was then added to the polymeric mixtures. The ratio of drug and polymer mixtures were taken as 1:2 in all the formulations; and mixed vigorously until uniform mixture was achieved. After that the resulting dispersions were added drop wise into calcium chloride solution of various concentrations (2.5%, 5%, and 7.5%) via a 26 gauge needle using a syringe. The solution was allowed to stir continuously for 15 min at 50 rpm by using magnetic stirrer (REMI Lab Stirrer, India). Then microspheres were collected by decantation, washed with deionized water for three times and dried at 40°C up to 6 h. The dried microspheres will be stored in desiccator for further use.[20]

2.2.3 | Drug entrapment efficiency and percentage yield of microspheres

Total drug content in microspheres were evaluated by previously reported method.[20] Dried microspheres (20 mg) were placed in mortar and crushed with pestle. The crushed powder of microspheres were dissolved in phosphate buffer pH 7.4 and kept aside for 24 h at 40°C. Then the sample was sonicated (Digital Ultrasonic Cleaner, Equitron PVT. LTD., India) for 15 min. After that aliquot was taken from the supernatant and analyzed by using a UV spectrophotometer (Shimadzu, Japan) at 276 nm.[20] The percentage of encapsulation efficiency was calculated by the following formula.

$$EE(\%) = \frac{ED}{AD} \times 100. \quad (1)$$

where EE (%) is the percentage encapsulation efficiency; ED is the amount of encapsulated drug; and AD is the amount of added drug.

The percentage yield of microspheres was calculated using the following formula.[21]

$$YD(\%) = \frac{C_m}{C_s} \times 100 \quad (2)$$

where YD (%) is the drug percentage yield, C_m denotes total mass of microspheres and C_S denotes the quantity of total added solid component.

2.2.4 | Microspheres size

Mean particle size of microspheres was determined according to the method described by Rastogi et al.,[22] using optical microscope (Olympus India Private Ltd.). The ocular micrometer was previously calibrated using stage micrometer.

2.2.5 | Swelling study

Swelling study of all formulated microspheres was carried out in two different solutions, namely, 0.1 N HCl (pH 1.2) and phosphate buffer (pH 7.4).[23] Briefly, 20 mg of dried microspheres (W_d) were placed in each two petriplates; and filled with 20 ml of 0.1 N HCl (pH 1.2) and phosphate buffer (pH 7.4). Petriplates were then kept aside for 24 h. The swelled microspheres (W_s) were removed from the petriplates and weighed accurately after drying the surface of microspheres using tissue paper. The percentage of swelling index was calculated by the following equation.

$$\text{Swelling index}(\%) = \frac{W_s - W_d}{W_d} \times 100. \quad (3)$$

where W_s is the weight of swollen microspheres and W_d is the weight of dried microspheres.

2.2.6 | In vitro release study

The release profile of capecitabine from microspheres in 0.1 N HCl (pH 1.2) and phosphate buffer (pH 7.4) were evaluated using a USP type 1 dissolution apparatus (Campbell Electronics, India) at 37°C ± 0.5°C with continuous stirring at 50 rpm.[24] Accurately weighed dried microspheres containing capecitabine (equivalent to 100 mg of drug) were placed into 900 ml of0.1 N HCl (pH 1.2) up to 2 h. Then it was kept at phosphate buffer (pH 7.4) for next 6 h. At predetermined intervals 1 ml of samples were withdrawn and replaced with fresh dissolution medium to maintain sink condition. The samples were diluted, filtered and the drug contents were determined by UV–Vis

spectrophotometer (Shimadzu, Japan) at 276 nm. The in vitro drug release data were plotted in various kinetic models like zero order, first order, Higuchi and Korsemeyer–Peppas to predict the drug release kinetics.[25]

2.2.7 | Surface morphology analysis

Surface morphology of optimized microsphere (F_6) was determined by SEM (Model: ZEISS EVO-18).[26] The sample was examined after coating with platinum by an auto fine coater operated at an acceleration voltage of 15 kV under ambient condition.[27]

2.2.8 | Atomic force microscopy

For the AFM imaging study the solution of microsphere were diluted upto 100 fold with water. Then 5 µl of aqueous solution of optimized microsphere was placed on the surface of 20 mm diameter of the mica sheet and then allowed to air dry till overnight.[28] The AFM data of optimized the microspheres were determined at room temperature with the help of Atomic Force Microscopy (Dimension Icon, Bruker, Karlsruhe, Germany) using silicon nitride probe having a resonance frequency of 150–350 kHz with constant force of 0.4 N/m, respectively. The images were analyzed by Pico View 1.12 version software.[29]

2.2.9 | Fourier transform infrared spectroscopy

FTIR spectrum of optimized microsphere (F_6) and individual components (gum odina, sodium alginate and capecitabine) were determined by FT-IR spectrometer (Shimadzu FTIR-8400S) in the range between 4000 and 500 cm^{-1} at a resolution of 4 cm^{-1} with scan speed of 1 cm/s.[30]

2.2.10 | X-ray diffraction study

XRD pattern of capecitabine and optimized formulation (F_6) were obtained by X-ray diffractometer (Ultima III theta – theta gonio) in the scanning range of 0–90°.[31] The X-ray tube was operated at 40 kV tube voltages and 30 mA tube current, using Cu as a radiation source.

2.2.11 | In vitro biodegradation study

The in vitro biodegradation study of optimized formulation (F_6) was carried out according to earlier reported method[32] with some modifications to study the biodegradability and morphological stability. Briefly, 20 mg of microspheres (W_0) were taken in physiological media (PBS 7.4) in presence of 0.2% (wt/vol) lysozyme and incubated for 28 days at 37°C. After every 7 days, sample (W_t) was taken out, washed with deionized water and dried. The percentage of degradation was calculated by using the following equation.

$$\text{Degradation}(\%) = \frac{W_0 - W_t}{W_t} \times 100. \quad (4)$$

2.2.12 | Moisture content study

Moisture content of optimized microsphere (F_6) was determined by adapting a method described by Wang et al.[33]Accurately weighed 250 mg (W_0) of optimized microsphere was placed in a desiccator (containing silica gel) at room temperature. The weight of optimized microsphere (W_t) was measured daily until a constant weight was achieved. Moisture content was determined by using following equation.

$$\text{Moisture content}(\%) = \frac{W_0 - W_t}{W_t} \times 100. \quad (5)$$

2.2.13 | Antioxidant activity (DPPH assay)

Antioxidant activity of the optimized formulation (F_6) was determined by its scavenging ability on the stable radical DPPH (2, 2-diphenyl-1-picrilhydrazil).[34] The formulation (F_6) was incubated with ethanolic solution of DPPH for 8 h in dark place at room temperature. After that 200 µl of sample solution was withdrawn and absorbance was measured using microtitreplate reader (Spectra Max M5, Molecular Devices, CA) at 517 nm (A_S). Absorbance of control experiment was measured as $\boldsymbol{A_c}$. The free radical scavenging activity (%) was calculated according to the following equation.

$$\text{The percentage of free radical scavenging activity}(\%) = \frac{A_c - A_s}{A_c} \times 100. \quad (6)$$

2.2.14 | Cell culture

HT29 Human colon cancer cell line was purchased from the National Centre for Cell Sciences (NCCS), Pune, India and were maintained in Dulbecco's Modified Eagle's Medium (DMEM), which was supplemented with

10% heat inactivated fetal bovine serum (FBS), 4.5 g/L glucose, 4 mM glutamine, 110 mg/L sodium pyruvate, 1.5 g/L sodium bicarbonate, 50 µg/ml streptomycin and 50 µg/ml penicillin.[35,36] HT29 cells were incubated in the humidified air containing 5% of CO_2 at 37°C. Cells were replenished and sub-cultured as per ATCC recommendations (ATCC, Manassus, VA).[37,38]

2.2.15 | Cell viability assay

The cell viability assay of optimized microsphere (F_6) was performed by (3-[4,5-dimethyl thiozol-2yl]-2,5 diphenyltetrazolium bromide) MTT assay on HT29 cell line.[39,40] Here only the viable cells were reduced MTT to the formazan crystals. In this event, viable cells were used the mitochondrial dehydrogenase enzyme. Cells were seeded into 96 well plates maintaining an optimal count of around 10^3 viable cells in each well. Cells were incubated for 1 day. Viability assay was performed with 4 µl of blank microsphere, optimized formulation, and capecitabine (drug) at different time points. We incubated the cells (after addition of the three compounds) for 2, 6, 12, 18, and 24 h. After treatment of the cells with the compounds, we replaced the media with the MTT containing media (1 mg/ml) and incubated them at 37°C in a humidified 5% CO_2 for 4 h. After incubation period, supernatant was removed and diluted the cells in 100 µl of MTT solubilization solution DMSO and plats were gently shaken to solubilize the formazan crystals.[37] The relative formazan formation in each well was checked by determining the absorbance at 540 nm[20] using a microplate reader (MultiSkan, Thermo Scientific). The cell viability was calculated using the following formula.

$$\text{Cell viability}\,(\%) = \frac{\text{Mean OD samples}}{\text{Mean OD of control group}} \times 100. \quad (7)$$

2.2.16 | Statistical analysis

The experimental data were measured as mean ± *SD*. Each experiments were predicted in triplicate ($n = 3$). Statistical evaluation of data was performed using analysis of variance (ANOVA) with Graph Pad InStat 3.1 software. $P < 0.05$ was considered for statistically significant.

3 | RESULTS AND DISCUSSION

3.1 | Formation of microspheres

When polymeric mixture of sodium alginate and gum odina was added dropwise into calcium chloride solution, microspheres were formed instantaneously due to intermolecular cross linking among the divalent calcium chloride and negatively charged carboxyl group of alginic acid and gum odina. Capecitabine loaded freshly formulated microspheres appeared as spherical, translucent, white and elastic in nature. But after drying, the prepared microspheres became light brownish, smaller, dense and hard; which is very similar to the result observed in the previous study of mucoadhesive alginate beads.[41]

3.2 | Percentage yield and percentage drug entrapment efficiency

The percentage yield of different batches of capecitabine varies from 61.29% to 90.74% (Figure 1a) this might be due to agglomeration accompanied between sticking of polymers to blades of stirrer and wall of the beaker during microsphere formation. Drug entrapment efficiency was expressed as amount of total drug actually entrapped in microsphere. Drug entrapment efficiency of different formulations varies from 21.44 ± 0.87% to 49.5 ± 2.58% (Figure 1b) due to variation of composition of microsphere. It was found that an increased in the concentration of sodium alginate leads to enhance drug entrapment efficiency significantly ($p < 0.05$).This occurred due to highly dense internal structure of polymeric matrix thus, preventing migration of drug in to crosslinking solution.[15]Again drug entrapment efficiency increased with increasing concentration of cross linking agent which hardened outer layer of the polymeric microspheres leading to reduction of drug leaching into the external phase.[42]

3.3 | Microsphere size

Size of microsphere is an important parameter to determine drug release, biodistribution, cellular uptake as well as the stability of the formulations. Particle sizes of all microspheres (F_1, F_2, F_3, F_4, F_5, and F_6) ranged from 330.33 to 568.33 µm (Figure 2). It was observed that diameter of particles were increased significantly ($p < 0.05$) with increasing concentration of sodium alginate in the formulations. It might be due to increase in viscosity of polymeric mixture and subsequently decreased in flow of the polymeric mixture through the needle, resulting in formation of microsphere with larger diameter. Larger size microspheres have a high affinity to aggregate compared to smaller ones ensuing in sedimentation. Again smooth, spherical microspheres were formed with increasing concentration of calcium chloride with sodium alginate during formulation of microspheres.[41] The result could be attributed to the variations in the availability of binding sites for crosslinking agent.

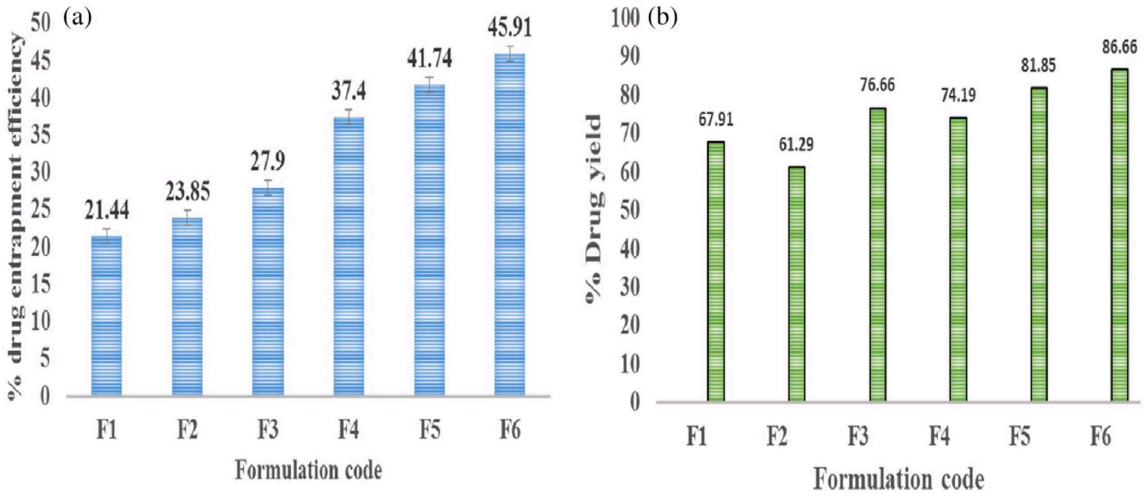

FIGURE 1 (a) % drug entrapment efficiency and (b) % drug yield of F_1, F_2, F_3, F_4, F_5, and F_6. Values were represented as mean ± *SD* in triplicate [Color figure can be viewed at wileyonlinelibrary.com]

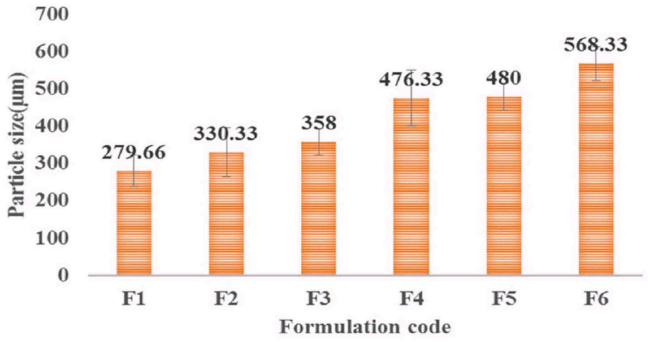

FIGURE 2 Particle size (μm) of F_1, F_2, F_3, F_4, F_5, and F_6. Values were represented as mean ± *SD* in triplicate [Color figure can be viewed at wileyonlinelibrary.com]

Moreover, excess of concentration of calcium chloride solution resulted in decreased average sizes of microspheres. This might be due to shrinkage of polymeric gel by higher degree of cross-linking agent.[42]

3.4 | Swelling study

Swelling behavior of capecitabine loaded gum odina - alginate microspheres were evaluated in 0.1 N HCl (pH 1.2) and phosphate buffer (pH 7.4). It was noticed that swelling index of formulated microspheres were minimum at acidic pH due to shrinkage of alginate,[41] whereas maximum swelling was observed in phosphate buffer pH 7.4 due to erosion of polymer matrix. Swelling characteristics of microspheres were performed in terms of equilibrium swelling condition. The result also indicated that swelling properties also dependent on concentration of cross-linking agent. It was found that decrease in concentration of crosslinking agent for formulation F_1, F_2, F_4, and F_5 swelling index also increased significantly ($p < 0.05$). The formulations (F_3 and F_6) with calcium chloride concentration more than 5% exhibited low swelling index due to of rigid polymeric matrix and less number of surface pores available for water penetration.[42]

3.5 | In vitro release study

The study of in vitro drug release from formulated microspheres (F_1–F_6) were performed in 0.1 N HCl, (pH 1.2) for the first 2 h and in phosphate buffer (pH 7.4) for the next 6 h has been depicted in Figure 3a,b. Rate of drug released from formulated microspheres were minimum at physiological environment of stomach, might be due to poor solubility and shrinkage of calcium alginate at acidic pH.[41] In phosphate buffer pH 7.4, faster release of drug from microspheres were found, which might be due to higher swelling rate of microspheres. In addition releases of capecitabine from microspheres were found to be slower with increasing crosslinking agent ($CaCl_2$) concentration. The higher concentration of cross linking agent could produce a rigid polymeric structure and facilitated poor entry of dissolution media in polymeric matrix, which could lower the drug release from microspheres. Drug release in 8 h from formulations F_1 to F_6 were within the range of 91.05 ± 2.77% to 73.27 ± 7.97% and this was found to be higher with decreasing of sodium alginate and gum odina ratio in polymeric mixture. For example F_1 containing 1:2 ratio of polymeric mixture exhibited initial drug release 52.62 ± 4.16% at 2 h whereas formulation F_6 containing 1:3 ratio of

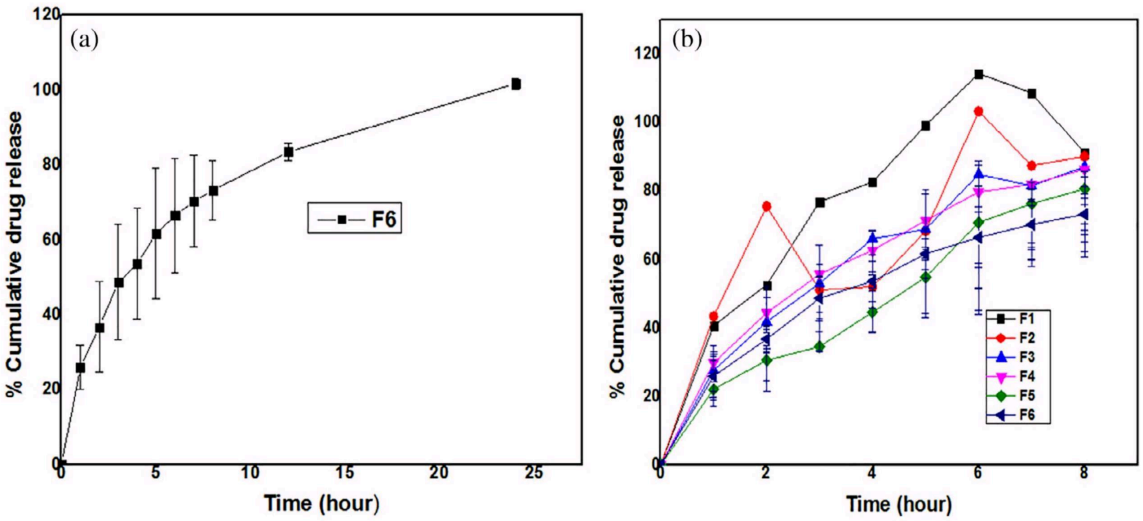

FIGURE 3 In vitro drug release profile of (a) capecitabine from F_6 and in vitro drug release profile of (b) capecitabine from F_1, F_2, F_3, F_4, F_5, and F_6. Values were represented as mean ± *SD* in triplicate [Color figure can be viewed at wileyonlinelibrary.com]

polymeric mixture reveled initial drug release 36.732 ± 12.06% at 2 h. The results indicate that the drug release gradually slow down significantly ($p < 0.05$) with increasing polymer concentration. In case of gum odina-alginate based microsphere containing higher amount of sodium alginate might formed viscous gel structure thus reducing the rate of swelling as well as release of the drug from polymeric matrix.[39] From Figure 3b it can be seen that formulation F_6 (73.27%) exhibited significant release of drug molecules for 8 h as compared to F_1, F_2, F_3, F_4, and F_5 (91.05%, 90.18%, 87.177%, 86.44%, and 80.67%) which consist of lower concentration of polymers. For formulation F_6cumulative percentage of drug release was continue up to 24 h and found that 83.52% release in 12 h and 100% release completed within 24 h.

Drug release kinetics study was examined by curve fitting method according to zero order, first order, Higuchi model (Table 1). It has been observed that the release of capecitabine from formulated microspheres followed Higuchi model kinetics on the basis of correlation coefficients (R^2) over a periods of 8 h. Release exponent data (n) of different formulations were evaluated by Korsemeyer–Peppas model. The results indicated formulation F_3, F_4, F_5, and F_6 followed nonfickian (anomalous transport) type ($1 < n < 0.5$)[41] whereas F_1 and F_2 followed fickian transport mechanism (Table 1). Anomalous transport refers to combination of both diffusion and erosion controlled rate release where fickian release only followed diffusion mechanism. From experimental studies it was found that formulation F_6 revealed best control of drug release with average swelling index and highest entrapment efficiency. Hence, F_6 was selected as an optimized formulation for carrying out of other crucial experiments.

3.6 | Surface morphology analysis

The surface morphology of F_6 microsphere was observed under SEM at different magnifications and was presented in Figure 4a,b. The SEM photographs of the microsphere showed spherical shape with a rough surface, exhibiting pores on it. The spherical shape of microsphere resulted from the coagulation process which occurred instantly during the interaction of polymeric mixture with the calcium ions. In addition, the porous structure might be resulted from shrinkage of polymeric matrix.[43] This porous structure of microsphere is desirable for water uptake, swelling, and release mechanisms. Presence of some polymeric debris on the surface of microsphere might be due to simultaneous gel preparation and formation of the polymer-blend matrix. Absence of capecitabine crystal on the surface of microsphere could be attributed to the complete dispersion of the drug throughout the polymeric matrix.[20] This physical state of drug in the formulated microsphere might be played a crucial role on drug release kinetics.

3.7 | AFM study

AFM topography images (Figure 5) of optimized formulation revealed that surface of microsphere was smooth, spherical in shape without any such huge number of cervices or cracks, which might be attributed to the presence of crosslinker (calcium chloride). Furthermore AFM data exhibited very tiny particles which formed micro size cluster with amplitude value 200 Mv and maximum height 1 μm. On the other hand crosslinking agent reduced porosity of matrix and normalizes microsphere surface and couture the matrix properties.[44] The

TABLE 1 Release profile of capecitabine from different formulation showing the R^2 value in different kinetics model

Formulation code	Correlation coefficients (R^2 value)			Model of best fit	Korsemeyer–Peppas model		
	Zero order	First order	Higuchi		Correlation coefficient (R^2 value)	Release exponent (n)	Release mechanism
F_1	0.780	0.484	0.915	Higuchi	0.894	0.487	Fickian
F_2	0.687	0.444	0.797	Higuchi	0.551	0.330	Fickian
F_3	0.909	0.540	0.985	Higuchi	0.985	0.567	Non-Fickian
F_4	0.902	0.520	0.994	Higuchi	0.978	0.516	Non-Fickian
F_5	0.948	0.618	0.974	Higuchi	0.957	0.660	Non-Fickian
F_6	0.898	0.526	0.996	Higuchi	0.993	0.510	Non-Fickian

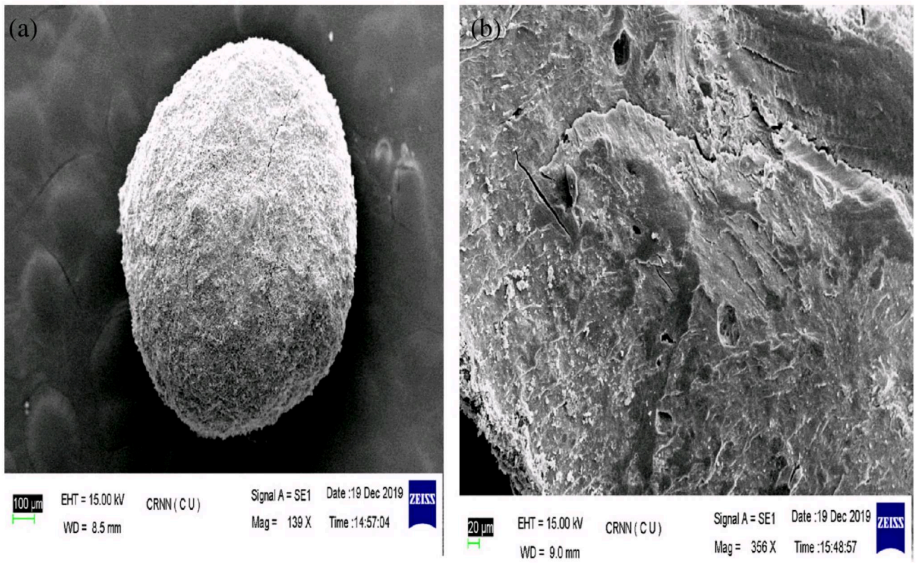

FIGURE 4 SEM images of (a) optimized microsphere (F_6) and (b) pores present on rough surface of microsphere [Color figure can be viewed at wileyonlinelibrary.com]

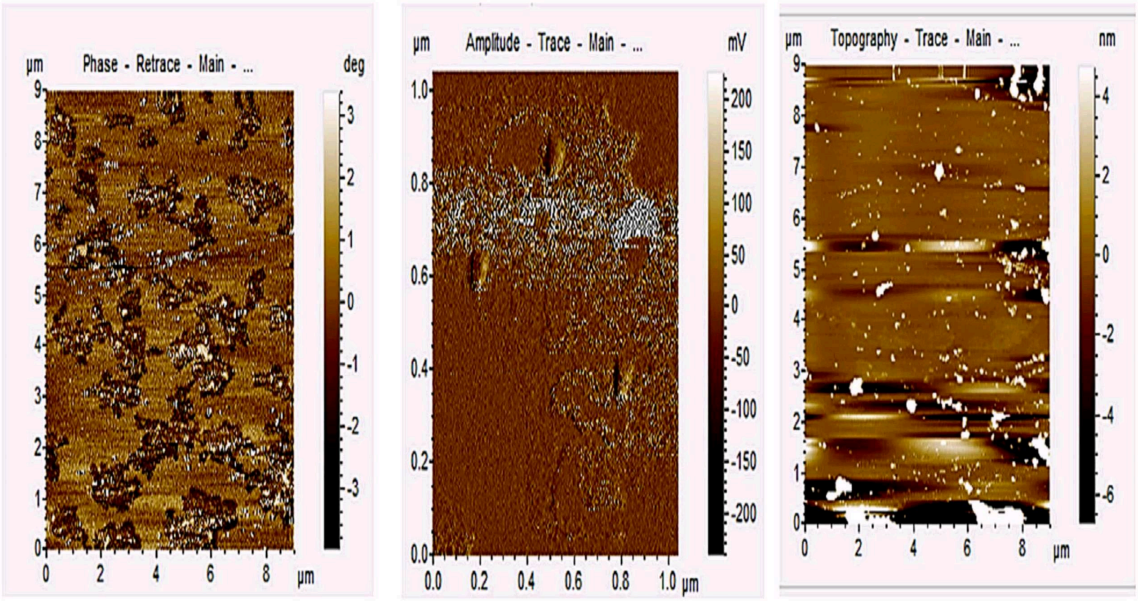

FIGURE 5 Atomic force microscopy images of F_6 [Color figure can be viewed at wileyonlinelibrary.com]

reduction in cracks and porosity to a certain extent, probably contributed to the controlled release of encapsulated drug molecule from microsphere to the targeted organ.[29]

3.8 | FTIR study

The FTIR spectra of sodium alginate, gum odina, capecitabine, and optimized formulation (F_6) were shown in Figure 6. The FTIR spectrum of sodium alginate (Figure 6a) showed the band appearing around 1415 and 1616 cm^{-1} for symmetric and asymmetric C–O stretching vibrations of COO− anions, respectively and wideband appeared due to the OH stretching vibrations at 3441 cm^{-1}.[20] In case of gum odina (Figure 6b), characteristic band at 3304, 2920, 1598 cm^{-1}, indicated that the stretching of –OH, CH, −COO (asymmetric). Several peaks at 1413.50 cm^{-1} (CH_2 bending), 1050–1015 cm^{-1} (C—C stretching and OH-bending) were observed.[45] The characteristics peaks of pure drug capecitabine (Figure 6c) at the wavenumber of 3520, 3215, 2958, 2861 cm^{-1} and at 1716 cm^{-1} indicated OH stretching, NH stretching, CH stretching, aldehyde group (CHO) vibrations and CO carbonyl group of stretching vibrations respectively. Peaks at 1502, 1245, 1042, and 1202 cm^{-1} showedNO bending vibrations, CN bending vibrations. C–F stretching vibrations as well as the presence of tetrahydrofuran ring respectively.[31] The FTIR spectrum of F_6 (Figure 6d) showed various characteristic peaks of sodium alginate, gum odina, and capecitabine without any significant shifting of these peaks suggested that blending of drug molecules with other formulating agents did not make any significant changes in the individual characteristics of the components. Thus, it can be concluded from the FTIR data that no possible chemical interaction took place between the drug candidate and polymeric mixture, suggesting that the chemical nature of the drug were preserved during formulation of microsphere, making the microsphere formulation good enough to facilitate the prevention of colon cancer.

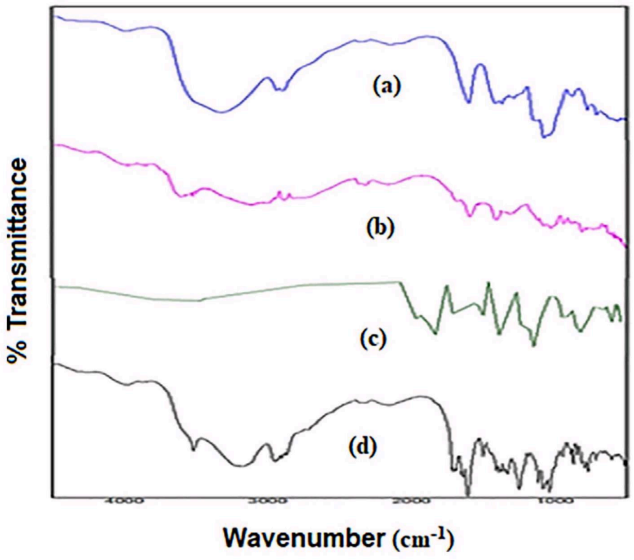

FIGURE 6 FTIR spectra of (a) gum odina, (b) sodium alginate, (c) capecitabine and (d) F [Color figure can be viewed at wileyonlinelibrary.com]

3.9 | X-ray diffraction study

The X- ray diffraction pattern of drug and drug loaded microsphere (F_6) were presented in Figure 7a,b. Capecitabine exhibited sharp intense peaks at 2θ of 5, 20, and 25° indicating crystalline nature of drug. Absence of characteristic crystalline peaks of the drug in the formulation (F_6) could be due to progressive amorphization of the capecitabine after entrapping into polymeric matrix.[31] The conversion of crystalline to amorphous nature of the drug significantly exhibited greater hygroscopicity, dissolution rate, solubility, and bioavailability of the capecitabine at desired side of action (colon).[46]

3.10 | Degradation studies

In vitro biodegradation study of optimized microsphere was done after incubation in PBS 7.4 to find out morphological stability as well as biodegradation. The formulation F_6 showed degradation of 11 ± 0.74%, 22.45 ± 0.023% and 35.55 ± 0.20% after 7, 14 and 28 days, respectively. Results showed that degradation of optimized microsphere in PBS 7.4 occurred in controlled manner up to 28 days. The decreased in weight of microsphere at PBS could be attributed to biodegradation of polymeric matrix (gum odina, sodium alginate) due to the large surface area, porous nature of microsphere to absorb fluid and swell, causing the outer polymer matrix to degrade. Result of in vitro biodegradation study indicated that extent upon concentration of crosslinking agent with polymeric mixture which tends to prevent the rapid erosion of microsphere and consequently retard their degradation.[47] The steady degradation at pH 7.4 confirms biodegradation of microsphere at the site of the colon (pH of nearly 7.4). There by capecitabine loaded gum odina-sodium alginate based polymeric microsphere significantly used as potent biodegradable formulation for colon targeted drug delivery system.

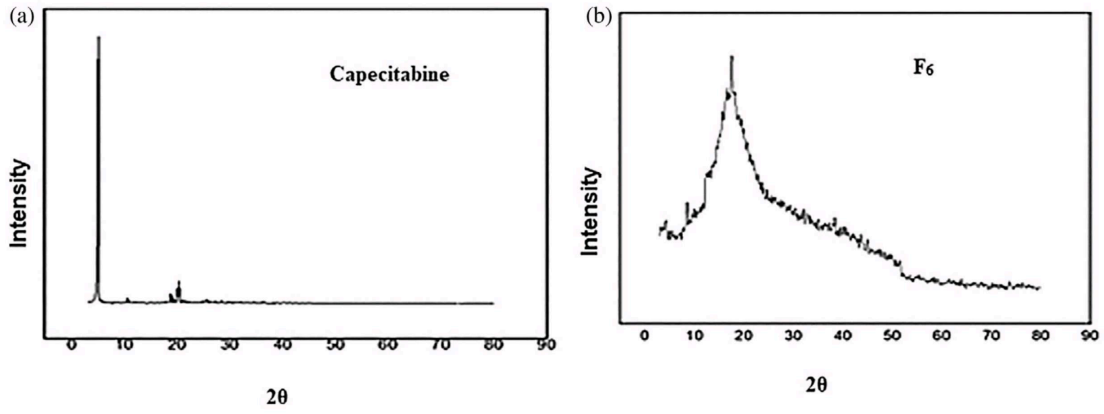

FIGURE 7 X-ray diffraction study of Capecitabine (a) and F_6 (b)

3.11 | Moisture content study

The moisture content (%) of optimized microsphere (F_6) showed 9.92 ± 5.38%. Sander et al.,[48] stated that moisture content of microsphere generally less than 10%. High moisture content in the formulation leads to particle agglomeration thus reducing the stability of the microsphere and there active components. In this study water was used as a medium of chemical reaction; hence, normally low moisture contents should be highly desirable since, it may impede interparticle cohesion, avoid drug degradation, and maintain long-term stability. Certain amount of moisture content in microsphere may prevent from being dry, brittle and also improve the stability of the microspheres.[33] Formulating agents gum odina, sodium alginate are hydrophilic in nature which could be played a significant role by moistening the microspheres and reducing them from being brittle.[49] De et al.,[18] has been already reported that gum odina has low moisture content value which indicated that potential uses as a carrier of moisture sensitive drugs. Moreover presence of adequate amount of water molecules in the surface of microspheres facilitated better flow and wetting properties of the particles and subsequently increased in the process of drug dissolution.[50]

3.12 | Antioxidant activity (DPPH assay)

Antioxidant capacity of optimized microsphere was determined by DPPH scavenging activity. Results of DPPH assay of F_6 indicated 40.58 ± 1.46%, 46.16 ± 0.16%, 83.51 ± 0.44% and 88.13 ± 0.771% scavenging after 2, 4, 6, and 8 h, respectively (Figure 8). Data were expressed as mean ± *SD* of triplicate measurements. Antioxidant behavior of microsphere might be due to the formulation components such as gum odina[18] and sodium alginate.[51]

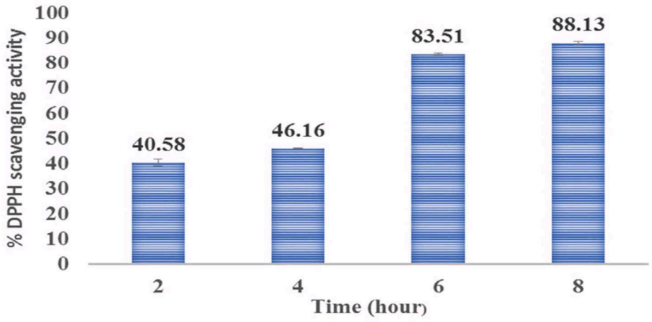

FIGURE 8 The antioxidant activity of F_6 at varying time intervals. Values were represented as mean ± *SD* in triplicate [Color figure can be viewed at wileyonlinelibrary.com]

Das et al.,[52] explained overproduction of oxidative stress due to deficiency of antioxidant mechanisms. The oxidative stress has been associated with many pathogenic diseases including cardiovascular diseases, cancer, inflammatory disease, and so forth. Antioxidants are chemo preventive by slowing progression of cancer.[53] This antioxidant property of formulation F_6 would be contributed to inhibit the tumor cell growth by antioxidant enzymes which directly resist the oxidant attack and may protect cells against lipid peroxidation and DNA damage. The antioxidant efficacy of F_6 did not promote any significant changes of other formulating agents after incorporation of drug molecules. Moreover optimized formulation (F_6) may very much effective against oxidative stress and along with reactive oxygen species (ROS) which contributed to the development of colon cancer.

3.13 | In vitro cytotoxicity assay

MTT assay of drug, blank microsphere, and drug loaded optimized microsphere (F_6) were performed on HT 29 cell

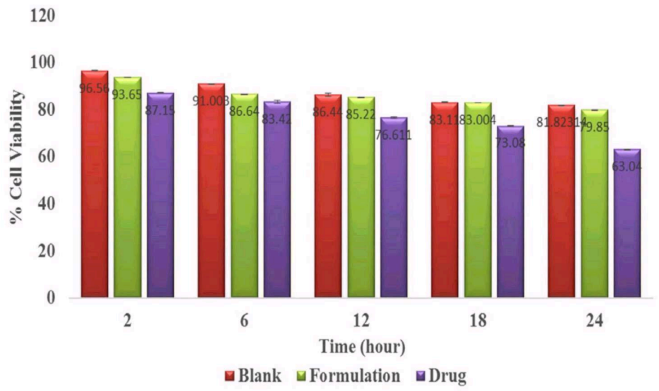

FIGURE 9 In vitro cytotoxicity profile of blank, formulation and drug. Values were represented as mean ± *SD* in triplicate [Color figure can be viewed at wileyonlinelibrary.com]

line at different time point; and this results might be attributed a higher degree of cell viability for the blank microsphere, indicating their safe use as a drug delivery system (Figure 9).[20] Capecitabine exhibited 12.85% cell death in 2 h when incubated with HT29 cell line which means only 87.15 ± 0.0558% cell was viable[20] but higher extent of cell viability was observed for blank microsphere (95.56 ± 0.048%) and formulation F_6 (93.65 ± 0.037%). The results might be attributed that optimized microsphere exhibited lesser cytotoxicity before they reach the colonic region.[20] Moreover pure drug capecitabine upto 6 h enhanced cell death and decreased the cell viability upto 83.42 ± 0.15% where in case of the blank microsphere and F_6, 91.00 ± 0.17% and 86.64 ± 0.60% cell viability was observed,[54] which represented that formulation F_6 was not released in the stomach region, and intended for colon targeting. From the experimental study it could be attributed that reduction cell viability statistically significant ($p < 0.005$) from 2 to 24 h in case of both blank microsphere and F_6, due to negatively charged carrier gum odina - alginate microsphere easily amalgamated with positively charged proteins present in damaged tissues of colonic mucosa.[55] These in vitro cytotoxicity results of formulation F_6 was quite similar with alginate-based chitosan hybrid polymer enhancing cell attachment and proliferation.[55] Ganguly et al.,[56] also reported 5-fluorouracil loaded enteric-coated PEG cross-linked chitosan microspheres induced apoptosis of HT29 tumor cell for prolong period of time, until the degradation of the polymer matrices. The overall result suggested that blending of capecitabine with other formulating agents like sodium alginate and gum odina, could be make the formulation (F_6) much effective for targeting colon cancer.

4 | CONCLUSION

In this study, novel capecitabine loaded gum odina – sodium alginate based microsphere for controlled delivery of capecitabine into colon was successfully developed and evaluated. The result of drug entrapment efficiency of optimized microsphere was found to be maximum (45.91 ± 2.94) than others. The in vitro drug release from optimized microsphere followed a sustained release pattern (Higuchi kinetics) with non-Fickian mechanismover 8 h in phosphate buffer (pH 7.4).The result of FTIR analysis confirmed the compatibility of the capecitabine with polymer mixture. The SEM and AFM images revealed that spherical shape with porous structure of optimized microsphere. The outcome of XRD study demonstrated that amorphous nature of the drug in optimized formulation. The antioxidant activity showed that regulation in the production of ROS indicated anticancer efficacy of the formulation. In vitro cytotoxicity assay of optimized formulation on HT29 cell line indicated reduction in abnormal cell proliferation significantly at sustained manner (from 2 to 24 h).

Additionally, further research is underway to investigate the stability of microsphere along with apoptosis assay; cell imaging; pharmacological & pharmacokinetic parameters on a mice model (in vivo study). Overall on the basis of correlation between physicochemical and biological parameters we concluded that capecitabine loaded gum odina-alginate based microsphere could be a promising oral delivery system for controlled drug delivery of capecitabine so as to reduce the dosage toxicity, dosing interval and also allow precise colon targeting.

ACKNOWLEDGMENTS

Ahana Hazra is thankful to University Grants Commission RUSA for providing the fellowship. The authors also acknowledge CRNN-Kolkata, India for SEM study. The authors are thankful to Department of Metallurgical and Material Engineering, Jadavpur University, Kolkata for FTIR, XRD study. The authors are highly grateful to the Department of Pharmaceutical Technology of Jadavpur University, India for providing all other necessary facilities to complete research work. Dwipanjan Sanyal acknowledges the Department of Science and Technology (DST) for doctoral fellowship (DST-INSPIRE). Dwipanjan Sanyal and Krishnananda Chattopadhyay acknowledge the Director, IICB.

CONFLICT OF INTEREST

The authors declare no conflicts of interest.

AUTHOR CONTRIBUTION

Ahana Hazra: Conceptualization, Investigation, Methodology, Writing - original draft. Dwipanjan Sanyal: Cell line study, In vitro cell cytotoxicity assay, Data curation, and analysis, Writing - review & editing. Arnab De: Formal analysis, Writing - review & editing. Sohini Chatterjee: Formal analysis. Krishnananda Chattopadhyay: Writing - review. Amalesh Samanta: Project administration, Supervision, Writing - review & editing.

DATA AVAILABILITY STATEMENT

The data that support the findings of this study are available on request from the corresponding author. The data are not publicly available due to privacy or ethical restrictions.

ORCID

Amalesh Samanta https://orcid.org/0000-0002-8502-7151

REFERENCES

[1] M. Arnold, M. S. Sierra, M. Laversanne, I. Soerjomataram, A. Jemal, F. Bray, *Gut* **2017**, *66*, 683.
[2] R. L. Siegel, K. D. Miller, S. A. Fedewa, D. J. Ahnen, R. G. Meester, A. Barzi, A. Jemal, *Cancer J. Clin.* **2017**, *67*, 177.
[3] F. A. Haggar, R. P. Boushey, *Clin. Colon Rectal. Surg.* **2009**, *22*, 191.
[4] C. Rosty, D. G. Hewett, I. S. Brown, B. A. Leggett, V. L. Whitehall, *J. Gastroenterol.* **2013**, *48*, 287.
[5] V. Sanna, A. M. Roggio, A. M. Posadino, A. Cossu, S. Marceddu, A. Mariani, V. Alzari, S. Uzzau, G. Pintus, M. Sechi, *Nanoscale Res. Lett.* **2011**, *6*, 260.
[6] S. Amidon, J. E. Brown, V. S. Dave, *AAPS PharmSciTech* **2015**, *16*, 731.
[7] D. Karuna, U. Udhumansha, G. Rathnam, M. Ganesh, H. Jang, *Turkish J. Pharm. Sci.* **2016**, *13*, 68.
[8] C. Kelly, N. Bhuva, M. Harrison, A. Buckley, M. Saunders, *Eur. J. Cancer* **2013**, *49*, 2303.
[9] R. Siegal, K. D. Miller, A. Jemal, *Cancer J. Clin.* **2014**, *64*, 9.
[10] X. Fu, Q. Ping, Y. Gao, *J. Microencapsul.* **2005**, *22*, 705.
[11] A. K. Nayak, H. Bera, M. S. Hasnain, A. De, D. Pal, A. Samanta, *Biopolymer-Based Nanomaterials in Drug Delivery and Biomedical Applications*, Academic Press, Cambridge **2021**, p. 313.
[12] J. Malakar, A. K. Nayak, D. Pal, *Int. J. Biol. Macromol.* **2012**, *50*, 138.
[13] N. Patel, D. Lalwani, S. Gollmer, E. Injeti, Y. Sari, J. Nesamony, *Prog. Biomater.* **2016**, *5*, 117.
[14] R. S. Al-Kassas, O. M. Al-Gohary, M. M. Al-Faadhel, *Int. J. Pharm.* **2007**, *341*, 230.
[15] D. Pal, A. K. Nayak, *Drug Deliv.* **2012**, *19*, 123.
[16] D. Mitra, A. Basu, B. Das, A. K. Jena, A. De, M. Das, S. Bhattacharya, A. Samanta, *RSC Adv.* **2017**, *7*, 29129.
[17] D. Mitra, A. K. Jena, A. De, M. Das, B. Das, A. Samanta, *Food Funct.* **2016**, *7*, 3064.
[18] A. De, D. Malpani, B. Das, D. Mitra, A. Samanta, *Carbohydr. Polym.* **2020**, *250*, 116950.
[19] C. Y. Wen, J. Y. Sun, *Chemistry Select* **2017**, *2*, 10885.
[20] P. Sinha, U. Udhumansha, G. Rathnam, M. Ganesh, H. T. Jang, *Int. J. Biol. Macromol.* **2018**, *117*, 840.
[21] H. L. Yu, Z. Q. Feng, J. J. Zhang, Y. H. Wang, D. J. Ding, Y. Y. Gao, W. F. Zhang, *BioMed Res. Int.* **2018**, *2018*, 9073420.
[22] R. Rastogi, Y. Sultana, M. Aqil, A. Ali, S. Kumar, K. Chuttani, A. K. Mishra, *Int. J. Pharm.* **2007**, *334*, 71.
[23] W. C. Lin, D. G. Yu, M. C. Yang, *Colloids Surf., B* **2005**, *44*, 143.
[24] P. Sinha, U. Ubaidulla, A. K. Nayak, *Int. J. Biol. Macromol.* **2015**, *72*, 1069.
[25] A. K. Jena, M. Das, A. De, D. Mitra, A. Samanta, *Asian J. Pharm. Clin. Res.* **2014**, *7*, 5.
[26] A. K. Jena, A. K. Nayak, A. De, D. Mitra, A. Samanta, *Future J. Pharm. Sci.* **2018**, *4*, 71.
[27] F. N. Parin, K. Yildirim, P. Terzioğlu, *J. Innov. Sci. Eng.* **2020**, *4*, 56.
[28] B. Saha, S. Chowdhury, D. Sanyal, K. Chattopadhyay, S. Kumar, *ACS Omega* **2018**, *3*, 2588.
[29] D. Dutta, A. Chakraborty, B. Mukherjee, S. Gupta, *ACS Appl. Bio Mater.* **2018**, *1*, 1538.
[30] F. N. Parın, K. Yıldırım, *Fibres Text. East. Eur.* **2021**, *1*, 17.
[31] S. A. Agnihotri, T. M. Aminabhavi, *Int. J. Pharm.* **2006**, *324*, 103.
[32] S. Das, A. De, B. Das, B. Mukherjee, A. Samanta, *J. Appl. Polym. Sci.* **2021**, *138*, 50057.
[33] S. Wang, Y. Sun, J. Zhang, X. Cui, Z. Xu, D. Ding, W. Zhang, *J. Front. Pharmacol.* **2020**, *11*, 230.
[34] B. Das, A. De, M. Das, S. Das, A. Samanta, *S. Afr. J. Bot.* **2017**, *109*, 16.
[35] S. Sarkar-Banerjee, S. Chowdhury, D. Sanyal, T. Mitra, S. Roy, K. Chattopadhyay, *Cell. Physiol. Biochem.* **2018**, *51*, 1658.
[36] S. Hazra, C. Bodhak, S. Chowdhury, D. Sanyal, S. Mandal, K. Chattopadhyay, A. Pramanik, *Anal. Bioanal. Chem.* **2019**, *411*, 1143.
[37] F. N. Parın, Ç. İ. Aydemir, G. Taner, K. Yıldırım, *J. Ind. Text.* **2021**, *112*, 1.
[38] S. Das, T. K. Dey, A. De, A. Banerjee, S. Chakaborty, M. K. A. Das Bhaskar, B. Mukherjee, A. Samanta, *Int. J. Pharm.* **2021**, *606*, 120892.
[39] S. Mukherjee, S. Hazra, S. Chowdhury, S. Sarkar, K. Chattopadhyay, A. Pramanik, *J. Photochem. Photobiol. A: Chem.* **2018**, *364*, 635.
[40] F. N. Parin, S. Ullah, K. Yildirim, M. Hashmi, I. S. Kim, *Polymer* **2021**, *13*, 3594.
[41] S. K. Dey, P. K. De, A. De, S. Ojha, R. De, A. K. Mukhopadhyay, A. Samanta, *Int. J. Biol. Macromol.* **2016**, *89*, 622.
[42] S. R. Soni, A. Ghosh, *Carbohydr. Polym.* **2017**, *174*, 812.
[43] P. Sinha, U. Ubaidulla, M. S. Hasnain, A. K. Nayak, B. Rama, *Int. J. Biol. Macromol.* **2015**, *79*, 555.
[44] G. A. Islan, G. R. Castro, *Drug Deliv.* **2014**, *21*, 615.
[45] A. De, B. Das, D. Mitra, A. K. Sen, A. Samanta, *Polym. Adv. Technol.* **2020**, *31*, 1814.
[46] A. Sahoo, R. Suryanarayanan, R. A. Siegel, *Mol. Pharm.* **2020**, *17*, 4401.
[47] M. Z. I. Khan, H. P. Štedul, N. A. Kurjaković, *Drug Devel. Indus. Pharm.* **2000**, *26*, 549.

[48] C. Sander, K. D. Madsen, B. Hyrup, H. M. Nielsen, J. Rantanen, J. Jacobsen, *Eur. J. Pharm. Biopharm.* **2013**, *85*, 682.
[49] K. Müller, M. Schmid, *Foods* **2018**, *7*, 10.
[50] N. Motlekar, B. B. Youan, *Drug Des. Devel. Ther.* **2008**, *2*, 39.
[51] S. Sellimi, I. Younes, H. B. Ayed, H. Maalej, V. Montero, M. Rinaudo, M. Nasri, *Int. J. Biol. Macromol.* **2015**, *72*, 1358.
[52] B. Das, A. De, S. Podder, S. Das, C. K. Ghosh, A. Samanta, *Inorg. Nano-Met. Chem.* **2021**, *51*, 1066.
[53] W. L. Stone, K. Krishnan, S. E. Campbell, V. E. Palau, *World J. Gastrointest. Oncol.* **2014**, *6*, 55.
[54] T. T. Jubeh, Y. Barenholz, A. Rubinstein, *Pharm. Res.* **2004**, *21*, 447.
[55] N. Iwasaki, S. T. Yamane, T. Majima, *Biomacromolecules* **2004**, *5*, 828.
[56] K. Ganguly, A. R. Kulkarni, T. M. Aminabhavi, *Drug Deliv.* **2016**, *23*, 2838.

How to cite this article: A. Hazra, D. Sanyal, A. De, S. Chatterjee, K. Chattopadhyay, A. Samanta, *J. Appl. Polym. Sci.* **2022**, *139*(26), e52374. https://doi.org/10.1002/app.52374

Volume 139 | Issues 25-26 2022
Included In This Print Edition:
Issue 25 (July 5, 2022)
Issue 26 (July 10, 2022)

JOURNAL OF Applied Polymer SCIENCE

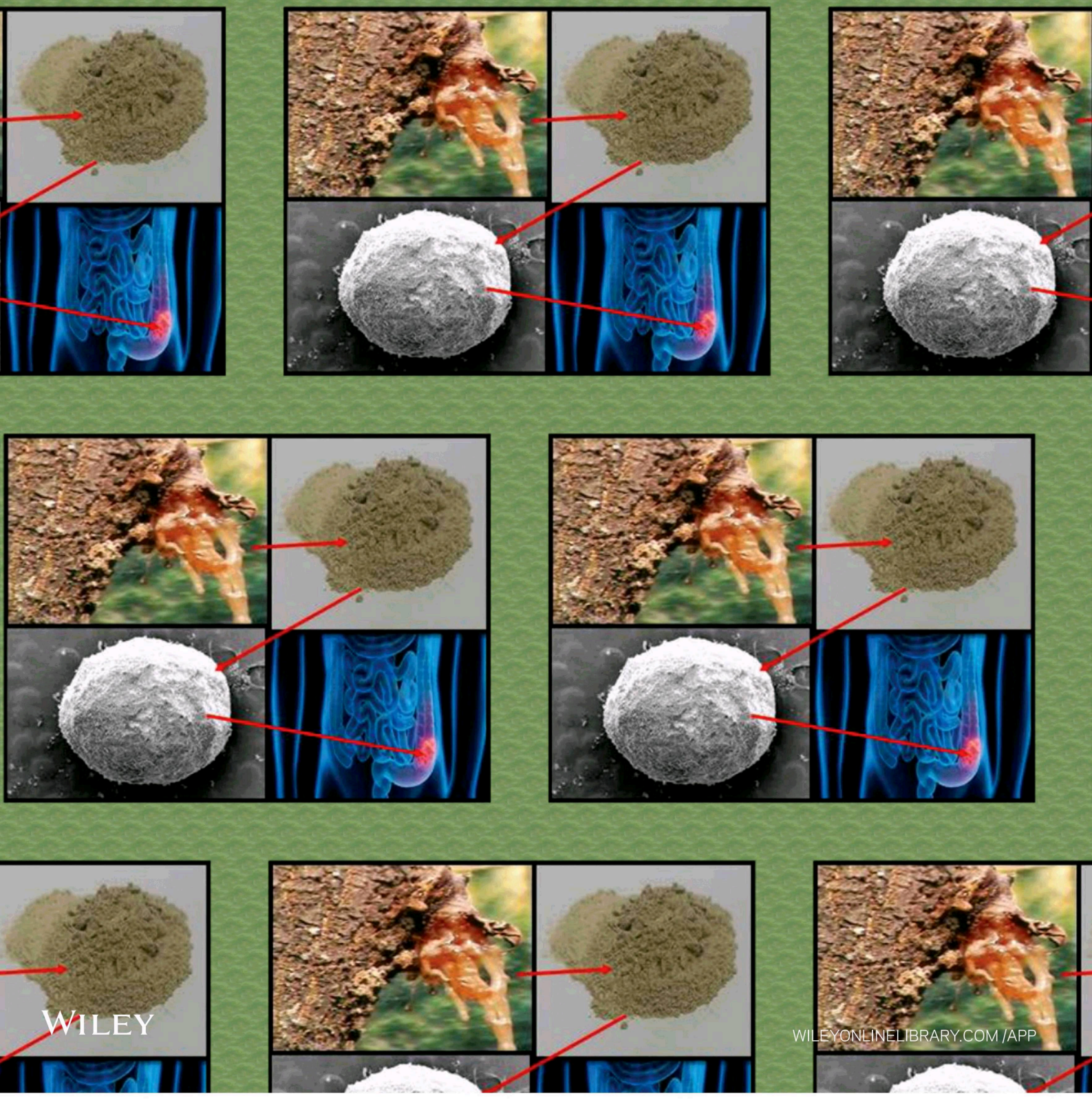

WILEY

WILEYONLINELIBRARY.COM /APP

Received: 12 April 2023 | Revised: 21 June 2023 | Accepted: 23 June 2023

DOI: 10.1002/pat.6139

REVIEW ARTICLE

polymers advanced technologies WILEY

A review on fungal pullulan as a natural polymer focusing on targeted therapy for colon cancer and other pharmaceutical applications

Ahana Hazra | Sohini Chatterjee | Abhishek Mohanta | Pankaj Paul | Amalesh Samanta

Division of Microbiology and Pharmaceutical Biotechnology, Department of Pharmaceutical Technology, Jadavpur University, Kolkata, India

Correspondence
Amalesh Samanta, Division of Microbiology and Pharmaceutical Biotechnology, Department of Pharmaceutical Technology, Jadavpur University, 188 Raja S C Mullick Road, Kolkata 700032, India.
Email: asamanta61@yahoo.co.in and amalesh.samanta@jadavpuruniversity.in

Abstract

Colon cancer is the second most invasive cancer and fourth most common malignant neoplasm worldwide. Targeted oral colonic drug delivery systems have attracted considerable attention in the treatment of colon cancer due to their superior properties. However, the delivery of drugs safely and effectively to the target site of the colon tumor is a hindrance due to the complexity of the gastrointestinal structure. Herein, to achieve an effective delivery system specifically targeting the colon, we have taken concern by using natural polymer such as pullulan, signifying its flexibility and relevance in biomaterials science to design antineoplastic approaches. Here, we summarize the physicochemical properties, different pullulan derivatives and their biomedical application, several colon cancer-related treatment, and pullulan and its derivatives-based delivery systems towards colonic tissue.

KEYWORDS
anticolon cancer activity, application, drug targeting, pullulan, sources

1 | INTRODUCTION

Colon cancer is the third leading cause of cancer-related death worldwide, accounting for up to 600,000 deaths every year. The lifespan of cancer-affected patients varies significantly depending on the stage of the tumor. The survival rate of colon cancer patients is ~90% in the early stages and drops down to around 10% once metastasis has been established.[1] Colorectal cancer-related death is mainly found in Australia, New Zealand, and so forth. In India every year more than 66,000 cases of colon cancer are reported.[2] Colorectal cancer is mostly found in those aged 50 years and over. Many previous reports proposed that this malignancy mostly arises with the growth of polyps, which be able to benign or non-cancerous and later develop into cancerous lesions. Control of colon cancer is a leading clinical challenge for us because of its complexity, heterogeneity, and aggressiveness.[3]

The concept of the conventional drug delivery approach is altering; nowadays researchers are progressively more concerned with developing natural polymer-based novel targeted drug delivery ahead of the approach of traditional and non-targeted systems.[4] Because naturally occurring polymers are biodegradable and biocompatible with higher bioavailability and lower toxicity.[5] Several biodegradable naturally obtained polymers including gum odina,[6] gum arabic,[7] pullulan, gellan gum,[8] gelatin, chitosan, and hyaluronic acid have been investigated for use as tissue engineering,[7] scaffolds, protein delivery, drug deliver,[9] and so forth.[10] Hence here we have taken the proposal of a natural polymer's targeted delivery system to overcome the aforementioned problems.

Chemotherapy is the most common treatment for colon cancer. Traditional chemotherapy remains a significant barrier in the diagnosis and treatment of colon cancer.[11] Moreover, in the case of metastases sometimes drug resistance might be associated, which could be another risk factor, leading to a tumor's relapse and a failure in treatment.[12] Currently, the concept of adjuvant chemotherapy is increasing significantly in cancer therapy. Novel adjuvant chemotherapy obstructs some of the drawbacks of conventional chemotherapies

International Journal of Biological Macromolecules 267 (2024) 131410

Contents lists available at ScienceDirect

International Journal of Biological Macromolecules

journal homepage: www.elsevier.com/locate/ijbiomac

Gum odina prebiotic induced gut modulation for the treatment of colon cancer on Swiss albino mice: By using capecitabine loaded biopolymeric microsphere

Ahana Hazra, Mousumi Tudu, Abhishek Mohanta, Amalesh Samanta *

Division of Microbiology and Pharmaceutical Biotechnology, Department of Pharmaceutical Technology, Jadavpur University, 188 Raja S C Mullick Road, Kolkata 700032, India

ARTICLE INFO

Keywords:
Capecitabine
Acute toxicity and colon cancer

ABSTRACT

A complex illness with a current global hazard, colon cancer has many different manifestations. The efficacy of colon cancer therapy can be affected by the bacteria in the digestive tract. It is hypothesised that novel prebiotics like Gum Odina is emerging as preventative therapy to fight chronic gut illnesses by gut microbiota modulatory therapy when compared to traditional intervention. The first-line chemotherapy drug for colon cancer, capecitabine, lacks a carrier that can extend its half-life. Here, we use the prebiotic gum odina – sodium alginate conjugate to create a capecitabine loaded biopolymeric microspheres, which were previously established as excellent tools for colon cancer therapy. The accelerated stability study exhibited that the alteration in physicochemical properties was found to be negligible. When administered orally to mice with colon cancer, capecitabine raises intra-tumoral capecitabine concentration and slows drug elimination in the blood. Optimized formulation improves anti-tumor immunity over free capecitabine and decrease the tumor volume from $8 \pm 6.59\ mm^3$ to $5.21 \pm 2.79\ mm^3$. This prebiotics based microsphere combine's gut microbiota manipulation with chemotherapy to offer a potentially effective colon cancer treatment.

1. Introduction

Colon cancer is the fourth leading cause of cancer-related diseases worldwide and accounts for up to 600,000 deaths every year. The life expectancy of colon cancer patients varies radically depending on the tumor stage [1]. 90 % of patients might survive up to 5 years in the early stages of detection and it could drop down to approximately 10 % once metastasis has occurred. Capecitabine is an oral fluoropyrimidine carbonate with antineoplastic activity and exerts its effect as an antimetabolite drug. A prodrug of 5-flurouracil, capecitabine has been used extensively as a chemotherapeutic medication for the treatment of colon cancer for many years. It was the preferred medication for the treatment of colon cancer due to its excellent tolerability and intratumor drug concentration [2]. But it has been not as effective as this drug has short plasma half-life <0.85 h that leads to rapid elimination from the body. High dose (1250 mg) of capecitabine is needed twice per day leads to common over dose related toxicity like bone marrow depression, cardiotoxicity, diarrhea, nausea, vomiting, dermatitis, thrombocytopenia and hyperbilirubinemia so forth. To overcome this problem of capecitabine a colon-specific drug delivery approach has been taken as an important tool for effectively targeting the drug to cancer cells with a lower dose and less systemic side effects [3]. The microbiota in the gastrointestinal tract can have an impact on the effectiveness of colon cancer therapy [4]. Prebiotics distribution into the gut is a more manageable way for gut microbiota modulatory therapy when compared to traditional intervention. Here, we use the prebiotic gum odina to create a capecitabine –loaded microsphere to achieve the site-specific action of the drug at the optimal rate and dose regimen [5]. We choose gum odina here as it acts as a prebiotic which upon metabolism liberates lactic acid, acetic acid, and other short-chain organic the immune system by increasing IgA against any kind of infection in the colon [6]. In this study, due to the low viscosity of gum odina [7], sodium alginate was used in the formulation of microsphere. Additionally, sodium alginate might act as an effective material for the formulation of microspheres due to its nontoxicity, immunogenicity, and good matrix-forming ability. As previously mentioned, the specific process for formulating capecitabine-loaded microspheres was described Hazra et al., 2022 [5]. In brief, calcium chloride was added as a cross-linker

* Corresponding author.
E-mail address: amalesh.samanta@jadavpuruniversity.in (A. Samanta).

https://doi.org/10.1016/j.ijbiomac.2024.131410
Received 14 September 2023; Received in revised form 26 March 2024; Accepted 3 April 2024
Available online 4 April 2024

dropwise to the polymeric mixture of gum odina and sodium alginate. The experiential microsphere was loaded with capecitabine (F6). In order to determine the significant property of anticolon cancer activity, both blank and drug-loaded microspheres were manufactured for this investigation and their therapeutic efficacy was assessed. According to experimental investigations, formulation F6 had the best drug release control (94.62 ± 4.16 %) up to 24 h, had an average swelling index (568.33 μm ± 1.47), and had the maximum entrapment efficiency (45.91 ± 2.58 %). F6 was chosen as an improved formulation to conduct additional essential studies. The drug-loaded formulation was developed and marked as F6 [5]. HT29 cells treated with capecitabine loaded microsphere (F6) showed a marked reduction in proliferation when compared to cells treated with the capecitabine alone. However, the percentage cell inhibition rate was 20.25 ± 3.65 % when using the capecitabine, but incubation with F6, the cell inhibition rate increased to 76.00 ± 3.21 % after 24 h of treatment. These results demonstrated that the F6 increased the permeability of capecitabine, enabling the cells to be exposed to greater drug concentrations as well as preventing the growth of colon cancer cells.

Physicochemical characterizations and in vitro study on the HT29 cell line of a prepared microsphere on their own are not satisfactory so that in vivo study is necessary to evaluate a better predictive value for determining the proof-of-concept. Physicochemical properties of the prepared microspheres might deteriorate upon storage condition due to absorption of moisture hence, the stability study of the optimized microsphere was performed. Moreover, the antiproliferative activity of gum odina – sodium alginate based microsphere in colorectal carcinoma cells was evaluated followed by pharmacokinetic activity and in vivo efficacy in a mouse model of colorectal cancer.

2. Materials and methods

2.1. Materials

Capecitabine, dimethylhydrazine (DMH), formaldehyde, chloroform, dipotassium hydrogen phosphate, potassium dihydrogen phosphate, sodium chloride, and dextran sulfate sodium (DSS) were purchased from Sigma-Aldrich, Germany. Gum odina (GO) exudate was collected and purified as stated previously. Double distilled water was used for the preparation of formulations as well as their analysis.

2.2. Preparation of microsphere

The formulation procedure of capecitabine-loaded gum odina and sodium alginate based microspheres was explained earlier [5]. Briefly, a certain amount of gum odina, and sodium alginate were blended and a solution of capecitabine was added to the polymeric mixture solution. Calcium chloride was incorporated dropwise into the solution as a crosslinker. A sequence of different microspheres was formulated by taking a variable ratio of gum odina and sodium alginate and evaluated the optimized formulation (F6) with all desired characteristics of an ideal in the treatment of colon cancer was found in 1:3 ratio of gum odina and sodium alginate. The medications were added to the optimized F6 microsphere at a concentration of 130 μg/mL, calculated from 1 % *w*/w of the total polymer (sodium alginate and gum odina) in the formulation [5].

Entrapment efficiency of formulated microspheres were determined by taking approx. 20 mg were added to the mortar and pestle. Crushed microsphere powder was added to phosphate buffer (pH 7.4), allowed to dissolve, and then kept at 40 °C overnight. After that samples were sonicated in bath sonicator (Digital Ultrasonic Cleaner, Equitron PVT. LTD., India) for 15 min and the absorbance of collected supernatant was analyzed by using a UV spectrophotometer (Shimadzu, Japan) at 276 nm. The in vitro drug release profile of capecitabine from microspheres in 0.1 N HCl (pH 1.2) and phosphate buffer (pH 7.4) was measured using a USP type 1 dissolution apparatus (Campbell Electronics, India) while stirring continuously at 50 rpm. Exact weighted dried microspheres containing capecitabine were allowed to soak for up to 2 h in 900 ml of 0.1 N HCl (pH 1.2). It was then maintained in a phosphate buffer (pH 7.4) for the following 6 h. To keep the sink condition, the 1 ml aliquot samples were removed and replaced with new dissolving media. The samples were correctly diluted and filtered, and a UV-VIS spectrophotometer (Shimadzu, Japan) set at 276 nm was used to determine the drug concentrations [5].

2.3. Stability study

The stability study is generally used to find out the stability potential of the capecitabine and other formulating agents present in the formulated microsphere. The accelerated stability study was carried out for up to 6 months according to the ICH guidelines under the following conditions: 40 ± 2 °C/75 % RH ± 5 % using a stability chamber (THERMOLAB, Humidity Chamber) for optimized microspheres (F6) [6]. The physicochemical stability of the optimized microsphere (F6) was evaluated by using several physicochemical parameters like entrapment efficiency, in vitro drug release study, FTIR, DSC, and TGA described by Hazra et al. 2023 to evaluate whether the optimized microsphere is stable or not during storage. Drug entrapment efficiency of optimized dry microspheres approx. 20 mg were added to the mortar and pestled to test the effectiveness of drug entrapment. Crushed microsphere powder was added to phosphate buffer (pH 7.4), allowed to dissolve, and then kept at 40 °C overnight. After that samples were sonicated in bath sonicator (Digital Ultrasonic Cleaner, Equitron PVT. LTD., India) for 15 min and the absorbance of collected supernatant was analyzed by using a UV spectrophotometer (Shimadzu, Japan) at 276 nm. The optimized formulation F6 was used to compute the percentage of encapsulation efficiency [5]. The in vitro drug release profile of capecitabine from optimized microspheres in 0.1 N HCl (pH 1.2) and phosphate buffer (pH 7.4) was measured using a USP type 1 dissolution apparatus (Campbell Electronics, India) while stirring continuously at 50 rpm. Exact weighted dried microspheres containing capecitabine were allowed to soak for up to two hours in 900 ml of 0.1 N HCl (pH 1.2). It was then maintained in a phosphate buffer (pH 7.4) for the following six hours. To keep the sink condition, the 1 ml aliquot samples were removed and replaced with new dissolving media. The samples were correctly diluted and filtered, and a UV-VIS spectrophotometer (Shimadzu, Japan) set at 276 nm was used to determine the drug concentrations [5].

2.4. Experimental animals

Swiss albino mice aged 6–8 weeks and male Wistar rats weighing 200–250 g at the age of 8 weeks were obtained from Chakraborty Enterprise. According to the recommendations of the Institutional Animal Ethics Committee (IAEC) of Jadavpur University, India (Ref No. JU/IAEC-22/05), all animals were acclimated to the laboratory settings in the Department of Pharmaceutical Technology, Jadavpur University, Kolkata, for a week prior to dosing [7]. The animals were kept with pellet food and water in an air-conditioned room with a 12-h light-dark cycle, a relative humidity of 50–15 %, and a temperature of 25 ± 2 °C. Every effort was made to lessen the pain and suffering of animals.

2.5. Acute toxicity study of gum odina

To evaluate the pharmacological safety of the gum odina acute repeated toxicity studies were carried out by administering the gum odina at 2000 mg/kg body weight for 14 days. This study was carried out on male wistar rats following the guidelines of the Organization for Economic Co-operation and Development (OECD). Throughout the course of the experiment, all the animals were observed daily for changes in physical appearance, damage, pain, and symptoms of illness as well as clinical evidence of toxicity, mortality, and behavioral

anomalies. Both before treatment and after treatment, body weight was monitored. The rats were sedated and blood samples were drawn from a heart puncture into tubes containing anticoagulants after 14 days of dosing. Hematological and biochemical analyses were performed on the blood that was drawn. The rats were then put to sleep, and their essential organs—their hearts, livers, and kidneys—were removed, preserved in 10 % formalin, and then set in paraffin. The slides were examined using an optical microscope (Magnus microscope, Chennai) following hematoxylin and eosin staining to look for any noticeable morphological alterations [8].

2.6. Pharmacokinetic study

Swiss albino mice were given a single dosage of capecitabine and capecitabine-loaded microspheres at a dose of 30 mg/kg body weight and were split into two groups ($n = 6$). Colon tissue samples were maintained at 80 °C until usage after complete dosing blood samples were obtained at several time periods including 2, 4, 8, 12, 24, and 48 h. In PBS 7.4, colon tissues were weighed and homogenized. A cardiac puncture was used to extract about 1 ml of blood into EDTA tubes. Serum was extracted from the blood and stored at −20 °C before to analysis. Blood was allowed to centrifuge at 5000 rpm for 10 min. The analysis was carried out using the HPLC method (Cyberlabs, Millbury, USA; column size: 4.6250 mm, 5 m) [8].

2.7. DMH + DSS induced colon cancer in mice model

There were four categories total for the animals. Group I acted as a vehicle control group and was made up of the control group ($n = 3$). Group II, often known as the positive control group, had six participants and received DMH and DSS at a dose of 20 mg/kg body weight. After administering DMH for five weeks, 3 % DSS was added to drinking water for one week, followed by another two weeks of monitoring. Group III ($n = 6$) began receiving DMH + DSS at the beginning of the first remission cycle and continued until the completion of the research. They also got capecitabine (30 mg/kg body weight; orally). The improved formulation was suspended and given orally to Group IV (n = 6) for up to 4 weeks at a dose of 30 mg/kg body weight of the animals [9].

2.8. Histopathological examination

The colons were promptly removed, flushed with saline, cut lengthwise along the major axis, and then rinsed with saline when the treatment time was complete. The mice were then painlessly killed. These colonic sections were preserved in a 10 % formalin solution for up to 24 h, at which point they were dehydrated in ethanol solutions of increasing strength before being embedded in paraffin wax and cut into tissue sections with a thickness of 5 μm. Utilizing ethanol and xylene, the paraffin-embedded colonic tissue segment was deparaffinized. The sections were then stained for histological analysis with hematoxylin and eosin reagents [10].

2.9. In vivo antitumor efficacy study

Swiss albino mice were used to compare the antitumor activity of capecitabine and a gum odina-based sodium alginate-based capecitabine loaded optimum formulation. Each week, records of the experimental animals' body weight changes and food and water intake were made. Following an 8-week course of DMH and DSS, two groups of rats received separate 4-week courses of capecitabine and a capecitabine-loaded optimal formulation. The animals were killed after 4 weeks in order to separate the colon tumors, and their volumes were calculated using slide calipers. All animals' body weight changes over the course of the trial were noted in order to assess body weight changes in DMH + DSS-treated animals and those receiving formulations following that treatment in order to monitor the growth and shrinkage of the tumor [11].

2.10. Tumor marker detection test

The tumor marker test relied on a monoclonal antibody directed against an antigen from a colon cancer cell line that had undergone metastasis. The retro-orbital plexus was used to obtain the blood sample, and centrifugation was used to obtain the serum. Using an electrochemiluminescence immunoassay equipment (Roch Modular E170 electrochemiluminescence), the blood levels of CA19-9 and CA125 were measured to examine cancer before and after treatment. The reference range for CA19-9 and CA125 was 0 to 35 kU/L and 0 to 35 kU/L, respectively [12].

2.11. Statistical analysis

All the experimental values were expressed as mean ± standard deviation (S·D). Each experiment was predicted in triplicate ($n = 3$). Statistical difference was evaluated by using analysis of variance (ANOVA) followed by Tukey's test using Graph Pad Prism 3.1 software. The levels of statistical significance were considered at $P < 0.05$.

3. Results and discussions

3.1. Stability study

The entrapment efficiency of the optimized formulation (F6) after 6 months was found to be 42.92 ± 1.30 %, which might be similar to the value of the freshly prepared formulation (49.5 ± 2.58 %). No significant difference ($p > 0.05$) in drug entrapment efficiency was observed between the freshly prepared microsphere and the 6 months' storage-formulated microsphere. The result of the percentage cumulative drug release (Fig. 1 a and b) of capecitabine from freshly prepared microspheres was 73.27 ± 7.97 %, and after 6 months storage, microspheres exhibited mostly similar results with a small amount of variance (87.49 ± 6.74 %). This variation might have occurred due to the formation of fractures or voids on the surface of the microsphere. From this result, it could be predicted that the elevated temperature does not affect the integrity of the microsphere [13].

From the FTIR analysis study, we might conclude that the optimized formulation during the storage period of 6 months did not exhibit any shifting or disappearance of the characteristic peak. In the FTIR study, peaks of capecitabine in optimized formulation (F6) were observed at a wavenumber of 3520 cm^{-1}, 3215 cm^{-1}, 2958 cm^{-1}, and 2861 cm^{-1}, and at 1716 cm^{-1}, which indicated OH stretching, NH stretching, CH stretching, aldehyde group (CHO) vibrations, and CO carbonyl group stretching vibrations, respectively. The presence of another characteristic peaks at 1502 cm^{-1}, 1245 cm^{-1}, 1042 cm^{-1}, and 1202 cm^{-1} showed NO bending vibrations and CN bending vibrations and C—F stretching vibrations as well as the presence of tetrahydrofuran rings [14]. But F6 formulation exhibited no significant change in characteristics peak after 6 months of storage under accelerated condition compared to freshly prepared microsphere. This result supported the stability of drug release study of the entrapped drug molecules (capecitabine) from the F6 matrix. (Fig. 2 a and b). The shape and appearance of the capecitabine-loaded microsphere were analyzed before and after 6 months using DSC studies. The sharp endothermic peak of the capecitabine-loaded formulation did not exhibit a peak at 121.9 °C, and it corresponded to the melting point of capecitabine (105–120 °C). But, this peak was absent in gum odina and sodium alginate-based formulations before and after the 6-month storage period. This might be due to the complete entrapment of the drug in the polymeric matrix and the conversion of the crystalline form to an amorphous state (Fig. 3 a and b) [15].

In the case of TGA analysis, there was a slight shifting of the TGA curve observed in the optimized formulation (F6) before and after

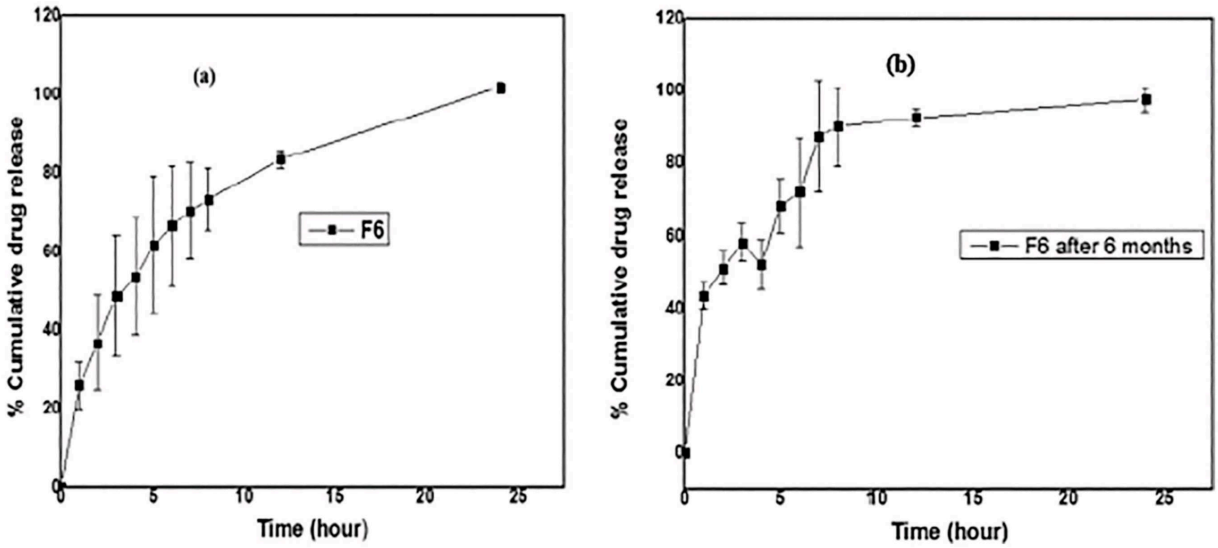

Fig. 1. (a) In vitro drug release profile of (a) capecitabine at initial day and (b) after 6 months storage were represented as mean ± SD in triplicate.

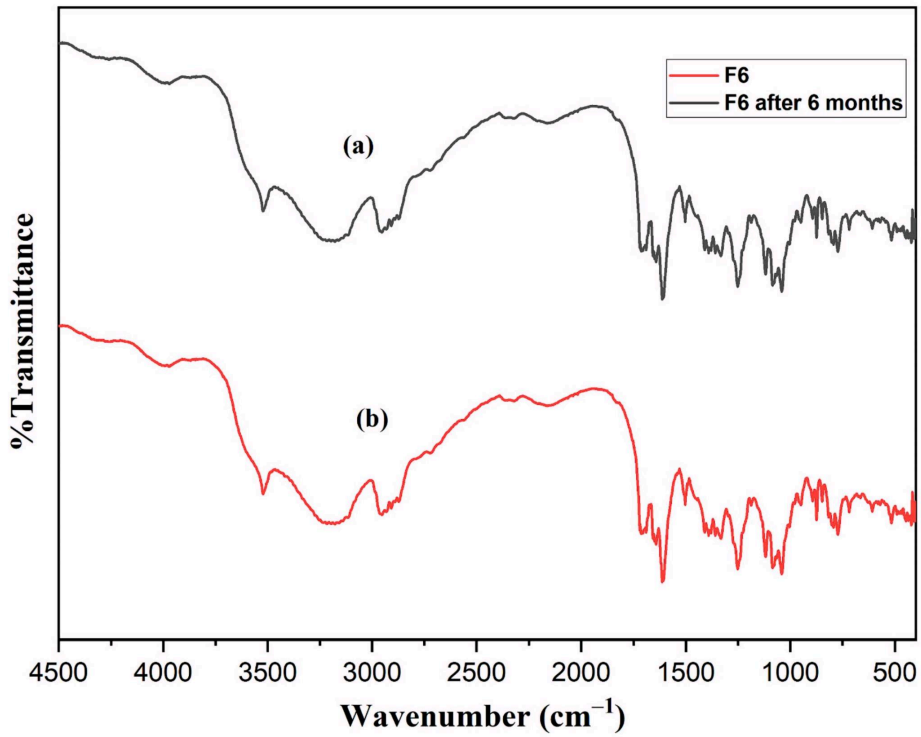

Fig. 2. The FTIR results demonstrate the existence of characteristic peaks of (b) capecitabine of 6 months stored in F6 as (a) similar to the freshly prepared microsphere.

storage, which might have occurred due to the presence of moisture. In the TGA curve of capecitabine, this first stage of thermal degradation and weight loss occurred at 137 °C, and about 7.5 % of it might be water evaporation, which was raised to 43 % at 174.35 °C, 54 % at 302 °C, and 75 % at 694 °C. In the case of optimized formulation F6, after storage conditions, initial weight loss was 7.96 % at 219 °C (Fig. 4 a and b), which was enhanced steadily with successive increases in temperature, i.e., 21.82 %, and 60 % at temperatures 515 and 567.86 °C, which might be almost analogous to the freshly prepared microsphere. Hence, in the case of total weight loss in optimized formulation before and after storage conditions, 60 % was above 567.86 °C, which was very low in the case of capecitabine. This result revealed that after the encapsulation of capecitabine into a polymeric matrix, thermal stability increased before and after storage conditions by shifting the denaturation temperature to a higher value [16]. Hazra et al. [4] have already reported that capecitabine exhibited sharp, intense peaks at *2*° of 5°, 20°, and 25°, indicating the crystalline nature of the drug. The XRD study of Fig. 5 (a and b) showed that the prepared microsphere did not display crystalline peaks of the drug before and after 6 months of the formulation. Despite the above studies, the analysis of surface morphology played a key role in the stability study as drugs tend to convert from an amorphous to crystalline nature in the formulation during storage conditions, which probably obstructs the in vitro drug release pattern. SEM photographs Fig. 6 (a) of the microsphere showed a spherical shape with a rough

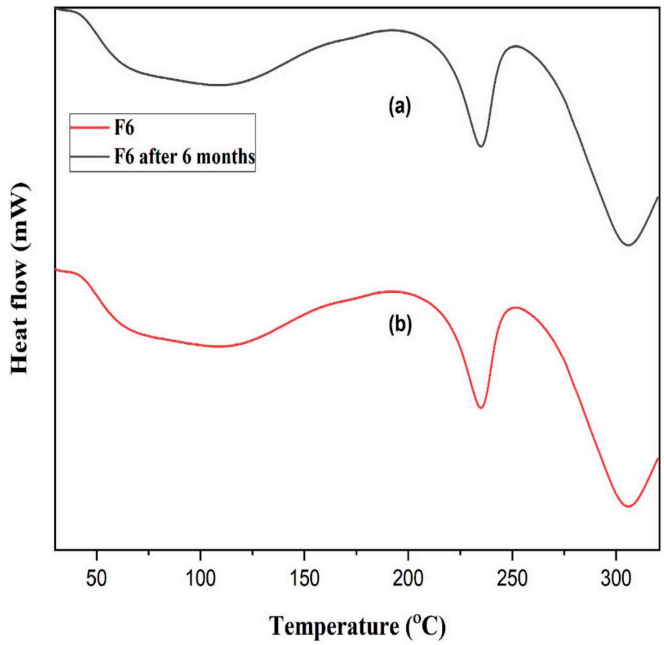

Fig. 3. The DSC thermogram of (a) F6 at the initial period and F6 after 6 months of storage.

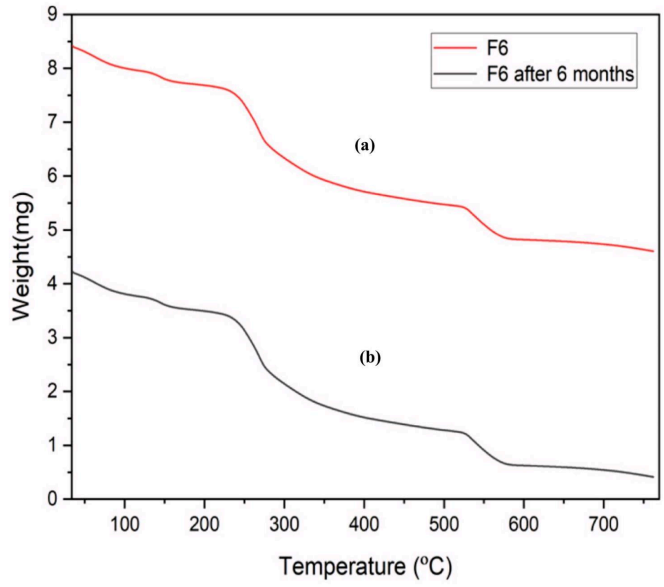

Fig. 4. The TGA thermogram of (a) F6 at initial period and F6 after 6 months storage.

surface exhibiting pores on it. This porous structure of the microsphere is desirable for water uptake, swelling, and release mechanisms. Fig. 6 (b, c) shows that the absence of capecitabine crystals on the surface of the microsphere could be attributed to the complete dispersion of the drug throughout the polymeric matrix [17]. This physical state of the drug in the formulated microsphere might play a crucial role in drug release kinetics. From Fig. 6 (a, b, and c), we concluded that there was no confirmation of crystals of drugs either in freshly prepared F6 or formulations stored under storage conditions for up to 6 months [18].

3.2. Acute toxicity study of gum odina

Male Wistar rats were subjected to acute toxicity testing to investigate the potential impact of gum odina on hematological parameters, biochemical parameters, visual examination, and the histology of critical organs. There were no behavioral abnormalities, acute toxicological effects, or significant weight loss observed in any of the therapy groups. The average body weights of rats at 1, 7, and 14 days were found to be 196.05 ± 13.43, 200.74 ± 82.71, and 241.4 ± 4.82 g, respectively. Additionally, all the treatment groups showed normal urea, serum creatinine, and liver function of the liver like ALT, AST, total protein, total bilirubin hemoglobin counts, platelet counts, total red blood cell counts, differential white blood cell counts, etc., with no significant variance ($p < 0.05$) as compared to control groups of animals represented in Table 1.

In the case of the control group, rats (Fig. 7a) did not exhibit any kind of necroscopy or abnormal morphological changes in the kidney (glomeruli, tubules, interstitium, and blood vessels). Microscopic evaluation of the histology of rat kidneys (Fig. 7 b) exhibited slight morphological changes, including a lessening of glomerulus cells (black star) and an extension of the bowman space (black arrow), found in gum odina-treated groups as compared with control groups. Results suggested that histological assessment of kidneys revealed a minor variant in the morphology of kidneys in 2000 mg/kg body weight-treated rats. Alternatively, biochemical parameters of renal function in all rats treated showed no significant changes. Hence, based on the biochemical and histological results of the kidneys, it might be concluded that gum odina did not display adequate nephrotoxicity to cause a variation in the functions of the kidneys [19]. Histology of the liver sections of control rats (Fig. 7 c) did not show any histologic abnormalities in conjunction with well-maintained hepatic cells and visible central veins. Rats treated with 2000 mg/kg of gum odina were exposed to certain alterations in the histology of the liver (Fig. 7d), like slight dilation of sinusoids and atrophy of hepatic cords (black arrow), moderate hepatocytes, and some binucleated cells (black star). Most of the bioactive compounds were exhibited in the liver and metabolized to other compounds, which may or may not be hepatotoxic to the mice. However, 2000 mg/kg body weight of gum odina in mice models showed a remarkably significant elevation of ALT, AST, creatinine, and urea, which are probably good indicators of liver and kidney functions. Therefore, the moderate variations presented on histology of the liver sections are not attributed to the toxic effect of the gum odina [20]. Comparing treated groups to control groups, the histological cross-section of the treated groups' hearts revealed regularly arranged and conserved polarity of myocytes organized in muscular bundles, with no signs of heart necrosis or haemorrhage (Fig. 7 e). The study revealed that upon oral administration of gum odina in rat models, there were no adverse effects exhibited, and hence, they might be safe for potential use as a polymer for the development of oral formulations [21].

Several hematological and serum biochemical parameters and the histopathological images of the vital organs like the liver, kidney, and heart did not show any significant difference between the test and control groups. Further in the experiment, the mortality of the animals was zero, which suggested the LD50 value of gum odina was set at 2000 mg/kg of body weight. Hence, gum odina was categorized under "category 5" with "zero toxicity," indicating safety for drug delivery through the oral route [22].

3.3. Pharmacokinetic studies

An in vivo pharmacokinetic study was performed on optimized formulation F6, which was compared with the standard drug capecitabine at an orally administered dose equivalent to 30 mg/kg body weight of mice in two study groups I and II, respectively (Table 2). The plasma concentration of the capecitabine-loaded optimized formulation showed a value of 24 %, which is higher as compared to capecitabine administration [23]. Significant changes in $t_{1/2}$ and AUC total values were also detected in the case of F6 as compared to free drug access, and the $t_{1/2}$ value of the optimized formulation suggested that drug release from microspheres occurs after reaching the colon [24]. According to the

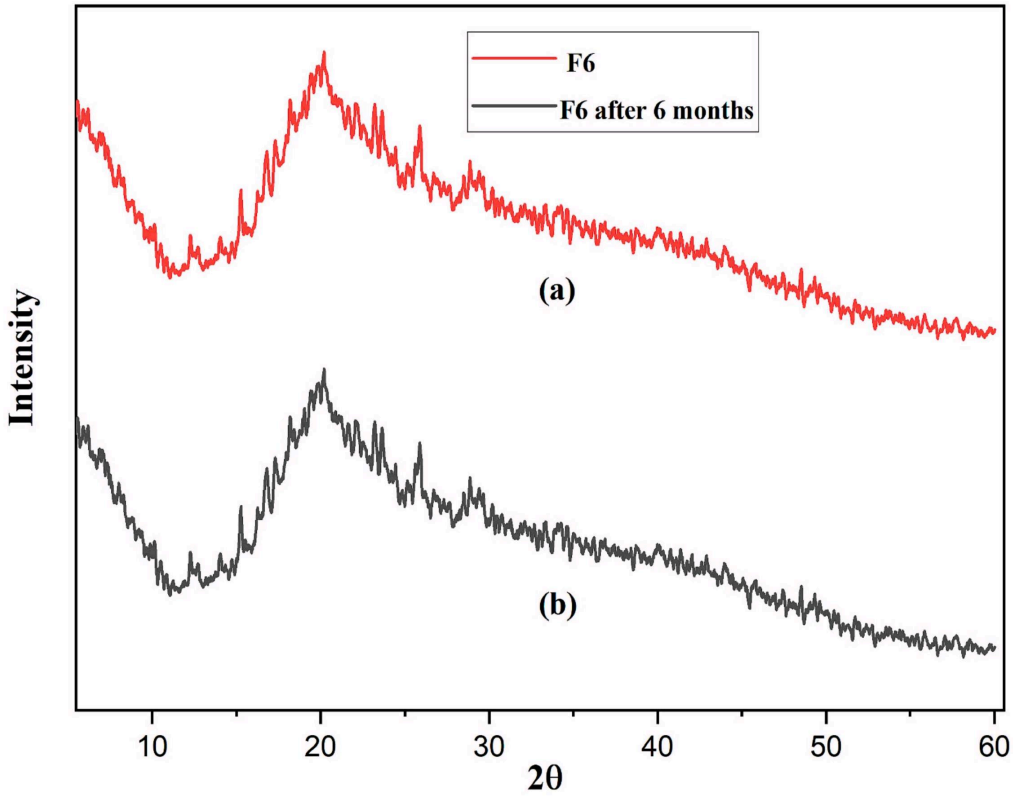

Fig. 5. XRD diffraction study of (a) F6 microsphere at 0 months and (b) after 6 months storage.

pharmacokinetic data, capecitabine loaded microspheres were shown to have the greatest C_{max} of medication in the colon. AUC values, delayed biological $t_{1/2}$ values, and low elimination rate constants all pointed to the distinct advantage of optimized formulation based treatment over free drug capecitabine treatment in terms of the bioavailability of capecitabine in colon tissue and plasma. These results showed that the rate of drug absorption followed in a sustained manner in the systemic circulation, satisfying one of the objectives of controlled release formulation. The value of area under the curve (AUC) indicated the extent of absorption, which was considerably greater for formulation F6, suggesting a prolonged duration of action above the free drug, signifying that the capecitabine-encapsulated optimized formulation might fruitfully control the release of capecitabine [25].

3.4. Histopathological changes in colon carcinoma tissue before and after treatment of capecitabine-loaded microsphere

The diagnosis of various stages of colorectal cancer depends greatly on histopathological characteristics. The term colon cancer refers to cancers that start in the colon or rectum. Hematoxylin and eosin histopathological staining of colorectal cancer tissue shows various tumor grades of colorectal carcinoma. [18]. The most common type of colorectal cancer that begins in the epithelial cells lining the colon's mucosa layer are adenocarcinomas. Oncogenes and tumor suppressor genes begin to undergo genomic changes as the lesion grows. The serrated pathway of colorectal cancer development may account for the development of colorectal cancer in hyperplastic polyps, according to mounting data. The histopathology study of colon tissue was viewed under a light microscope at several magnifications to explore the histological morphology of colonic mucosa [19]. As seen in Fig. 8, colonic cells largely generated an adenoma or polyp after being treated with DMH + DSS at the various time periods, which gradually might reach the uncontrolled cell division stage before its infiltration into the next layer, i.e., submucosa. The adenoma-carcinoma sequence may be broken by this pre-existing adenomatous precursor (polyps) in the colon interfering with the natural processes that control epithelial renewal. When they are further advanced, they may enter blood vessels, spread to other tissues, and eventually develop metastasis [20]. The colon of the control group (Fig. 8a) showed normal mucosa and submucosal layers and normal colonic architecture without apparent abnormality in colonic cells. In DMH+ DSS-induced group (Fig. 8b, c) showed clear degeneration of tubular glands in the mucosal and submucosal layer, aberrant crypts, and growth of polyps on the lining of colon cancer cells. The adenoma-carcinoma sequence may be broken by this pre-existing adenomatous precursor (polyps) in the colon interfering with the natural processes that control epithelial renewal. When they are further advanced, they may enter blood vessels, spread to other tissues, and eventually develop metastasis [21]. Mice treated with the standard drug capecitabine exhibited hyperplastic crypts with cell infiltration and a slight change in the muscular layer architecture [22]. Mice treated with optimized formulation exhibited a reduced incidence of polyps and showed normal crypts as compared to cancer-induced mice. This result showed that optimized formulation was well tolerated in a healthy colon and did not harm or significantly alter the histology of the colonic tissues. Along with the submucosal and muscular layers, which were both structured properly, the epithelial layer was also present. Additionally, this shows that optimized formulation was not harmful to the healthy colon (8d) [23].

3.5. In vivo antitumor efficacy study

Animals taking DMH + DSS alone were seen to gradually lose body weight (184.7 ± 1.83 g), and this was followed by a variety of behavioral changes, including decreased food intake, slower locomotion, increased resting, and a propensity for infrequent outbursts of anger. With the addition of capecitabine and capecitabine loaded optimized formulation, the body weight began to rise (192.05 ± 2.63, and 239.4 ± 1.32 g) which was quite similar to result of Wang et al.,2022 reported method

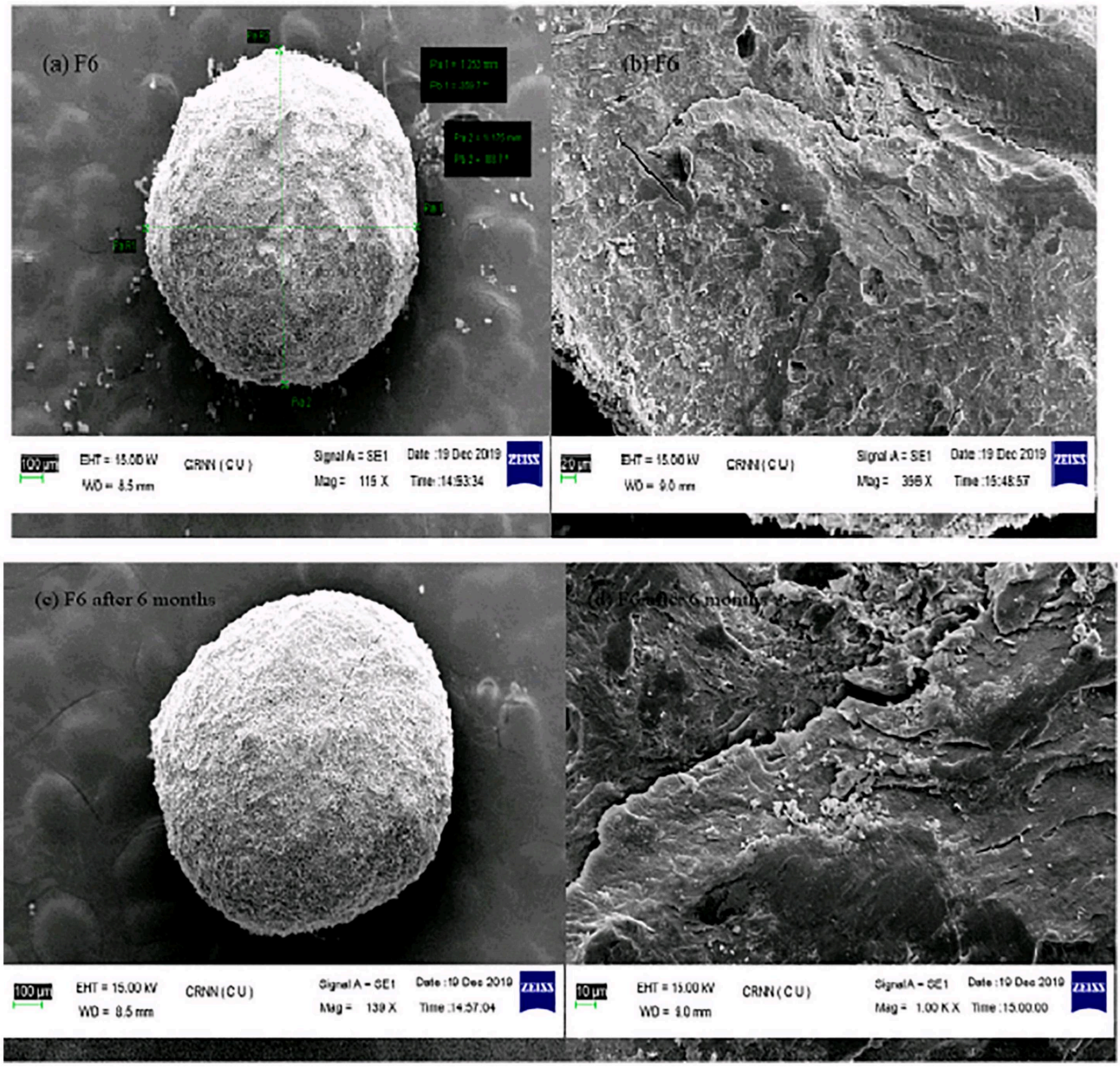

Fig. 6. SEM study shows the morphological stability of the F6 microsphere. The SEM image of (a) freshly formulated F6 and (b) 6 months stored F6.

Table 1
Hematological and biochemical parameters in male wistar rat treated for 14 days with gum odina (mean ± SD, $n = 6$).

Parameters (Unit)	Control	Treatment
White blood cells	8.5 ± 1.10 10^3/mm^3	8.31 ± 0.38 10^3/mm^3
Hemoglobin	12.24 ± 0.05 g/dL	10.62 ± 0.71 g/dL
Total red blood cells	4.81 ± 0.53 10^6/mm^3	5.166 ± 1.088 10^6/mm^3
Mean corpuscular volume	41.34 ± 4.15 fL	46.34 ± 4.15 fL
Mean corpuscular hemoglobin	20.80 ± 9.38 pg/cell	20.12 ± 1.34 pg/cell
ALT	44.56 ± 4.53 mg/dl	42.16 ± 1.45 mg/dl
AST	0.54 ± 0.05 mg/dl	0.59 ± 0.028 mg/dl
Total protein	35.8 ± 2.97 IU/L	35.84 ± 1.61 IU/L
Total bilirubin	103 ± 46.76 IU/L	110.45 ± 4.87 IU/L

[24]. Moreover, optimized formulation (F6) treated groups exhibited statistical ($p < 0.05$) enhancement in weight growth compared to carcinogen-treated rats. A group of mice were slaughtered and their colon tissues were extracted after receiving DMH therapy for 8 weeks. Different-sized tumors in the tissues were discovered, and the majority of them were mostly visible under a microscope. To establish a general idea of the average tumor volume, their volumes were measured. It was challenging to determine the weights of the majority of the tumors because they were often so tiny and intertwined with colonic epithelium [25]. We sacrificed a different group of mice and looked at changes in the tumor morphology after the mice had been given capecitabine and optimized formulation treatment for 4 weeks. The volumes of the isolated tumors were calculated. Tumors were isolated, and their volumes were measured. The tumor volume was found to be 13.16 ± 7.36 mm^3 for the DMH-DSS treated colorectal cancer mice (Fig. 9 A), whereas volumes of 8 ± 6.59 mm^3 (Fig. 9b) and 5.21 ± 2.79 mm^3 (Fig. 9 C), were found in the case of capecitabine and capecitabine loaded optimized formulation respectively.

3.6. Tumor marker detection test

Serum concentrations of CA 19–9 and CA 125 played an important role in the clinical purpose of detecting the degree of angiogenesis, the

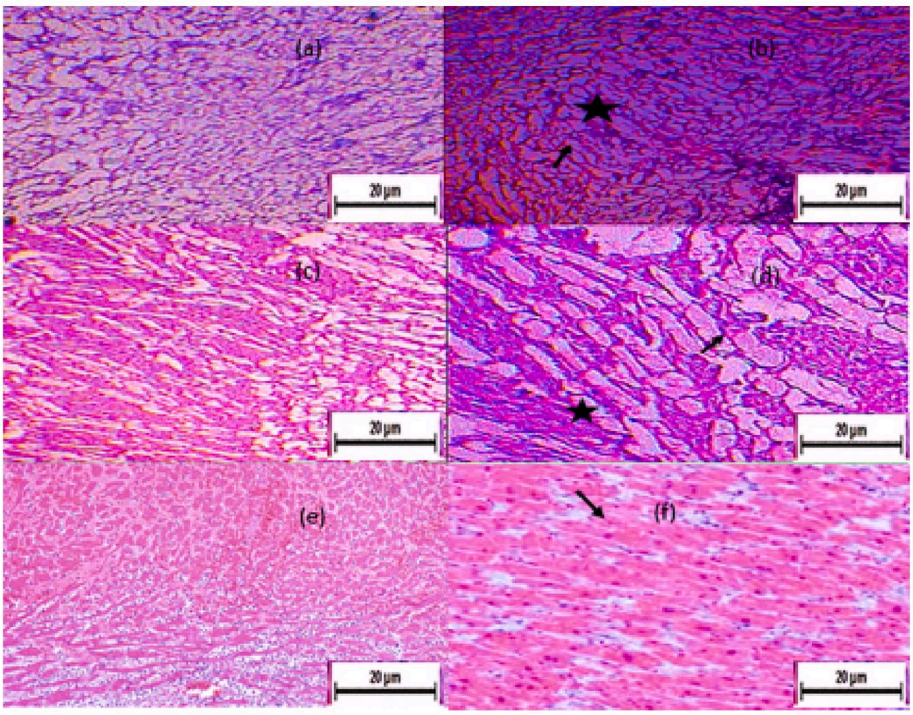

Fig. 7. (a) Histopathological examination of kidney on controlled and non-treated male rats (10× and 60× magnifications) and (b) treated rats (10× and 60× magnifications), (c) histopathological examination of the liver on controlled and untreated male rats (10× and 60× magnifications) and (d) treated rats (10× and 60× magnifications) and (e) histopathological examination of the heart on controlled and untreated male rats and 10× and 60× magnifications (f) treated rats (10× and 60× magnifications). Scale bar used in 10× and 60× magnification panels represent 20 µm respectively.

Table 2
Pharmacokinetic parameters of capecitabine and capecitabine loaded microsphere treated with different groups of mice.

Pharmacokinetic Parameters	In-vivo pharmacokinetic data of free capecitabine	In-vivo pharmacokinetic data of capecitabine loaded optimized formulation
C_{max} (ng/mL)	30.64 ± 2.85	51.16 ± 5.68
AUC_{0-t} (ng h/mL)	62.79 ± 48.36	102.32 ± 11.37
$AUC_{0-infinity}$ (ng h/mL)	324.08 ± 68.29	350.5 ± 1.06
AUC total (ng h/mL)	386.87 ± 18.77	454. 32 ± 11.37
$t_{1/2}$ (h)	5.27 ± 0.66	11.38 ± 0.45

presence of endothelial cells, and cellular proliferation. We first evaluated the sensitivity of individual markers, followed by CA 19–9 and CA 125, whose displayed values were 33.4 U/mL and 29 U/mL on cancer-induced mice. These results suggested that these tumor markers revealed a positive correlation with the advancement of tumor stages [26]. In addition, the increase of such indicators as CA19-9 and CA125 was also influenced by lymph node metastasis, vascular invasion, nerve infiltration, vascularization or angiogenesis, and TNM staging. In capecitabine loaded microsphere treated mice, CA 19–9 and CA 125 values were obtained at 1.05 U/mL and 0.27 U/L, respectively after 9 weeks of treatment is very similar to the results obtained in the study of Carcinoembryonic antigen, CA 19–9, and CA 125 in normal and carcinomatous human colorectal tissue [27]. CA 19–9 and CA 125 have proven to be useful in monitoring the effect of therapy and are pertinent prognostic tools for clinical use. This has given evidence of the successful development of our formulation for the treatment of colorectal carcinoma. These results clearly express that serum CA 19–9 and CA 125 tests are probably most applicable for colon cancer diagnosis, postoperative surveillance, and the monitoring of treatment effects [28].

The above results indicate that capecitabine-loaded microspheres might be related to the increased cellular availability of the drugs in the tumor due to the polymeric matrix of gum odina and sodium alginate, which enhance permeation and retention of drugs; however, a thorough comparison with respective free drug capecitabine-treated groups and pharmacokinetic studies would be applicable to confirm this hypothesis.

4. Conclusion

This study found that microspheres (F6) made of sodium alginate and loaded with capecitabine made the best treatment for colon cancer. The optimized microsphere didn't significantly change during storage in terms of its physiochemical properties. Evaluation of F6's drug entrapment effectiveness and drug release characteristics during the course of the stability research showed no deterioration of the drug's encapsulated capecitabine in the optimized microsphere. In addition, FTIR spectra did not show any kind of additional peaks or peak shifting after 6 months of an accelerated stability study of the formulation. In XRD images, the formulation exhibited no crystallinity during the storage period, which indicated a positive consequence for the amount of drug release from F6 after 6 months. The acute oral toxicity study of gum odina did not show any toxic effect on Wistar rats, and no abnormal results have appeared in histological sections of the liver, kidney and heart, suggesting that gum odina is safe and harmless for internal use. The in vivo pharmacokinetic study of the optimized formulation displayed a $t_{1/2}$ of 11.32 h, whereas the free drug was exposed for 5.27 h, while C_{max} was significantly different ($p < 0.05$), a sufficient condition for controlled release of capecitabine from the surface of the matrix. In vivo, *the* biomarker test was an important tool for screening and diagnosis and one of the main measures to reduce the incidence and mortality of colon cancer. DMH + DSS-induced histological abnormalities of the colon in Swiss albino mice were also exhibited and developed significantly. Hence, the results confirmed that the capecitabine-loaded optimized microsphere showed an advantageous material for the improvement of oral bioavailability and anti-colon cancer activity.

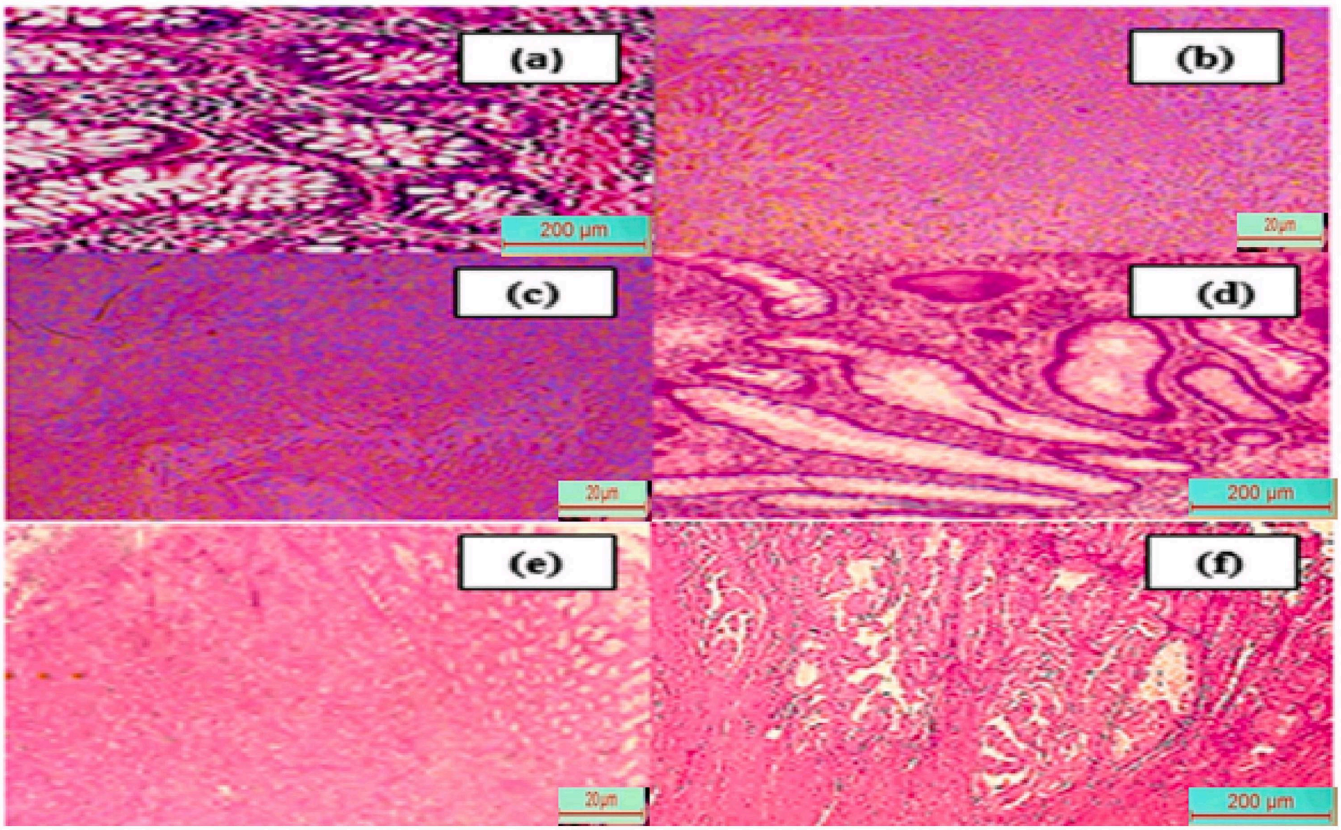

Fig. 8. Histopathological morphology of (a) normal colonic tissue at 10× and 60× magnifications, (b), (c) and (e) exhibiting different grades of cancer progression after treatment with DMH + DSS for a 4 weeks (at 10× and 60× magnifications respectively), (d) carcinogen-treated mice received optimized capecitabine loaded microsphere (at 10× and 60× magnifications respectively), and (f) carcinogen-treated mice treated with standard drug (at 10× and 60× magnifications respectively). Scale bar used in 10× and 60× magnification panels represent 200 μm and 20 μm respectively.

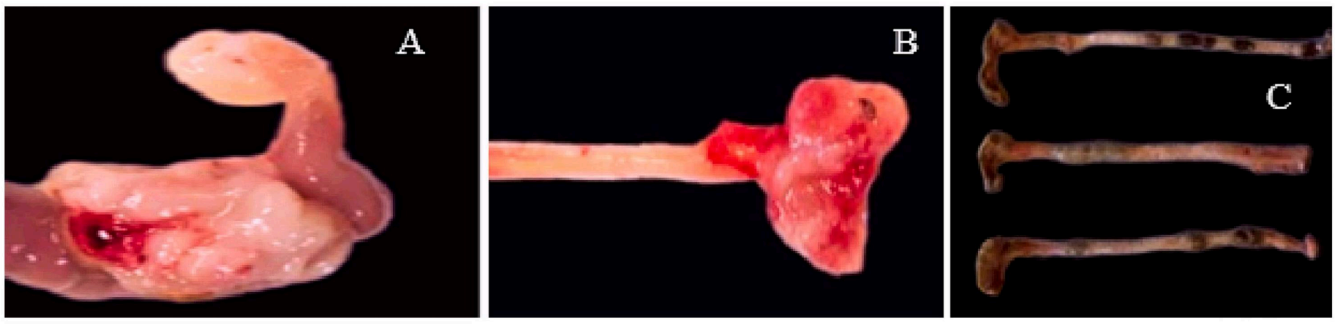

Fig. 9. Anatomical images of A) colon after treatment with DMH + DSS for a 4 weeks B) carcinogen-treated mice received standard drug capaecitabine, C) carcinogen-treated mice received optimized capecitabine loaded microsphere.

CRediT authorship contribution statement

Ahana Hazra: Conceptualization, Writing – original draft, Writing – review & editing. **Mousumi Tudu:** Formal analysis. **Abhishek Mohanta:** Writing – review & editing. **Amalesh Samanta:** Project administration, Supervision.

Declaration of competing interest

The authors report no conflict of interest.

Data availability

The data that has been used is confidential.

Acknowledgments

A.H. is thankful to University Grants Commission RUSA and SVMCM for providing the fellowship. The authors also acknowledge CRNN-Kolkata, India for the SEM study. The authors are thankful to the Department of Metallurgical and Material Engineering, Jadavpur University, Kolkata for FTIR, XRD, and TGA studies. The authors are highly grateful to the Department of Pharmaceutical Technology of Jadavpur University, India for providing all other necessary facilities to complete research work.

References

[1] J. Ferlay, I. Soerjomataram, R. Dikshit, S. Eser, C. Mathers, M. Rebelo, D.M. Parkin, D. Forman, F. Bray, Cancer incidence and mortality worldwide: sources, methods

and major patterns in GLOBOCAN 2012, Int. J. Cancer 136 (2015) E359–E386, https://doi.org/10.1002/ijc.29210.
[2] H. Ameli, N. Alizadeh, Targeted delivery of capecitabine to colon cancer cells using nano polymeric micelles based on beta cyclodextrin, RSC Adv. 12 (2022) 4681–4691, https://doi.org/10.1039/D1RA07791K.
[3] M. Upadhyay, S.K.R. Adena, H. Vardhan, S.K. Yadav, B. Mishra, Development of biopolymers based interpenetrating polymeric network of capecitabine: a drug delivery vehicle to extend the release of the model drug, Int. J. Biol. Macromol. 115 (2018) 907–919, https://doi.org/10.1016/j.ijbiomac.2018.04.123.
[4] J. Shi, Y. Wang, L. Cheng, J. Wang, V. Raghavan, Gut microbiome modulation by probiotics, prebiotics, synbiotics and postbiotics: a novel strategy in food allergy prevention and treatment, Crit. Rev. Food Sci. Nutr. (2022) 1–17, https://doi.org/10.1080/10408398.2022.2160962.
[5] A. Hazra, D. Sanyal, A. De, S. Chatterjee, K. Chattopadhyay, A. Samanta, Development and in vitro characterization of capecitabine loaded biopolymeric vehicle for the treatment of colon cancer, J. Appl. Polym. Sci. 139 (2022) e52374, https://doi.org/10.1002/app.52374.
[6] D. Mitra, A. Basu, B. Das, A.K. Jena, A. De, M. Das, S. Bhattacharya, A. Samanta, Gum odina: an emerging gut modulating approach in colorectal cancer prevention, RSC Adv. 7 (2017) 29129–29142.
[7] S. Das, T.K. Dey, A. De, A. Banerjee, S. Chakraborty, B. Das, A.K. Mukhopadhyay, B. Mukherjee, A. Samanta, Antimicrobial loaded gum odina - gelatin based biomimetic spongy scaffold for accelerated wound healing with complete cutaneous texture, Int. J. Pharm. 606 (2021) 120892, https://doi.org/10.1016/j.ijpharm.2021.120892.
[8] D. Dutta, A. Chakraborty, B. Mukherjee, S. Gupta, Aptamer-conjugated apigenin nanoparticles to target colorectal carcinoma: a promising safe alternative of colorectal cancer chemotherapy, ACS Appl. Bio Mater. 1 (2018) 1538–1556, https://doi.org/10.1021/acsabm.8b00441.
[9] S. Kumar, N. Agnihotri, Piperlongumine, a piper alkaloid targets Ras/PI3K/Akt/mTOR signaling axis to inhibit tumor cell growth and proliferation in DMH/DSS induced experimental colon cancer, Biomed. Pharmacother. 109 (2019) 1462–1477, https://doi.org/10.1016/j.biopha.2018.10.182.
[10] B. Bhattacharya, P. Pal, A. Lalee, D.K. Mal, A. Samanta, Available online through www.jpronline.info in vivo and in vitro anticancer activity of Coccinia grandis (L.) Voigt. (Family: Cucurbitaceae) on Swiss albino mice, J. Pharm. Res. (2011).
[11] R. Muthu, M. Vaiyapuri, Synergistic and individual effects of umbelliferone with 5-fluorouracil on tumor markers and antioxidant status of rat treated with 1,2-dimethylhydrazine, Biomedicine & Aging Pathology 3 (2013) 219–227, https://doi.org/10.1016/j.biomag.2013.08.007.
[12] C. Pablo Carmignani, R. Hampton, C.E. Sugarbaker, D. Chang, P.H. Sugarbaker, Utility of CEA and CA 19-9 tumor markers in diagnosis and prognostic assessment of mucinous epithelial cancers of the appendix, J. Surg. Oncol. 87 (2004) 162–166, https://doi.org/10.1002/jso.20107.
[13] C. Wang, T. Li, P. Lin, Y. Tao, X. Jiang, X. Li, Q. Wen, Y. Cao, Pharmacokinetic and safety comparison of two capecitabine tablets in patients with colorectal or breast cancer under fed conditions: a multicenter, randomized, open-label, three-period, and reference-replicated crossover study, Adv. Ther. 38 (2021) 4798–4814, https://doi.org/10.1007/s12325-021-01817-4.
[14] N. Vilaça, R. Amorim, A.F. Machado, P. Parpot, M.F. Pereira, M. Sardo, J. Rocha, A. M. Fonseca, I.C. Neves, F. Baltazar, Potentiation of 5-fluorouracil encapsulated in zeolites as drug delivery systems for in vitro models of colorectal carcinoma, Colloids Surf. B: Biointerfaces 112 (2013) 237–244.
[15] S. Afshar, A. Farshid, R. Heidari, M. Ilkhanipour, Histopathological changes in the liver and kidney tissues of Wistar albino rat exposed to fenitrothion, Toxicol. Ind. Health 24 (2008) 581–586, https://doi.org/10.1177/0748233708100090.
[16] M.M. Brzoska, J. Moniuszko-Jakoniuk, B. Piłat-Marcinkiewicz, B. Sawicki, Liver and kidney function and histology in rats exposed to cadmium and ethanol, Alcohol Alcohol. 38 (2003) 2–10.
[17] A. Kumar, P.K. Singh Arya, A. Jindal, Modulation of intestinal permeability of 5-fluorouracil via phospholipid interaction based lipophilic complex designing and pharmacokinetic assessment, J. Dispers. Sci. Technol. (2024) 1–13, https://doi.org/10.1080/01932691.2024.2325398.
[18] R. Narayan, S. Gadag, S.P. Cheruku, A.M. Raichur, C.M. Day, S. Garg, S. Manandhar, K.S.R. Pai, A. Suresh, C.H. Mehta, Chitosan-glucuronic acid conjugate coated mesoporous silica nanoparticles: a smart pH-responsive and receptor-targeted system for colorectal cancer therapy, Carbohydr. Polym. 261 (2021) 117893.
[19] M. Upadhyay, S.K.R. Adena, H. Vardhan, S.K. Yadav, B. Mishra, Locust bean gum and sodium alginate based interpenetrating polymeric network microbeads encapsulating Capecitabine: Improved pharmacokinetics, cytotoxicity &in vivo antitumor activity, Mater. Sci. Eng. C 104 (2019) 109958.
[20] D. Kumar, A. Gautam, P.P. Kundu, Synthesis of acrylamide-g-melanin/itaconic acid-g-psyllium based nanocarrier for capecitabine delivery: in vivo and in vitro anticancer activity, Int. J. Pharm. 635 (2023) 122735.
[21] K. Barkat, M. Ahmad, M.U. Minhas, I. Khalid, N.S. Malik, Chondroitin sulfate-based smart hydrogels for targeted delivery of oxaliplatin in colorectal cancer: preparation, characterization and toxicity evaluation, Polym. Bull. 77 (2020) 6271–6297, https://doi.org/10.1007/s00289-019-03062-w.
[22] C. Karthika, R. Sureshkumar, D.V. Sajini, G.M. Ashraf, M.H. Rahman, 5-fluorouracil and curcumin with pectin coating as a treatment regimen for titanium dioxide with dimethylhydrazine-induced colon cancer model, Environ. Sci. Pollut. Res. 29 (2022) 63202–63215.
[23] R.K. Kang, N. Mishr, V.K. Rai, Guar gum micro-particles for targeted co-delivery of doxorubicin and metformin HCL for improved specificity and efficacy against colon cancer, In Vitro and In Vivo Studies, AAPS PharmSciTech 21 (2020) 48, https://doi.org/10.1208/s12249-019-1589-3.
[24] Amelioration of DMH-induced colon cancer by eupafolin through the reprogramming of apoptosis-associated p53/Bcl2/Bax signaling in rats - Congcong Wang, Xiao Qiao, Jingwen Wang, Jia Yang, Chen Yang, Yi Qiao, Yue Guan, Aidong Wen, Liuqin Jiang, 2022, (n.d.). https://doi.org/10.1177/20587392211069771 (accessed March 21, 2024).
[25] Y. Goyal, A. Koul, P. Ranawat, Ellagic acid modulates cisplatin toxicity in DMH induced colorectal cancer: studies on membrane alterations, Biochemistry and Biophysics Reports 31 (2022) 101319.
[26] S. Desai, A.K. Guddati, Carcinoembryonic antigen, carbohydrate Antigen 19-9, cancer Antigen 125, prostate-specific antigen and other cancer markers: a primer on commonly used cancer markers, world, J. Oncol. 14 (2023) 4–14, https://doi.org/10.14740/wjon1425.
[27] A. Quentmeier, P. Möller, V. Schwarz, U. Abel, P. Schlag, Carcinoembryonic antigen, CA 19-9, and CA 125 in normal and carcinomatous human colorectal tissue, Cancer 60 (1987) 2261–2266, https://doi.org/10.1002/1097-0142(19871101)60:9<2261::AID-CNCR2820600926>3.0.CO;2-P.
[28] Preoperative Serum Carcinoembryonic Antigen, Carbohydrate Antigen19-9 and carbohydrate Antigen 125 as prognostic factors for recurrence-free survival in colorectal cancer, Asian Pac. J. Cancer Prev. 12 (2011) 1251–1256.

Department of Biotechnology and Medical Engineering
National Institute of Technology, Rourkela
Odisha, India

National Conference
BIOENGINEERING-2019

Certificate of Participation-cum-Presentation

is presented to

Ahana Hazra

for his/her participation-cum-presentation in **BIOENGINEERING-2019** conference, held during December 06-07, 2019.

Convenor

Virtual Scientific Conclave - 2021

A platform for comprehensive discussion on challenges and prospects in the field of science and technology

27-01-2021 to 29-01-2021

Organized by

Faculty of Pharmaceutical Science,
Assam down town University (AdtU), Guwahati, Assam

In association with

Defence Research Laboratory, DRDO, Tezpur, Assam

Certificate of Participation

Faculty of Pharmaceutical Science Assam down town University highly appreciates

Ms. Ahana Hagra for his/ her active participation in virtual scientific conclave - 2021

Prof. (Dr.) B. K. Dey
Chairperson
Organizing committee

Shri. Ashim Barman
Addl. Registrar
AdtU

RESEARCH PLATEAU
PUBLISHERS

International Conference on

Recent Trends in Materials Science & Devices 2023

ICRTMD 2023

22-23 JULY, 2023

Organised by
Research Plateau Publishers
&
G.A.V. Degree College, Patauda, Jhajjar, Haryana, India

CERTIFICATE

This is to certify that

Ms. Uzma Hazra

presented a paper entitled "Orally active capecitabine-loaded biopolymeric microsphere inhibiting the proliferation of human colon cancer: in vitro and in vivo evaluation" at an International conference on Recent Trends in Materials Science & Devices 2023 (ICRTMD-2023) held in Online Mode from 22-23 July 2023 organized by Research Plateau Publishers in association with G.A.V. Degree College, Patauda, Jhajjar, Haryana, India

Dr. Amrita Hooda
Organizing Secretary

Dr. Sandeep Kaushik
Convener

Dr. Ram Niwas Chauhan
Co-Convener

2023 AMBT
ADVANCED MATERIALS FOR BETTER TOMORROW

International Conference
on
Advanced Materials for Better Tomorrow-II

Organized by
Department of Physics, Banaras Hindu University
&
Society for Interdisciplinary Research in Materials & Biology (SIRMB)

Certificate of Participation
Poster Presentation

This certificate is presented to

Ahana Hazra

Jadavpur University

Place : Varanasi
Date : October 10-13, 2023

Dr. Jayeeta Lahiri
Conference Convener